Direct-photon production in high-energy collisions*

T. Ferbel

Department of Physics, University of Rochester, Rochester, New York 14627

W. R. Molzon

Department of Physics, University of Pennsylvania, Philadelphia, Pennsylvania 19104

The authors review the experimental evidence for the observation of single photons in hadronic reactions, summarize the phenomenology used in parametrizing the dynamics of the process, provide a survey of the current status of the experimental program, and discuss expectations from future investigations of direct-photon production at large transverse momenta.

CONTENTS

I. OVERVIEW

A. Introduction

It has been known for decades that photons are produced copiously in hadronic collisions. The overall inclusive yield is, in fact, comparable to that observed for pions (see, for example, Boggild and Ferbel, 1974). The source of these photons can, of course, be largely attributed to $\pi^0 \rightarrow \gamma + \gamma$, $\eta \rightarrow \gamma + \gamma$, $\Sigma^0 \rightarrow \Lambda^0 + \gamma$, and other electromagnetic decays of directly produced hadrons. These secondary sources, although interesting in their own right, are not the subject of this review. Here we will be concerned with primary sources, that is, with prompt photons that are produced directly in high-energy interactions.

The interest in direct production of photons in hadronic collisions stems from the fact that, from a purely qualitative perspective, a substantial yield of photons, particularly at large transverse momentum (p_T), would suggest the presence of pointlike charged objects within hadrons. Considering the great success of the quark model in describing the spectrum and properties of the elementary particles (Rosner, 1981), and of the parton model in accounting for deep-inelastic scattering of leptons from nucleons (Yan, 1976), one could hardly regard such an implication as controversial. Nevertheless, the observation of direct photons would be important, because such data could provide a new probe for investigating the substructure of hadrons and lead to a more thorough understanding of the nature of the hadronic constituents and their interactions.

Direct production of photons at low transverse momenta, at a level of 1% of hadroproduction, has been expected and observed from pion inner bremsstrahlung processes (Goshaw *et al.*, 1979); another relatively weak source of prompt photons has been expected from the direct coupling of neutral vector mesons to photons (see, for instance, Perl, 1974, p. 454); also, arguments based on thermodyanmic models have suggested that direct photon production, particularly at high energies, might compete quite favorably with hadron production (Feinberg, 1974). Finally, prior to the discovery of a prompt photon yield at large p_T, calculations based on the hard scattering of partons predicted that the ratio of γ/π production in hadronic reactions would exceed 10% at large p_T (Escobar, 1975; Farrar and Fraustschi, 1976).[1]

*Research supported by the United States Department of Energy.

[1]The initial stimulation for predictions of large yields of direct photons appear to have been the excess of leptons observed at large transverse momenta. This could not be accounted for by standard mechanisms and was attributed, particularly by Farrar, to the decay of virtual photons [see, for example, Lederman (1975)]. Measuring l^+l^- pairs at low mass is, in fact, an alternate way to study direct photons. This approach was first employed by Cobb *et al.* (1978).

There is now overwhelming evidence that the yield of single prompt photons at large p_T approaches that observed for low-lying meson states. Although anticipated from several viewpoints, this is nevertheless a remarkable result and particularly noteworthy, because, both from general arguments and specific calculations based on quantum chromodynamics (QCD), copious production of direct photons is indeed expected at large p_T (Fritzsch and Minkowski, 1977; Halzen and Scott, 1978; Rückl *et al.*, 1978; Field, 1978; Contogouris *et al.*, 1979). The investigation of prompt photon production therefore offers an important tool for examining the essential validity of QCD and of the associated phenomenology.

B. Leading-order processes

In any scattering among constituents in which a strongly coupled vector gluon (g) is emitted from a quark (q), the gluon can be replaced by an electromagnetically coupled photon. This is illustrated in the diagrams shown in Fig. 1. Two illustrative QCD processes of order α_s^2 (where α_s is the strong coupling constant of QCD) are given at the top, and the appropriate diagrams that contribute to direct photon production are shown at the bottom. The photon emission probability relative to the gluon yield is reduced essentially by the ratio of α_s/α (α is the fine-structure coupling constant). Figures 1(c) and 1(d) provide the leading-order contributions to direct photon production in hadronic reactions at large p_T, where a perturbative expansion in QCD is expected to be valid. Figure 1(c), which is the QCD analog of Compton scattering, is commonly referred to as the Compton graph, while, for obvious reasons, Fig. 1(d) is referred to as the annihilation graph.

The importance of direct photon production arises from the well-understood electromagnetic (pointlike) coupling of a photon to a quark and the consequent anchor that this process can provide in helping unfold the underlying quark-gluon dynamics and hadron structure. In particular, from Fig. 1 we see that when a photon appears in the final state, either it is accompanied by a gluon, or the hard scattering is initiated by a gluon. If the contributions from these two leading-order graphs can be isolated, prompt γ production can be used to extract information on both gluon fragmentation[2] and on the gluon structure of hadrons (i.e., the momentum distribution of gluons within hadrons).

Although, in principle, Figs. 1(a) and 1(b) have equivalent physics content to Figs. 1(c) and 1(d), the great advantage of using direct photons is that they emerge from the collision as free particles, and consequently provide pristine information about the hard scattering. In contrast, gluons or quarks must fragment into hadrons (of reduced p_T), and the resulting hadrons must first be associated with their respective partons before the extraction of the physics of constituent interactions can take place. Two possible approaches are available for associating the produced hadrons with their parent partons. One alternative is to detect all the parton fragments—that is, to capture and identify the complete jet of hadrons. Aside from the experimental difficulties of such a task (De Marzo *et al.*, 1982; Wolf, 1982), there are inherent theoretical ambiguities in the definitions of constituent jets (Hoyer *et al.*, 1979; Anderson *et al.*, 1980) that limit the utility of this kind of procedure, particularly for quantitative studies of the elementary subprocesses. Nevertheless, recent experiments using unbiased jet triggers have been able to extract quantitative information on scattering of constituents at large p_T (Åkesson *et al.*, 1982b; Banner *et al.*, 1982; Arnison *et al.*, 1983). The other approach involves selecting single hadrons of large p_T that reflect the properties of the scattered protons. However, because selection of a particle with high p_T tends to bias events to the kind in which the fragmenting parton gives most of its momentum to that single hadron, in this approach the extracted cross section for parton interactions is rather sensitive to the nature of the fragmentation process. Finally, we note that for hadron-triggered experiments there is no direct way of distinguishing which of the subprocesses contribute to the measured cross sections for scattering of constituents.[3]

C. Triggering and general design considerations

Because cross sections for hard collisions are rather small, it is important in any experimental investigation of such reactions to develop efficient probes and analysis methods that can be used to associate data with interesting parton-level processes. As discussed above, photons emerge from interactions carrying the full momentum of the partonic collision; consequently, photons can provide

[2]Fragmentation is the mechanism whereby colored constituents "dress" themselves, that is, evolve into visible color-singlet hadrons, as they emerge from the collision. This process can be characterized by a fragmentation function that specifies the probability of emitting a hadron that has some given fraction of the momentum of the constituent. The fragmentation probability decreases rapidly as the momentum fraction of the hadron increases [see, for instance, Sehgal (1977)].

[3]It should also be pointed out that even at the Born level there are considerably more graphs that can contribute to jet production than to the direct-photon yield. For example, it is thought that the order α_s^2 process $gg \rightarrow gg$ accounts for essentially all jet production studied at the $\bar{p}p$ collider at CERN (Banner *et al.*, 1982; Arnison *et al.*, 1983). Because only gluons are involved in these subprocesses, there are no analogous contributions to direct-photon production (in lowest order). Consequently, it is not surprising that the phenomenology for direct photons is less complicated than for jets.

There is now overwhelming evidence that the yield of single prompt photons at large p_T approaches that observed for low-lying meson states. Although anticipated from several viewpoints, this is nevertheless a remarkable result and particularly noteworthy, because, both from general arguments and specific calculations based on quantum chromodynamics (QCD), copious production of direct photons is indeed expected at large p_T (Fritzsch and Minkowski, 1977; Halzen and Scott, 1978; Rückl *et al.*, 1978; Field, 1978; Contogouris *et al.*, 1979). The investigation of prompt photon production therefore offers an important tool for examining the essential validity of QCD and of the associated phenomenology.

B. Leading-order processes

In any scattering among constituents in which a strongly coupled vector gluon (g) is emitted from a quark (q), the gluon can be replaced by an electromagnetically coupled photon. This is illustrated in the diagrams shown in Fig. 1. Two illustrative QCD processes of order α_s^2 (where α_s is the strong coupling constant of QCD) are given at the top, and the appropriate diagrams that contribute to direct photon production are shown at the bottom. The photon emission probability relative to the gluon yield is reduced essentially by the ratio of α_s/α (α is the fine-structure coupling constant). Figures 1(c) and 1(d) provide the leading-order contributions to direct photon production in hadronic reactions at large p_T, where a perturbative expansion in QCD is expected to be valid. Figure 1(c), which is the QCD analog of Compton scattering, is commonly referred to as the Compton graph, while, for obvious reasons, Fig. 1(d) is referred to as the annihilation graph.

The importance of direct photon production arises from the well-understood electromagnetic (pointlike) coupling of a photon to a quark and the consequent anchor that this process can provide in helping unfold the underlying quark-gluon dynamics and hadron structure. In particular, from Fig. 1 we see that when a photon appears in the final state, either it is accompanied by a gluon, or the hard scattering is initiated by a gluon. If the contributions from these two leading-order graphs can be isolated, prompt γ production can be used to extract information on both gluon fragmentation[2] and on the gluon structure of hadrons (i.e., the momentum distribution of gluons within hadrons).

Although, in principle, Figs. 1(a) and 1(b) have equivalent physics content to Figs. 1(c) and 1(d), the great advantage of using direct photons is that they emerge from the collision as free particles, and consequently provide pristine information about the hard scattering. In contrast, gluons or quarks must fragment into hadrons (of reduced p_T), and the resulting hadrons must first be associated with their respective partons before the extraction of the physics of constituent interactions can take place. Two possible approaches are available for associating the produced hadrons with their parent partons. One alternative is to detect all the parton fragments—that is, to capture and identify the complete jet of hadrons. Aside from the experimental difficulties of such a task (De Marzo *et al.*, 1982; Wolf, 1982), there are inherent theoretical ambiguities in the definitions of constituent jets (Hoyer *et al.*, 1979; Anderson *et al.*, 1980) that limit the utility of this kind of procedure, particularly for quantitative studies of the elementary subprocesses. Nevertheless, recent experiments using unbiased jet triggers have been able to extract quantitative information on scattering of constituents at large p_T (Åkesson *et al.*, 1982b; Banner *et al.*, 1982; Arnison *et al.*, 1983). The other approach involves selecting single hadrons of large p_T that reflect the properties of the scattered protons. However, because selection of a particle with high p_T tends to bias events to the kind in which the fragmenting parton gives most of its momentum to that single hadron, in this approach the extracted cross section for parton interactions is rather sensitive to the nature of the fragmentation process. Finally, we note that for hadron-triggered experiments there is no direct way of distinguishing which of the subprocesses contribute to the measured cross sections for scattering of constituents.[3]

C. Triggering and general design considerations

Because cross sections for hard collisions are rather small, it is important in any experimental investigation of such reactions to develop efficient probes and analysis methods that can be used to associate data with interesting parton-level processes. As discussed above, photons emerge from interactions carrying the full momentum of the partonic collision; consequently, photons can provide

[2]Fragmentation is the mechanism whereby colored constituents "dress" themselves, that is, evolve into visible color-singlet hadrons, as they emerge from the collision. This process can be characterized by a fragmentation function that specifies the probability of emitting a hadron that has some given fraction of the momentum of the constituent. The fragmentation probability decreases rapidly as the momentum fraction of the hadron increases [see, for instance, Sehgal (1977)].

[3]It should also be pointed out that even at the Born level there are considerably more graphs that can contribute to jet production than to the direct-photon yield. For example, it is thought that the order α_s^2 process $gg \to gg$ accounts for essentially all jet production studied at the $\bar{p}p$ collider at CERN (Banner *et al.*, 1982; Arnison *et al.*, 1983). Because only gluons are involved in these subprocesses, there are no analogous contributions to direct-photon production (in lowest order). Consequently, it is not surprising that the phenomenology for direct photons is less complicated than for jets.

physics have now been completed, and the next series of investigations at CERN and at Fermilab are either in progress or in advanced stages of construction. The pioneering experiments (Amaldi *et al.*, 1979a; Diakonou *et al.*, 1979; Anassontzis *et al.*, 1982a; Baltrusaitis *et al.*, 1979; Angelis *et al.*, 1980; McLaughlin *et al.*, 1983; Donaldson *et al.*, 1976; Darriulat *et al.*, 1976) that discovered the existence of direct photons were not truly optimized for such studies. Even the best of these (Anassontzis *et al.*, 1982a) suffered from limited acceptance. Although not all of the current experiments (Antille *et al.*, 1980; Bachman *et al.*, 1980; Bamberger *et al.*, 1980; Hagelberg *et al.*, 1980; Anassontzis *et al.*, 1981; Camilleri *et al.*, 1981; Baker *et al.*, 1981; Binkley *et al.*, 1981) were designed specifically to examine direct-photon physics, they will nevertheless have excellent capabilities to do this.

II. PHENOMENOLOGICAL DISCUSSION

A. Phenomenology of the elementary processes

The diagrams displayed in Fig. 1 correspond to fundamental subprocesses among the constituents. To obtain a cross section in leading order of perturbative QCD for the production of a photon in a hadronic collision, we must convolute the cross section for the elementary process with the gluon or quark contents of the participating hadrons. The appropriate kinematics for the reaction $A+B\rightarrow\gamma+$anything are shown in Fig. 2. The p_i are four-vectors of the physical particles and of the partons; $\hat{s}$ and $\hat{t}$ are, respectively, the square of the energy in the constituent (a,b) center of mass and the square of the four-momentum transferred in the subprocess. The invariant cross section for the reaction can be written in a factorized form as follows:

$$E_\gamma\frac{d\sigma}{d^3p_\gamma}(A+B\rightarrow\gamma+\cdots)=\int\frac{dx_a}{x_a}\frac{dx_b}{x_b}F(a,A;x_a)F(b,B;x_b)\frac{E_\gamma d\hat{\sigma}}{d^3p_\gamma}\ , \tag{1}$$

where the invariant cross section for the subprocess $a+b\rightarrow c+\gamma$ can be written as

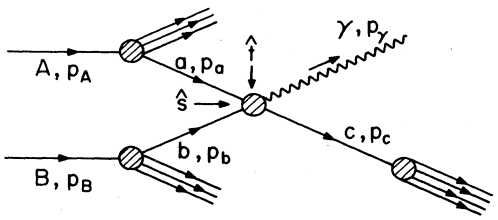

FIG. 2. The kinematics for the inclusive production of photons in collisions of particles A and B are shown in terms of the interactions of their constituents a and b.

$$E_\gamma\frac{d\hat{\sigma}}{d^3p_\gamma}=\frac{\hat{s}}{\pi}\frac{d\sigma}{d\hat{t}}\delta(\hat{s}+\hat{t}+\hat{u})\ , \tag{2}$$

with $\hat{u}$ being the third Mandelstam variable for the subprocess. The particular δ function is appropriate for partons of zero mass. The x_i are the fractions of the four-momenta of the incident particles that are carried away by the partons. The F's are structure functions of the hadrons; namely, they provide the probabilities of finding any particular constituent with some prescribed value of x. The structure functions are related to the number distributions G: $G(a,A;x_a)=F(a,A;x_a)/x_a$ (Baier *et al.*, 1979). For the Compton graph the elementary cross section can be written as (see, for example, Fritzsch and Minkowski, 1977; Halzen and Scott, 1978b; Rückl *et al.*, 1978)

$$\frac{d\sigma}{d\hat{t}}(qg\rightarrow q\gamma)=-\frac{\pi\alpha\alpha_s}{3\hat{s}^2}e_q^2\frac{\hat{u}^2+\hat{s}^2}{\hat{s}\hat{u}}\ , \tag{3}$$

and for the annihilation diagram:

$$\frac{d\sigma}{d\hat{t}}(\bar{q}q\rightarrow g\gamma)=\frac{8\pi\alpha\alpha_s}{9\hat{s}^2}e_q^2\frac{\hat{u}^2+\hat{t}^2}{\hat{u}\hat{t}}\ , \tag{4}$$

e_q is the charge of the interacting quark. For production at 90° in the (a,b) center of mass, for example, where $\hat{s}=-2\hat{u}=-2\hat{t}$, the cross sections for the two subprocesses are comparable. However, their respective contributions to the direct-photon yield of Eq. (1) is clearly a function of the nature of the constituent distributions within any hadron.

The $(\hat{s})^{-2}$ form in $d\sigma/d\hat{t}$ leads naturally to an inclusive photon cross section from Eq. (1) that scales in the parton model as p_T^{-4}. That is, if we assume that the structure functions depend only on the x_i and not on the momentum transfers (i.e., we assume scaling in the structure functions), then for any given $x_T\equiv 2p_T/\sqrt{s}$ and scattering angle θ in the center of mass, the cross section becomes (Farrar, 1977; Berman *et al.*, 1971)

$$E_\gamma\frac{d\sigma}{d^3p_\gamma}(AB\rightarrow\gamma+\cdots)\simeq\frac{f(x_T,\theta)}{s^2}\simeq\frac{g(x_T,\theta)}{p_T^4}\ . \tag{5}$$

In fact, without scaling violations, the cross sections for production of jets and single hadrons at large p_T should also follow Eq. (5), but with different forms for the functions $g(x_T)$, reflecting different parton-level processes (Rückl *et al.*, 1978).[5] As we shall see, the experimental p_T dependence for photons is closer to p_T^{-6}. This softer distribution can be accommodated because of the presence of higher-order corrections and scaling violations, to which we now turn.

[5]It is important to realize that, because the functions $g(x_T)$ can be different for photons, hadrons, and jets, the relative yield of these objects at a fixed $\sqrt{s}$ will generally change with p_T (see footnote 4).

Modifications in the p_T dependence of Eq. (5) can arise in two ways. First, in perturbative QCD, the strong "running coupling constant" has a Q^2 dependence, which, to lowest order in corrections to the gluon propagator, is given by (see, for instance, Aitchison and Hey, 1982; Quigg, 1983)

$$\alpha_s(Q^2)=\frac{12\pi}{(33-2f)\ln Q^2/\Lambda^2}\ , \tag{6}$$

where Q^2 is the square of an appropriate momentum transfer (of order p_T^2) that characterizes the collision, f is the number of flavors that can contribute to the scattering, and Λ is a parameter that sets the scale for Q^2. Expression (6) is valid only for $Q^2 \gg \Lambda^2$ [and $\ln Q^2 \gg \ln(\ln Q^2)$], i.e., when $\alpha_s \ll 1$. It is clear from Eq. (6) that if the number of flavors is less than 17 (at SPS/Fermilab energies $f=4$), then $\alpha_s \to 0$ as $Q^2 \to \infty$. This "asymptotic freedom" provides the justification for a perturbative QCD (Gross and Wilczek, 1973; Politzer, 1973).[6]

The other source for modifications to the p_T dependence in Eq. (5) arises from the presence of scaling violations in the structure functions. That is, the functions F in Eq. (1) have a Q^2 dependence, which originates in the strong "radiative" corrections of QCD (Georgi and Politzer, 1974; Gross and Wilczek, 1974; De Rujula *et al.*, 1977). Because there is no theory of confinement for hadrons, there is no fundamental prescription for the structure functions; they are often parametrized using parton counting rules (Brodsky and Farrar, 1975; Farrar, 1974; Gunion, 1974; Rückl *et al.*, 1978) for the x dependence and QCD-inspired parametrizations that satisfy the Q^2 evolution equations of QCD (Owens and Reya, 1975; Buras and Gaemers, 1978; Altarelli and Parisi, 1977). Scaling violations have been shown to be rather important in reducing the large-p_T components in the calculations of direct-photon yields (Contogouris *et al.*, 1979; Petrarca and Rapuano, 1979). The quark structure functions and scaling violations for nucleons have been measured in deep-inelastic lepton scattering (Perkins, 1981). Gluon structure functions of hadrons are not known very well, and one of the major goals of the direct-photon experiments is the extraction of that information from the data.

B. Ambiguities and corrections to lowest-order terms

Several problems and ambiguities present themselves in the evaluation of Eq. (1). First is the question of the proper definition for Q^2 in the estimation of the scaling violations and of $\alpha_s(Q^2)$. The kinematic domain in which most present-day calculations (leading $\ln Q^2$ terms) are appropriate corresponds to large s and p_T, and x_T near unity. Such a regime is characterized by $\hat{s} \sim -\hat{t} \sim -\hat{u}$. Consequently, it is appropriate to regard Q^2 of that same order of magnitude. When $\ln Q^2$ is large enough, the precise definition of Q^2 becomes unimportant; for example, if N is some constant of order unity, then it does not matter whether we define $Q^2=p_T^2$ or $Q^2=Np_T^2$, because $\ln Q^2=\ln p_T^2 \simeq \ln N p_T^2$. Unfortunately, at ISR, SPS, or Fermilab energies, the p_T values that can be reached are $p_T^2 \lesssim 200$ GeV^2, and the definition of Q^2 therefore has impact on the theoretical predictions. Commonly, Q^2 is chosen as $2p_T^2$ or as $\frac{4}{3}\ p_T^2$. The first choice corresponds to $-\hat{t}$ in Fig. 2, or to $-\hat{u}$ for the crossed Feynman graph; the second choice equals $2\hat{s}\hat{t}\hat{u}/(\hat{s}^2+\hat{t}^2+\hat{u}^2)$; both limits are for the case when the hard scattering is at 90°, i.e., $x_a=x_b=x_T=(\hat{s}/s)^{1/2}$, and $\hat{s}=-2\hat{u}=-2\hat{t}$ in Fig. 2.

Another ambiguity arises from the fact that the partons do not necessarily collide head on. That is, they have finite initial values of p_T because of their transverse Fermi motion within the hadrons. This "intrinsic k_T," as it is termed, is usually introduced in the form of a Gaussian smearing of the parton's transverse momentum. Such smearing is, of course, unimportant at very large p_T values, but cannot be ignored in the (5—10)-GeV/c range. Typical $\langle k_T \rangle$ values, estimated from hadronic interactions (see, for instance, Feynman *et al.*, 1978) and used in the literature, lie between 0.4 and 1.0 GeV/c. The effect of introducing k_T smearing is, typically, to increase the yield of direct photons, but to have less of an effect on the γ/π production ratio (Baier *et al.*, 1980).[7] There is also a degree of flexibility in the way k_T smearing is usually introduced. The partons can be treated as virtual off-mass-shell objects or as real particles of zero mass. The effect of the internal k_T is more pronounced for the latter case then for the kinematically preferred off-shell treatment (Caswell *et al.*, 1978; Horgan and Scharbach, 1979).

The most serious deficiency of the phenomenology described thus far is, of course, that higher-order contributions to the yield of direct photons have been neglected. Bremsstrahlung processes of the kind shown in Fig. 3 have been investigated in some detail (Rückl *et al.*, 1978; Aurenche and Lindfors, 1980; Horgan and Scharbach, 1981; Dechantsreiter *et al.*, 1981; Contogouris, Papadoupolos, and Papavassiliou, 1981; Nowak and Praszalowicz, 1983; Benary *et al.*, 1983) and should become important as the photon's x_T approaches 1. However, if the gluon structure of hadrons is relatively hard (does not fall rapidly with x), then the Compton graph could continue to dominate even at large x_T. The latest calculations indicate that the $qq \to qq\gamma$ processes contribute, for moderate x_T (0.1—0.3), at about 30% of the Born term for the Compton graph (Nowak and Praszalowicz, 1983). Data (discussed in the next section) appear to support the presence of relatively small bremsstrahlung contributions,

[6]We should point out that QCD provides only the form for the evolution of α_s with Q^2. The parameter Λ and the value of α_s at some fixed value Q_0^2 are not specified and must be extracted from data. Hadron production in e^+e^- annihilations appears to be the cleanest regime for determining α_s [see, for example, Adeva *et al.* (1983)]. The latest favored value of Λ is ~ 0.2 GeV/c.

[7]Corrections to π^0 production are larger than to the γ yield, because the p_T distribution for π^0's is steeper than for γ's.

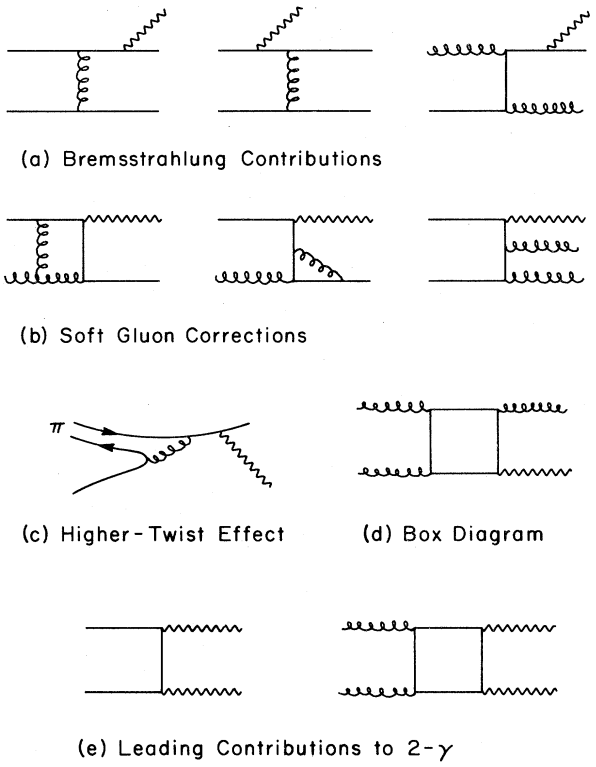

FIG. 3. Representative graphs for (a) lowest-order bremsstrahlung processes, (b) soft-gluon corrections of order $\alpha\alpha_s^3$ (virtual) and $\alpha\alpha_s^2$ (real), (c) a higher-twist contribution for $\pi q \to q\gamma$, (d) quark-box diagram of order $\alpha\alpha_s^3$, and (e) the leading contributions to the production of two prompt photons.

except possibly at largest x_T values. It is interesting to note that, although bremsstrahlung appears to be of order $\alpha_s^2\alpha$, in fact, because the fragmentation of a constituent into a photon is proportional to α/α_s (Rückl *et al.*, 1978; Frazer and Gunion, 1979), bremsstrahlung can be regarded as a process of order $\alpha\alpha_s$, that is, the same level as the Born terms in Figs. 1(c) and 1(d).[8]

Soft gluon (real and virtual) corrections to the Born terms have also been investigated and, as in the case of the Drell-Yan mechanism (Altarelli *et al.*, 1979; Kubar-Andre and Paige, 1979), found to be important (Contogouris, Papadoupolos, and Ralston, 1981, 1982). The kinds of graphs that have to be considered are also shown in Fig. 3. The soft gluon corrections to order α_s^2 are estimated to provide a factor of $\sim$1.5—2 increase in the direct-photon yield [analogous to the "k-factor" of $\sim$2—2.5 in Drell-Yan production (see, for example, Berger, 1982b)]. Again, there are some ambiguities in the calculation because of neglect of next-order contributions (beyond single-loop terms), the choices available for Q^2, and other problems inherent in the QCD perturbative expansion (Owens, 1981). There are also higher-order terms involving quark box diagrams that are not very important in the single-photon yield but cannot be neglected for two-photon production (Combridge, 1980; Carimalo *et al.*, 1981; Field, 1983).

Finally, there are "higher-twist" effects in which one of the incident particles interacts directly with a constituent from the other particle. Because of hadronic form factors, such processes have very small cross sections. Nevertheless, the direct-photon yield from higher-twist contributions can be important in certain restricted regimes of phase space (Berger, 1982a; Rückl *et al.*, 1978). A typical graph that dominates at small production angles and large p_T (and that scales as p_T^{-6} rather than p_T^{-4}) is also shown in Fig. 3.

C. Correlations, projectile dependence, two-photon yield, and nuclear dependence

Several phenomenological investigations have emphasized the desirability of measuring the correlation between direct photons and their associated jets of hadronic particles (Cormell and Owens, 1980; Halzen *et al.*, 1980; Baier *et al.*, 1980; Contogouris, Papadoupolos, and Papavassiliou, 1981; Horgan and Scharbach, 1981). In pp collisions, for example, direct-photon production should be dominated by the Compton graph. Consequently, away-side jets should be mainly fragments of quarks, and, in fact, primarily of u quarks [Eq. (3)]. Measuring the charge distribution of particles on the away side provides, therefore, information on the γ-production mechanism. Furthermore, because jets recoiling from π^0's or from charged hadrons can often be initiated by gluons, a comparison of away-side jets that accompany γ's with those that accompany hadrons can yield at least a qualitative measure of the difference between quark and gluon fragmentation. Also, prompt photons should not be accompanied by hadrons along their direction of motion (that is, on the "same side"); the presence of such hadrons would signal a likely contribution from quark bremsstrahlung (again, because of the dependence on e_q^2, for pp collisions these would be mainly u quarks). Consequently, comparisons of the density of same-side hadrons and their charges with those that, for example, accompany π^0's, provide probes of the underlying production mechanisms.

Using different projectiles for studying direct photon production provides additional constraints on the phenomenology. In particular, for $\pi^- p$ or $\bar{p}p$ collisions, because of the enhanced possibility of $\bar{u}u$ (valence) interactions, the annihilation graph, especially at large x_T, should contribute substantially to the yield of prompt photons. A calculation of the ratio of annihilation/Compton production as a function of x_T is shown in Fig. 4 for $\pi^- p$ collisions at $\sqrt{s}=23$ GeV (Kotański and Kubar, 1980). Because of the observed dependence on x_T,

[8]The above follows for quarks just from QED. However, because of higher-order QCD corrections, gluons also have a nonvanishing probability for photon fragmentation that scales as α/α_s. This and other phenomenological subtleties are discussed by Owens, 1981.

the character of the recoiling jet should change as the relative contributions of the Compton and annihilation graphs change.

Examining differences in prompt photon inclusive cross sections between $\pi^- p$ and $\pi^+ p$ (or between $\bar{p}p$ and pp) interactions provides the additional possibility of isolating specific production mechanisms. In particular, ignoring the sea antiquarks, it follows from Eq. (4) that the annihilation diagram is a factor of 8 greater in $\pi^- p$ than in $\pi^+ p$ interactions (the difference between $\bar{p}p$ and pp is, clearly, much greater). The Compton diagram is the same for the two channels. Consequently, forming the difference between $\pi^- p$ and $\pi^+ p$ cross sections isolates the annihilation term, and provides a means for extracting quark and gluon structure functions (Contogouris, Papadoupolos, and Papavassiliou, 1981; Kotański and Kubar, 1980; Hagelberg *et al.*, 1980; Cormell and Owens, 1980). The difference distribution for the characteristics of the recoil jets isolates properties of gluon fragmentation. Bremsstrahlung processes may confuse this simple picture; nevertheless, such difference measurements should prove of great interest in future experiments.

Correlation measurements between direct photons and their accompanying jets can be used to extract the x dependence of the gluon structure functions for some specific region of Q^2 (see, for instance, Cormell and Owens, 1980). This can be accomplished if the Compton contribution can be isolated and the momentum of the accompanying quark jets established. Then, just as in the case of the measurement of the pion structure functions in Drell-Yan production (Newman *et al.*, 1979; Badier *et al.*, 1979), the distribution of gluons can be determined directly. In fact, if k_T effects can be ignored, just the *direction* of the jet and the γ momentum suffice for the gluon determination. (If the accompanying jet is not measured, the data are sensitive only to the integral over the gluon distribution.) There are, of course, the standard theoretical and experimental uncertainties in the assignment of hadrons to jets that make the extraction here more ambiguous than for Drell-Yan production. Also, it may not be possible to separate the Compton contribution from other terms, such as the annihilation graph or bremsstrahlung, just on the basis of kinematics alone (see Sec. III.E). Nevertheless, as just discussed, a complete study of several incident channels should provide the required discrimination.

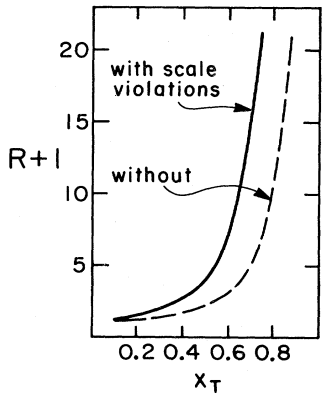

FIG. 4. Estimate of the ratio of contributions from the annihilation graph to that from the Compton graph (R), as a function of x_T, for prompt photon production in $\pi^- p$ interactions at $\sqrt{s}=23$ GeV (at 90° in c.m.). The quantity $(R+1)$ is shown with and without QCD scaling violations (Kotański and Kubar, 1980).

In addition to measuring just inclusive single-photon production, two-photon yields are of substantial importance. The main contributions expected for the two-photon yield are shown at the bottom of Fig. 3. Identifying the two photons specifies completely the kinematics and provides a method for measuring intrinsic k_T.[9] It has been emphasized that a study of the yield of direct-photon pairs relative to dileptons would be particularly valuable in gauging the importance of the two-gluon graph, and thereby provide a nontrivial check on the gluon structure of hadrons (Combridge, 1980; Carimalo *et al.*, 1981; Field, 1983). A comparison of two-photon yields with π^+ and π^- beams, or the ratio of dilepton to diphoton production, would also provide direct information on the electric charge of quarks (Krawczyk and Ochs, 1978). There is at present only one experimental result pertinent to the measurement of photon pairs (Kourkoumelis *et al.*, 1982).

Finally, a word concerning target material: Although, in principle, direct-photon production should be easiest to interpret for interactions of hadrons with proton targets, persuasive arguments can be made for using nuclear targets as well. It has been suggested (Hagelberg *et al.*, 1980), for example, that the best way to extract the contribution from the annihilation graph is through a subtraction of π^+ from π^- projectile data on isoscalar targets (e.g., carbon). In this way, any background due to strong π^0 or η production should cancel automatically, and the difference should correspond to the difference between the $\bar{u}u$ and $\bar{d}d$ annihilation processes. There are also interesting conjectures concerning the relative sizes of cross sections for scattering of quarks and gluons that can be tested by studying the behavior of recoil jets on different nuclei (Krzywicki *et al.*, 1979). In addition, the direct-photon yield as a function of atomic number is especially sensitive to higher-twist contributions (Berger, 1981). Nevertheless, although the unique physics possibilities from nuclear targets are important, it should be recognized that the phenomenology may require some modifications to take account of any nuclear effects. A particular case in point is the recent discovery that quark structure functions may not be the same in nuclei as in a proton (Aubert *et al.*, 1983; Bodek *et al.*, 1983; Krzywicki, 1976; Jaffe, 1983; Llewellyn Smith, 1983).

Before turning to the experiments and their analyses in

[9]The approximate momentum of the recoil jet accompanying single photons can also provide some constraint on k_T and can lead to a cleaner confrontation with theoretical predictions (Cormell and Owens, 1980).

terms of the above phenomenology, we wish to bring to the attention of the reader several recent reviews of direct-photon production that have appeared in the literature, namely, Willis (1981), Pretzl (1983), Halzen and Scott (1981), Owens (1981), and Field (1983).

III. EXPERIMENTAL TECHNIQUES AND RESULTS

This section is devoted to a survey of the experimental status of prompt photon production. First, we discuss the general techniques that can be used in such studies; this discussion is followed by a description of specific experiments and a comparison of their relative strengths and weaknesses; we then turn to results that have been reported on hadrons produced in association with direct photons. We delay to Sec. V our discussion of theoretical predictions and their comparison with measurements.

A. Overview of experimental techniques

As we mentioned briefly in the Introduction, the detection of prompt γ's requires the suppression of background from nonprompt sources (i.e., decays of short-lived particles) and from hadrons that can be misidentified as γ's. The primary source of background photons in hadron-hadron interactions arises from the decay of π^0 and η mesons and, to a lesser extent, from η' and ω decays. (Other known sources, e.g., $\Sigma^0 \to \Lambda\gamma$, can be ignored at large values of p_T.) Meson decays can give rise to background photons in the two following ways: (1) One of the γ's from a $\pi^0 \to \gamma\gamma$ or $\eta \to \gamma\gamma$ decay may not be detected and consequently yield an apparently isolated single γ, or (2) the two γ's from a meson decay may coalesce, i.e., may have a spatial separation that is too small to be resolved in the detector, and appear as a single photon. The ability to calculate such photon background requires precise information on the production characteristics of the major sources of background.

To illustrate the level of photon background expected from π^0 decay, let us consider, for example, an experiment in which γ's are detected using a single arm spectrometer of good spatial resolution but very small solid angle. Let us suppose that we wish to measure the photon yield at a momentum p_γ. Because, in the laboratory, the photons from the decay of a π^0 are distributed essentially uniformly in momentum between 0 and the momentum of the π^0 (p_0), and because all π^0's with $p_0 > p_\gamma$ can contribute to the photon spectrum at p_γ, we can write

$$\frac{d\sigma}{dp_\gamma} = 2\int_{p_0=p_\gamma}^{\sqrt{s}/2} \frac{d\sigma}{dp_0}\frac{dP}{dp_\gamma}dp_0 = 2\int_{p_\gamma}^{\sqrt{s}/2} \frac{d\sigma}{dp_0}\frac{dp_0}{p_0} . \quad (7)$$

Here dP/dp_γ is the momentum probability distribution for the decay photons ($\sim p_0^{-1}$), and the factor of 2 arises from the fact that two photons contribute. Ignoring the longitudinal momentum of the π^0 (that is, assuming $\theta_{\text{c.m.}} \simeq 90°$ for the position of the spectrometer), we can take Eq. (7) as a relationship between p_T spectra of π^0's and their γ-decay products. If we are not interested in p_T values close to the kinematic limit of $\sqrt{s}/2$, then we can replace the upper limit in the integral by $p_0 = \infty$.

At p_T values of ~ 5 GeV/c, for example, the π^0 cross section can be approximated by $d\sigma/dp_T \sim p_T^{-n}$, where n equals ~ 10 for $\sqrt{s} \sim 30$ GeV. Using this specific form in Eq. (7), and ignoring regions close to the edge of phase space, yields a daughter spectrum having the same shape as that of the π^0, but reduced in magnitude by a factor of $n/2$. Thus independent knowledge of the π^0 cross section could, in principle, be used to subtract this source of background in the measured γ signal. Because of the difficulty of measuring with sufficient accuracy absolute cross sections that have very steep falloffs in p_T, this method has not been useful in determining the presence of direct photons. Most evidence for direct-photon production to date has been derived using methods that normalize the observed prompt photon yield to the π^0 cross section measured in the same experiment. Because the detection techniques for γ's and π^0's are similar, systematic errors tend to cancel in the ratios of cross sections, and results in terms of a γ/π^0 production ratio tend to be more reliable.

Primarily two techniques have emerged for detecting prompt photons and for dealing with the large backgrounds to the γ signal. One is the "direct method," in which π^0's are detected simultaneously with single γ's, and a large fraction of the two photons from π^0 decays are resolved through a measurement of the $\gamma\gamma$ mass. The other is the "conversion method," in which π^0's and γ's are also detected simultaneously, but separated only statistically through the measurement of the conversion probability in a thin converter that is placed in front of a shower detector.

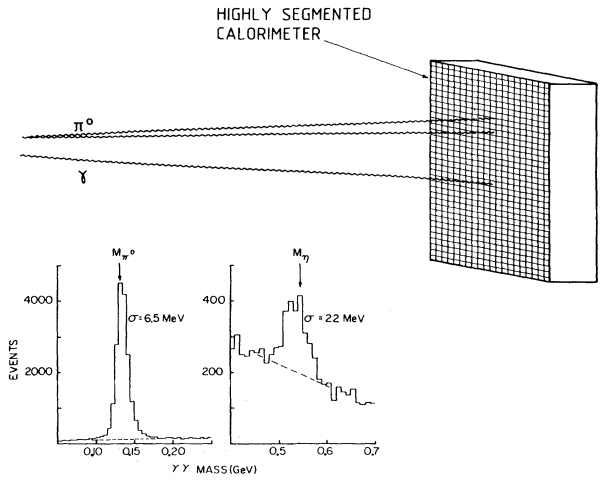

FIG. 5. A schematic drawing of a detector that can be used for the measurement of prompt γ's using the direct method. An electromagnetic shower detector of sufficient granularity to resolve the two photons from π^0 decays is used to detect γ's and π^0's. A typical $\gamma\gamma$ mass distribution in the π^0 and η mass range is also shown (Povlis *et al.*, 1983).

The elements of the first technique are illustrated schematically in Fig. 5. Typically, the detector consists of an array of lead glass counters, a sampling calorimeter, or an ionization chamber; the detector should have good acceptance for π^0's and sufficient spatial resolution for resolving the separate photons from $\pi^0\to\gamma\gamma$ decays. Figure 5 also displays a typical $\gamma\gamma$ mass spectrum observed in such direct-method measurements (Povlis *et al.*, 1983). Sensitivity to acceptance and to background calculations can be minimized in these experiments for the following reasons. Consider the case in which background is due only to $\pi^0\to\gamma\gamma$ decay. The observed γ to π^0 ratio is given by

$$\left.\frac{N(\gamma)}{N(\pi^0)}\right|_{\rm obs}=\frac{N(\gamma)A(\gamma\to\gamma)+N_{\pi^0}P(\pi^0\to\gamma)}{N(\pi^0)A(\pi^0\to\pi^0)}\ , \tag{8}$$

or the production ratio by

$$\left.\frac{N(\gamma)}{N(\pi^0)}\right|_{\rm prod}=\left[\left.\frac{N(\gamma)}{N(\pi^0)}\right|_{\rm obs}\frac{A(\pi^0\to\pi^0)}{A(\gamma\to\gamma)}\right]-\frac{P(\pi^0\to\gamma)}{A(\gamma\to\gamma)}\ . \tag{9}$$

Here $N(\gamma),N(\pi^0)$ are the experimentally observed (obs) or produced (prod) number of γ's or π^0's; $A(\pi^0\to\pi^0),A(\gamma\to\gamma)$ are efficiencies for detecting π^0's or γ's, and $P(\pi^0\to\gamma)$ is the probability that a π^0 will provide only one observed shower in the detector. Thus the γ/π^0 production ratio is given by the detected γ/π^0 ratio, corrected by ratios of calculable acceptances for γ's and π^0's. Clearly, to optimize the experiment, the last term in Eq. (9) should be made as small as possible, and the two acceptances should be made large.

As mentioned in the Introduction, four characteristics are required of a good detector: (1) fine transverse segmentation to detect the two photons from π^0 decays, (2) good capability for detecting low-energy photons, so as to be maximally sensitive to π^0 decays in which the two photons have substantially different energies ("asymmetric" decays), (3) large solid-angle coverage to minimize the occurrence of events in which one γ from a π^0 misses the detector, and (4) linearity in energy response.

The need for fine-grained transverse segmentation can be understood as follows: For large π^0 momenta, the distribution in opening angle between the two photons in the laboratory is sharply peaked at the minimum value $\theta_{\rm min}\simeq 2m_\pi/E_\pi$. Thus, if $d_{\rm min}$ is the minimum separation distance between the γ's at the detector, and l is the distance from the interaction point to the detector, $d_{\rm min}$ is given by $2m_\pi l/E_\pi$. For $\theta_{\rm c.m.}=90°$, $p_T=5$ Gev/c, and $l=2$ m, $d_{\rm min}$ is approximately 10 cm for collisions observed in the center of mass (e.g., at the ISR); hence a spatial resolution of $\lesssim 5$ cm would be required to resolve the two photons. Clearly, for different choices of l and p_T, $d_{\rm min}$ scales appropriately. In particular, for a laboratory beam momentum of 800 GeV/c and $l=10$ m, $d_{\rm min}$ is about 1.3 cm for $E_{\pi^0}=200$ GeV/c ($p_T=10$ GeV/c at $\theta_{\rm c.m.}=90°$), and the required segmentation is $\lesssim 0.6$ cm. It should be recognized that segmentation much beyond 0.5 cm may not prove valuable because of the limits placed by the inherent transverse dimensions of electromagnetic showers in these detectors.

Good detection of low-energy γ's, as mentioned above, is needed for detecting asymmetric π^0 decays. The asymmetry parameter A is given by $A\equiv|E_1-E_2|/(E_1+E_2)$. This parameter corresponds essentially to $|\cos\theta_\gamma^*|$, where θ_γ^* is the angle of the photon in the π^0 rest frame, measured with respect to the direction of the π^0 in the laboratory. Because π^0's are pseudoscalar mesons, the decay distribution in $\cos\theta_\gamma^*$, and consequently in A, is uniform. Thus the probability that either decay γ has less than some fraction f of the momentum of the π^0 is given by $2f$. Whenever f is small, the second γ has nearly the full π^0 momentum. Consequently, inefficiency in detecting low-momentum γ's can result in substantial background from large-energy (or large-p_T) photons from asymmetric π^0 decays.

Good solid-angle coverage is therefore needed to minimize background from π^0 decays in which one of the photons misses the detector. A large number of elements in any transverse dimension of the detector might also be required to satisfy both the segmentation and acceptance criteria in any particular experiment. Typically, 10—200 detector elements were employed in the first-generation measurements.

It should be pointed out that, although the opening angle for $\eta\to\gamma\gamma$ decays is ~ 4 times that for $\pi^0\to\gamma\gamma$, the branching ratio of $\eta\to\gamma\gamma$ is about 0.4, and the production ratio of η/π^0 is about 0.5; it is therefore not as important to have full acceptance for η's as for π^0's. Thus only a moderate increase in the size of an efficient π^0 detector will suffice for determining the η yield and its contribution to the direct-γ background.

Finally, we discuss the question of detector linearity. A calculation of the contribution from π^0 background to the direct-photon signal requires a precise measurement of the yield of π^0's relative to γ's. Given the steeply falling p_T dependence of the π^0 cross section, any small systematic shift in the measurement of π^0 energies relative to single-photon energies can induce large differences in the relative yields. In particular, because π^0's are detected as two γ's, each with about half of the energy of the π^0, while direct γ's produce single showers of full energy, nonlinearities in detector response can cause relative shifts in the measured p_T between π^0's and direct γ's.

For example, in an experiment that detects 5-GeV/c γ's and π^0's at 90° at the ISR, the π^0's will provide two photons, typically, of 2.5 GeV/c. If such 2.5-GeV photons are measured correctly in the detector, but single 5.0-GeV γ's are measured systematically higher as 5.25-GeV showers, then the π^0 background to γ's at 5.0 GeV will be predicted incorrectly using the yield of 5.25-GeV π^0's, and consequently the feed through from π^0's will be underestimated. In particular, if the p_T spectrum of π^0's falls as p_T^{-10}, then the expected γ background from π^0's at 5 GeV/c will be underestimated by about a factor of 2. In addition, of course, even if there is no background

from π^0's, the measured γ/π^0 ratio will be incorrect because of such a nonlinearity.

In Sec. III.B we discuss recent experiments that have used the direct technique and we indicate how the optimization of various criteria was carried out in order to improve the signal to noise ratio, but here we turn to the other method used for detecting prompt γ's, namely, the conversion method.

The technique is illustrated in Fig. 6. In this procedure, deposited energy is measured in an electromagnetic shower counter located downstream of a thin converter, but no attempt is made to distinguish $\pi^0 \rightarrow \gamma\gamma$ decays from single γ's. Scintillator hodoscopes are placed immediately upstream and downstream of the converter to determine whether a conversion occurred (shower was initiated) in the converter. Because an unresolved π^0 shower in the detector is caused by two γ's, the probability of observing a γ conversion in the thin front radiator is greater for a π^0 than for a single γ. Consequently, the technique for establishing a prompt γ signal is to measure the fraction of events that have conversions in the radiator (i.e., signals in the second, but not in the first, hodoscope of scintillators), and to compare this to the expected conversion probability assuming the absence of a direct-photon signal.

Consider, for example, a radiator of 1.0 radiation-length thickness. The nonconversion probability $P_\gamma(\mathrm{NC})$—that is the probability that a single γ *does not* convert—is given approximately by

$$P_\gamma(\mathrm{NC}) = e^{-7/9x} = 0.46 \ , \tag{10}$$

where x is the radiator thickness in units of radiation lengths. The probability $P_{\pi^0}(\mathrm{NC})$ that *both* of the γ's from a π^0 decay *do not* convert is given by the square of this probability. Consequently, by measuring the observed nonconversion probability $P_{\mathrm{obs}}(\mathrm{NC})$, one can obtain the fraction of *all* observed events that correspond to single photon showers, f_γ:

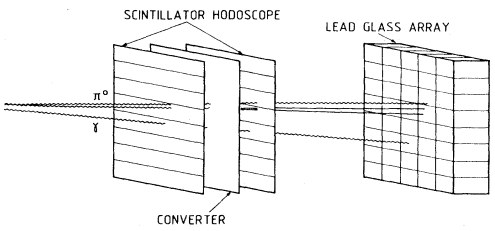

FIG. 6. A schematic drawing of a detector used in the conversion method of measuring prompt γ's. The electromagnetic shower detector does not have sufficient granularity to resolve the two photons from π^0 decays. Segmented scintillation hodoscopes are used to detect any photons that convert in a thin converter. One of the photons from a π^0 decay is shown converting in the converter.

$$P_{\mathrm{obs}}(\mathrm{NC}) = f_\gamma P_\gamma(\mathrm{NC}) + (1 - f_\gamma) P_{\pi^0}(\mathrm{NC}) \ . \tag{11}$$

The weak dependence of the photon conversion probability on energy must be taken into account when using this expression. Clearly, to obtain the correct average value of the nonconversion probability requires detailed information concerning the photon multiplicity in all events that can yield single (i.e., unresolved) showers, namely, the η, η', ω contributions, correlated π^0's, etc.

Although the conversion method requires less granularity and therefore fewer detector channels, it nonetheless puts stringent demands on the detector. In particular, (1) the absolute conversion probability must be known accurately, and (2) any nonlinearities introduced by energy loss in the converter must be well understood.

The first requirement follows from relationship (11), in that the fraction of observed events that correspond to single γ's depends directly on the deviation of $P_{\mathrm{obs}}(\mathrm{NC})$ from $P_{\pi^0}(\mathrm{NC})$. When the direct-γ fraction is small, the γ/π^0 ratio is particularly sensitive to the nonconversion probability. For example, for a true γ/π^0 ratio of 0.1, $P_{\mathrm{obs}}(\mathrm{NC})$ changes from 0.211 to only 0.234.

The requirement that any nonlinearities introduced by the converter be well understood is again important because of the steep p_T dependence of the cross sections. Since events with conversions deposit some energy in the radiator, the actual electromagnetic energy for the event is greater than just the energy observed in the detector. Thus, nonconverting events (more likely γ's) tend to be compared to converting events (usually π^0's) of higher energy. The measured nonconversion probability (or, equivalently, the energy of events with conversions) must be corrected for this effect on a statistical basis through a parametrization of the average energy loss in the converter.

The relative merits of the direct and the conversion methods depend on the absolute cross sections involved, the size of the γ/π^0 ratio, the amount of beam time that can be obtained, and the availability of resources. The advantages of the first technique are basically that, with sufficient detector optimization, most of the backgrounds (i.e., π^0's and η's) can be measured and removed, and any remnant background can be calculated reliably from the measured π^0 and η data. Clearly, this requires a device with a large number of channels that provides sufficient segmentation and large solid-angle acceptance. This technique is most advantageous when absolute cross sections are relatively large but the γ/π^0 ratio is small. The second technique has the advantage that it can provide large coverage with a relatively small number of channels. However, for small γ/π^0 ratios, systematic effects dominate the measurement. This method is therefore best suited to small absolute cross sections, but a reasonably large γ/π^0 ratio. In particular, because coalescence of separate showers does not affect the conversion method, there is no intrinsic upper limit to the p_T values that can be probed using this technique.

An additional advantage of the direct method is that it is more suitable for comparing the structure of prompt γ events with those containing high-p_T π^0's. As noted above, by using the direct method, the signal-to-background ratio for a given γ/π^0 ratio can be improved through an optimization of the detector. This is not true for the conversion technique, where the extraction of γ's is done on a statistical basis and where even nonconverting events have a relatively large π^0 contamination. For example, if we use a 1.0 radiation length converter and assume a γ/π^0 ratio of 0.5, the signal-to-background ratio is 1.0, even for the nonconverting sample. Experiments using the direct technique have achieved signal-to-background ratios of 1.0 for γ/π^0 ratios of only 0.1 (Åkesson *et al.*, 1983b; McLaughlin *et al.*, 1983). For measuring correlations between the trigger γ and recoiling jets, for example, a statistical subtraction must be performed based on the measured level of the signal-to-background ratio. The systematic error on this subtraction is often the limiting factor in such investigations.

In the foregoing discussion we have emphasized γ background from π^0 decays. However, as mentioned in the Introduction, decays of other mesons also contribute to the background, e.g., $\eta\to\gamma\gamma$, $\eta'\to\gamma\gamma$, $\omega\to\pi^0\gamma$, etc. Contributions from these sources are usually calculated either from directly measured individual meson yields, or from relative ratios, such as η/π^0, η'/π^0, etc., coupled with measured π^0 yields. The radiative decay of the ω corresponds to only $\sim 9\%$ of its total width. The η' contribution is also suppressed by its small branching fraction into modes that provide an energetic photon. (Decays into π^0's are already contained in the measured π^0 yields.) Other known sources of γ's are negligible at larger p_T, either because of low production cross sections, or small radiative branching ratios, or because of unfavorable decay kinematics (e.g., $\Sigma^0\to\Lambda\gamma$).

A final source of background that affects both techniques is that from hadron misidentification. Stable hadrons, produced at rates comparable to π^0's, can interact and produce signals in the electromagnetic-shower detectors. Charged hadrons can be rejected by requiring that no charged track pass in the immediate vicinity of the detected shower. Neutral hadrons, especially antineutrons for ISR experiments, can be more problematic. Because the shower detectors are typically thin, corresponding to about one hadronic interaction mean free path, only a small fraction of the hadronic energy is deposited in them. Consequently, in this situation, the steeply falling p_T spectrum helps to suppress the apparent photon background. Antineutrons, on the other hand, if they stop in the detector, can annihilate and deposit an additional ~ 2 GeV beyond their kinetic energy. At the ISR, especially at 90°, this can cause a significant problem. Away from $\theta_{\text{c.m.}}=90°$ at colliders, or at fixed-target machines, this sort of background becomes less important, because the energy from annihilation becomes a small fraction of the total hadron energy.

Techniques for rejecting hadronic background are based chiefly on characteristics of the transverse and longitudinal shower development. We shall discuss this in more detail as we describe the individual experiments, to which we now turn.

B. The first experiments

The first positive indications of prompt γ production at large transverse momenta were rather qualitative and subject to large systematic and statistical uncertainties. Subsequent experiments, both at the ISR and at Fermilab, were more convincing and provided useful measurements of inclusive cross sections in different regions of phase space.

The first published result on direct photons was obtained by CERN experiment R412 at the ISR, using the direct method (Darriulat *et al.*, 1976). The experiment was not originally designed for detecting prompt γ's and was ultimately limited by systematic uncertainties in detector linearity and $\bar{n}$ contamination.

Photons were detected in an array of lead glass blocks situated at 90° in the center of mass. The transverse segmentation was such that π^0's were resolved only for two-photon separations greater than 26 cm. In this geometry, π^0's were detected with reasonable efficiency between 0.9 and 3.6 GeV/c; above 3.6 GeV/c the photons tended to merge into single showers, while below 0.9 GeV/c the probability of missing one γ from a π^0 decay became unacceptably large. The experiment had tracking capability for charged particles via chambers of the Split Field Magnet Facility.

Figure 7 shows the value of the γ/π^0 ratio obtained by this group, corrected for all instrumental effects. The observed ratio of 0.15—0.30 in the range $2.8<p_T<3.8$ GeV/c was surprisingly large and is, in fact, inconsistent with present observations. As discussed by the authors, there were two important sources of systematic error which were not well controlled in the experiment: (1) possible nonlinearities in the detector response and (2) possible $\bar{n}$ contamination. The contributions to the systematic error in the γ/π^0 ratio from these sources were estimated to be ± 0.05 and ± 0.07, respectively; the uncertainty from the latter source was, however, not thought to be very re-

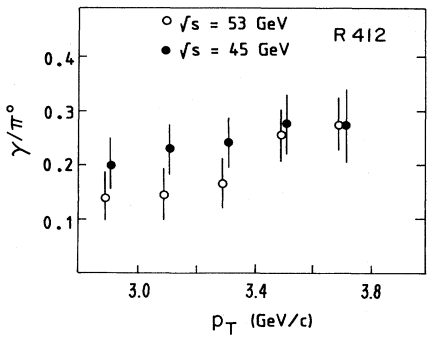

FIG. 7. The first published γ/π^0 ratio (Darriulat *et al.*, 1976), ostensibly corrected for all instrumental effects, but inconsistent with more recent measurements at the ISR.

liable. These systematic uncertainties are not shown in Fig. 7. Because of these problems, the group presented their results as only suggestive of prompt γ production.

There were two early indications of a possible direct-photon signal from experiments at Fermilab. The first of these (Donaldson *et al.*, 1976) was never published because of difficulties with background interactions from upstream of the target. The other result was presented at a conference (Cronin, 1977) by the Fermilab—Johns Hopkins group; the more recent and improved work of this collaboration will be discussed in Sec. III.C.3.

The second result reported from CERN, using essentially the same technique and similar apparatus as R412, was obtained by experiment R107 performed by a Rome, BNL, CERN group (Amaldi *et al.*, 1978) also working at the ISR. The experiment used an array of 9×15 lead glass blocks, each 10×10 cm^2 in area, to detect π^0's and η's. The detector was operated at two distances from the interaction region (4.7 and 1.47 m) so as to cover the p_T range between 2 and 5 GeV/c. To study backgrounds to the prompt γ signal, lead converters of various thicknesses were placed in front of the lead glass arrays.

For the distant configuration, data were recorded if any one of 15 nonoverlapping 3×3 subarrays of the detector contained energy above 1.25 GeV. [At 4.7 m, the minimum opening distance for π^0's is about 1.2 m/p_T (GeV/c).] In the closer configuration, data were recorded if any one of the central 15 blocks contained energy above 2.0 GeV.

A clustering algorithm was used to isolate individual showers. Only blocks with $E>50$ MeV were included in the search, and a cluster was defined whenever a set of blocks had a local energy maximum at its center. Single-photon candidates were defined as single clusters 2×2 blocks in size that did not have scintillator signals in a counter array in front of the blocks. Neutral pions were defined by two clusters with an invariant mass within an appropriate range of the π^0 mass.

The background in the γ sample from π^0's was calculated using the π^0 signal measured concurrently in the experiment. The π^0 acceptance for the two configurations differed substantially. For the nearby configuration it was typically 0.93, and for the far configuration it was 0.2. The background from η decays was calculated using their measured value for the cross section ratio η/π^0 of 0.50 ± 0.08, which is consistent with other measurements of this quantity in this p_T and energy range.

The two main sources of systematic uncertainty that limited the experiment of Darriulat *et al.* were controlled more effectively in this measurement. The blocks were calibrated individually in an electron beam and the response was corrected for an observed nonlinearity. In addition, during the running, the calibration was checked by monitoring the reconstructed π^0 mass. The latter corrections were small and only infrequently as large as 10%.

The $\bar{n}$ contribution was determined experimentally by exploiting the fact that γ's convert in thin lead plates (placed before scintillation counters in front of the lead glass arrays), while $\bar{n}$'s are hardly affected. Measurement of the nonconversion probability as a function of converter thickness was used to obtain the $\bar{n}$ contamination; this contamination was such as to increase the true γ/π^0 ratio by 0.02.

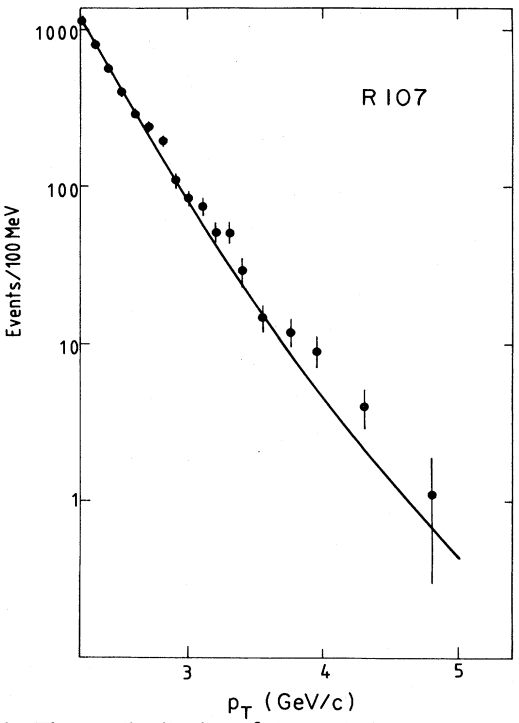

FIG. 8. The p_T distribution of detected photons, corrected for $\bar{n}$ and η contributions, compared with the prediction for the γ spectrum expected from π^0's (Amaldi *et al.*, 1978).

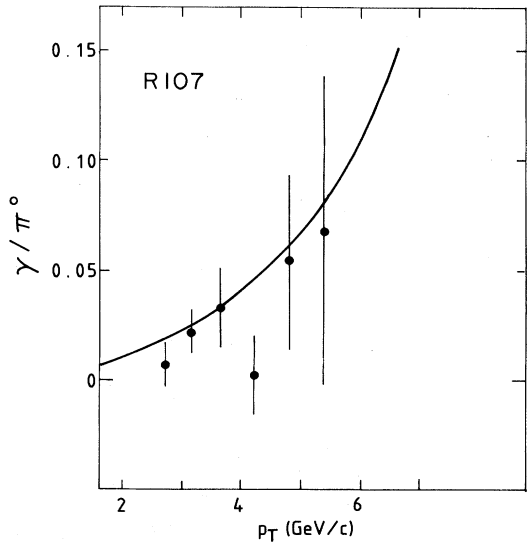

FIG. 9. The corrected γ/π^0 yield as a function of p_T for the data of Amaldi *et al.*, 1978. The error bars are statistical. The smooth curve is an early QCD calculation for the ratio (Field, 1978).

The prompt γ signal was extracted by subtracting the expected π^0, η, and $\bar{n}$ contamination from the observed single-shower data. At the 95% confidence level, the γ/π^0 ratio in the region $2.3 < p_T < 3.4$ GeV/c was found to be less than 0.027 and less than 0.023, for the near and far configurations, respectively.

Using the far configuration, the p_T range was extended to 5.7 GeV/c. Figure 8 shows the p_T distribution for detected photons (after subtracting the $\bar{n}$ and η contribution), compared with the prediction of the γ spectrum expected from π^0's. The ratio of the γ/π^0 yield, following subtraction of the π^0 background contribution, is shown in Fig. 9, where the errors are statistical. As the authors point out, bin by bin their measured γ/π^0 ratio is consistent within two statistical standard deviations with no effect whatsoever. Additional systematic uncertainties tend to weaken the experimental results further, and the authors consequently chose to present their findings in terms of conservative upper limits on the γ/π^0 production ratio.

At low p_T, using the near configuration, the principal source of systematic uncertainty was detector nonlinearity. Accounting for this uncertainty increased the upper limit on the γ/π^0 ratio from 4% to 6% in the region $2.3 < p_T < 3.4$ GeV/c. In the far configuration, the linearity error was not so important, since the detected π^0's were mostly asymmetric, with one of the photons carrying most of the energy. However, because of limited acceptance, the calculated background due to π^0 decays is larger (typically 60—90% of the detected γ signal for $p_T > 3.0$ GeV/c is from background) and presumably sensitive to systematic uncertainties in π^0 reconstruction efficiency. At larger p_T (> 5 GeV/c) the authors quoted an upper limit to the γ/π^0 ratio of 0.18.

C. More recent measurements

We next turn to a discussion of more recent experiments which have presented evidence for prompt γ production at high p_T. The experiments have been performed by

(1) an Athens-BNL-CERN group working at the CERN ISR (R806);
(2) a CERN-Columbia-Oxford-Rockefeller group working at the ISR (R108);
(3) a Fermilab—Johns Hopkins group working at Fermilab (E95);
(4) a CERN—BNL—Copenhagen—Lund—Penn—Pittsburgh—RAL—Tel Aviv—QMC group working at the CERN ISR (R807);
(5) a Fermilab—Michigan State—Minnesota—Northeastern—Rochester group working at Fermilab (E629).

Experiments 1, 3, 4, and 5 used the direct method, while experiment 2 used the conversion method. Table I summarizes the detector properties and kinematic regions covered in these experiments.

TABLE I. Properties of completed prompt-photon experiments.

Experiment	Beam	c.m. energy (GeV)	$\theta_{c.m.}$	Detector type	Number of elements	Method
R412						
Darriulat *et al.*, 1976	pp	45,53	90°	lead glass	$\sim 8\times 8$ hexagonal array	direct
R107						
Amaldi *et al.*, 1978	pp	31,53	90°	lead glass	9×5 square array	direct
R806						
Diakonou *et al.*, 1979	pp	31,45,53,63	90°	lead liquid argon	$32+64+64+10$ ϕ,u,v,θ strips	direct
R108						
Angelis *et al.*, 1980	pp	45,63	90°	lead glass	12×14 square array	conversion
E557						
Baltrusaitis *et al.*, 1980	pBe	19.4,23.7	90°—150°	lead glass	5×5 square array	direct
E629						
McLaughlin *et al.*, 1983	π^+C pC	19.4	90°	lead liquid argon	$64+112$ x,y strips	direct
R807						
Åkesson *et al.*, 1983	pp	63	11°	uranium scintillator sandwich	$24+24+24$ x,y,u strips	direct

1. The R806 experiments

The early experiments of the R806 group (Diakonou *et al.*, 1979) presented the first convincing evidence for the existence of prompt photons, and the follow-up experiments (Diakonou *et al.*, 1980b; Anassontzis *et al.*, 1982a) extended the measured range of prompt γ production to higher transverse momenta. All these experiments were performed at the ISR for pp collisions at 90°, and for p_T values up to 12 GeV/c. The major strength of these experiments was the use of a detector with very high granularity, good energy resolution, and moderate solid-angle acceptance. It was possible to detect π^0's with high efficiency and thereby achieve a correspondingly low level of background for prompt γ candidates.

The photon detector consisted of two identical lead—liquid-argon shower counters (Cobb *et al.*, 1979). A sketch of the counter geometry is given in Fig. 10. Longitudinally (along the direction of the incident γ), each device was segmented in three regions, of 2.5, 2.5, and 12.0 radiation lengths. The second layer consisted of two interleaved sets of channels that were read out independently. Transverse to the incident γ direction, the detectors had four types of strips. The first layer consisted of azimuthal ϕ strips, the second layer of U and V strips oriented at $\pm 20°$ with respect to the ϕ strips, and the last layer of polar-angle θ strips. The transverse granularity in the first two layers was 2 cm, and provided position resolution of 0.5 cm and two shower separation of 5.0 cm. The calorimeters were studied extensively in test beams, and the results compared with Monte Carlo calculations using the EGS code (Ford and Nelson, 1978). The test results were found to be in good agreement with the Monte Carlo, with the exception to be discussed below.

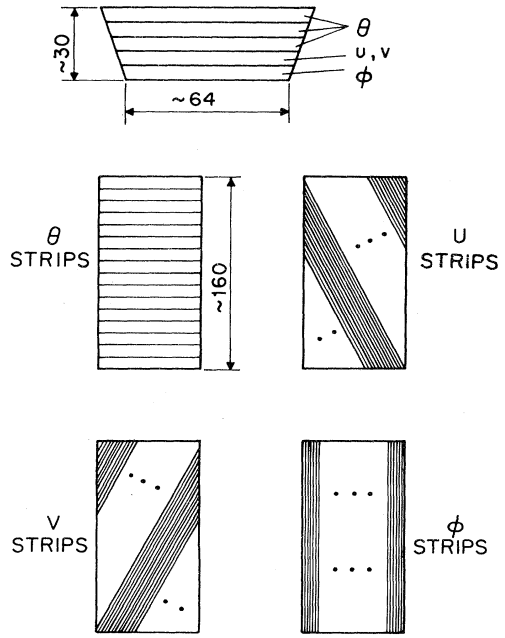

FIG. 10. Sketch of the geometry of the liquid-argon calorimeters used in R806 (Cobb *et al.*, 1979). Dimensions are given in cm. The top drawing shows a cut in the calorimeter in the plane perpendicular to the ISR beams. The layout of the strips is shown below that.

Data were recorded in three geometrical configurations: (1) Both calorimeters placed at a distance of 1.65 m from the ISR crossing, facing the c.m. motion of the ISR, but with centers of the detectors displaced by $+23.75°$ (and $-23.75°$) relative to the pp scattering plane. (2) Both calorimeters 2.15 m from the crossing, opposite to the ISR c.m. motion, and $+22.5°$ relative to the scattering plane. (3) Both calorimeters 2.15 m from the crossing, one in the scattering plane and opposite to the ISR motion, the other 31.9° below the scattering plane and also opposite to the direction of the ISR c.m. motion. Because of the different distances from the interaction point to the calorimeters, and because of the 14.5° crossing angle at the ISR, the effective solid angle (0.40, 0.17, and 0.17 sr, in configurations 1, 2, and 3, respectively) varied by more than a factor of 2 and the ability to resolve two photons varied by a factor of about 1.5 in these experiments. These differences provided important checks on possible uncertainties in the analysis.

Data were recorded when all the following conditions were satisfied: (1) A signal was detected in a set of scintillation counters around the intersection region or in counters positioned at small angles relative to the outgoing beam pipes. (2) An energy deposition was found in a localized region in U and V strips above some threshold and, for part of the running in configuration 2, an energy deposition above some threshold in the ϕ strips. (Unfortunately, because of late conversions, 12% of incident γ's deposited an insufficient amount of energy in the ϕ layer; consequently, the latter requirement produced a trigger inefficiency for γ's.) (3) The total energy deposited in the calorimeter was above a suitable threshold.

Using liquid argon as the active ionization medium provided very little variation in channel-to-channel response, and resulted in relatively stable detector performance. The overall gain of the calorimeter was established by normalizing the reconstructed π^0 mass to the accepted value of 135 MeV.

The linearity was checked in several ways. The electronics was monitored by injecting standard pulses onto the detector strips. Overall system linearity was determined using electrons of known momentum, and checked by measuring the η mass as a function of the momentum of one of the detected photons, as well as by comparing the J/ψ and Υ masses (in their e^+e^- decay modes) with expected values.

Data were analyzed first by correlating energies in the various layers to form showers. Ambiguities were resolved using both pulse-height matching in the U and V layers, and through stereoscopic reconstruction of the showers (using the ϕ, U, and V views). The two calorimeter modules were treated as independent and equivalent units.

The analysis was designed to maximize the acceptance

for π^0's while minimizing the background in the single-γ sample from π^0 decays in which one γ was lost, either because it missed the calorimeter or because it was not reconstructed as a good shower. To this end, cuts were made requiring all showers to be located within a restricted volume of the detector. Also, the longitudinal energy development was required to be consistent with that expected for electromagnetic showers. The energy in the first two layers that was not assigned to reconstructed showers had to be less than 35 MeV. Only one shower was allowed per calorimeter for γ candidates and two showers for π^0 candidates. In addition, prompt γ candidates were required to have a transverse shower size consistent with that expected for a single incident photon, and π^0's were required to have a $\gamma\gamma$ invariant mass within 45 MeV of the π^0 mass. The first criterion minimized background from events in which one photon from π^0 or η decay missed the calorimeter, while the cuts on unassigned energy and on the number of reconstructed showers reduced contributions to the single-γ sample from those asymmetric π^0 decays in which one of the photons was not reconstructed properly.

The effects of the reconstruction algorithms and of sundry analysis criteria were examined in a test beam and through Monte Carlo techniques. Monte Carlo studies were used to determine γ and π^0 reconstruction efficiencies and the probability that π^0's were detected as photons. Events were generated with the p_T spectra measured at the ISR (Kourkoumelis *et al.*, 1980b). The EGS shower generation code was used to simulate the calorimeter response. The results were found to be in good agreement with various aspects of the data, such as the π^0 mass resolution, the decay angular distribution of the photons, and the observed longitudinal shower development. As an example of the consistency, we compare in Fig. 11 a previously unpublished $\pi^0\to\gamma\gamma$ decay angular distribution for the data and the Monte Carlo calculation. Small differences observed in the transverse shower shape led to a 2% correction that was applied to the Monte Carlo efficiency.

The Monte Carlo calculation predicted a small (1%) deviation from linearity between 3 and 6 GeV/c and a slight deterioration with energy. The nonlinearity was caused by leakage of energy out of the back of the calorimeter. This leakage was compensated for (in the analysis) by just increasing the gain of the last section (θ strips) of the detector.

Using the above corrections, Kourkoumelis *et al.* (1980) found the overall efficiency for photons and π^0's to be nearly independent of momentum. For $p_T > 3.0$ GeV/c, the average efficiency was 73% for γ's and 57% for π^0's (integrated over asymmetry).

The same program that was used to calculate the γ and π^0 efficiencies was also used in determining the background expected in the prompt γ candidates from meson decays. Production ratios for π^0's, η's, $\eta'(958)$'s, and ω's were generated in the ratios of 1.0:0.55:1.0:0.9, using the same p_T dependences. For the case of the η's, this ratio was well known from a previous measurement using the same apparatus (Kourkoumelis *et al.*, 1979a). For $\eta'(958)$'s and ω's, the experimental uncertainties in the production spectra were greater (Diakonou *et al.*, 1980a), but the background contributions were smaller; the uncertainty in the production spectra contributed negligibly to the final error.

Contributions form the various sources of background are displayed in Fig. 12. The background has been expressed in terms of the individual contributions to the observed γ/π^0 ratio as a function of p_T. For example, at $p_T = 6$ GeV/c, for each detected π^0, 0.09 detected photons from π^0 decays are expected from events where one of the photons misses the calorimeter. Similarly, 0.06, 0.01, and 0.01 photons are expected from η, η', and ω decays, respectively. Finally, 0.04 detected photons from π^0 decays are expected in which both of the γ's fall within the acceptance of the detector, but of which one is not reconstructed properly.

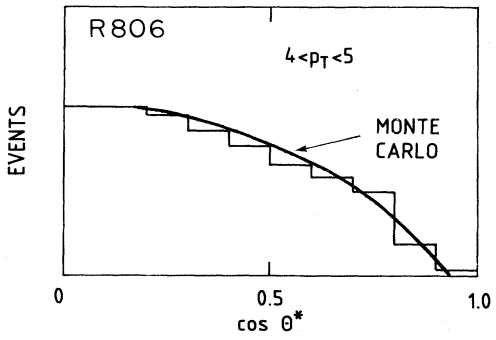

FIG. 11. A typical asymmetry distribution for π^0 decays in R806 compared to expectations of the EGS Monte Carlo.

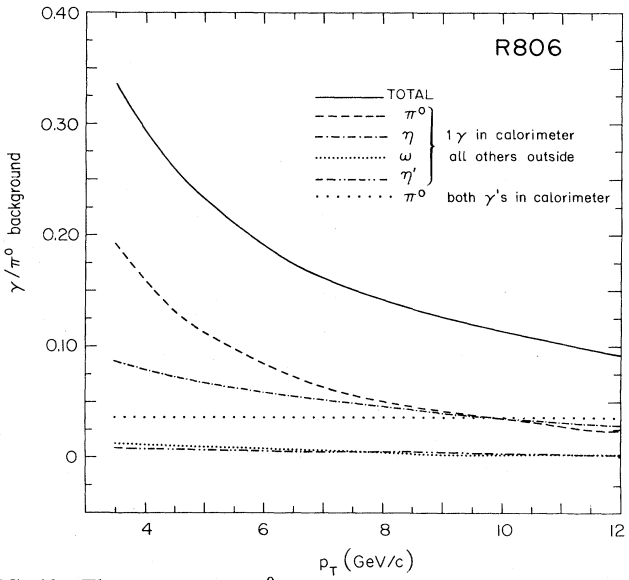

FIG. 12. The apparent γ/π^0 ratio due to known meson decays at $\sqrt{s} = 63$ GeV. The contributions of the π^0, η, η', and ω mesons are shown separately, as well as their sum, as a function of p_T (Anassontzis *et al.*, 1982).

The produced γ/π^0 ratio was determined from the following relationship:

$$\frac{\gamma}{\pi^0}=\left[\frac{N_\gamma}{N_{\pi^0}}-(R_{\pi^0}+R_\eta+R_{\eta'}+R_\omega)\right]\frac{A_{\pi^0}}{A_\gamma}\,, \qquad (12)$$

where the R_i are the Monte Carlo calculated ratios of observed background γ's to detected π^0's for each of the sources, and A_γ and A_{π^0} are products of geometric acceptance and reconstruction efficiencies for γ's and π^0's, respectively.

For $\sqrt{s}=63$ GeV, Fig. 13 shows the observed γ/π^0 ratio and the expected background as a function of p_T for the third geometrical configuration. The band on the background curve represents an estimate of the uncertainty in the calculation due to possible errors in production cross sections and other systematic uncertainties in the Monte Carlo. The inner error bars on the data represent statistical errors; the outer error bars include (in quadrature) uncertainties due to the estimated departure from linearity in the energy response of the detector. Results from all three configurations (not shown here) are consistent and provide evidence for a large direct-photon signal.

Several other sources of bias that could account for some of the signal were examined in detail. For example, the group calculated the nonlinearity needed to reproduce the entire direct-γ excess and found it incompatible with known characteristics of the detector. Data taken in special runs with no beams in the ISR essentially eliminated the possibility that cosmic-ray background was the source of the γ excess. Based on studies in a test beam, possible contamination from hadrons was calculated to be negligible. (The fact that hadrons normally deposit only a small fraction of their full energy in the calorimeter strongly suppresses this background; the measured hadron/γ rejection was greater than 250:1.) Showers caused by antinucleons were rejected, largely because their transverse sizes were incompatible with those expected for photon showers. This result was confirmed in the R807 experiment, in which only 0.1% of the identified $\bar{p}$ tracks associated with showers in the calorimeter passed the transverse shower size requirements used in the γ analysis.

Additional information from experiment R807, which followed R806 and had much enhanced charged particle detection capability, confirmed the hadron test beam results quoted above. Studies of charged particles reconstructed in a drift chamber and associated with showers in the calorimeter indicated that 0.6% of γ's from π^0 decays had tracks associated with them, and that 1.8% of all γ candidates had charged tracks pointing to the showers. These results are consistent with the known photon conversion probability in the beam pipe and with an essentially negligible (1.2%) hadron contamination. From all available information, the group estimated a hadron contamination contribution of less than 0.02 to the γ/π^0 ratio.

After correction for backgrounds and for relative γ/π^0 reconstruction efficiencies, γ/π^0 production ratios were calculated. These are shown in Figs. 14—16 for the three

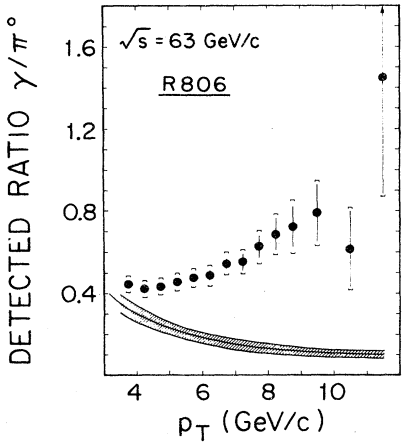

FIG. 13. Observed ratio of γ/π^0 at $\sqrt{s}=63$ GeV. Inner error bars are statistical. The outer errors include possible systematic effects due to calorimeter nonlinearity. The solid curve shows the Monte Carlo prediction for the ratio assuming no direct γ production. The shaded area indicates the one-standard-deviation systematic errors on the Monte Carlo simulation. Results are for data obtained with the third arrangement (Anassontzis *et al.*, 1982).

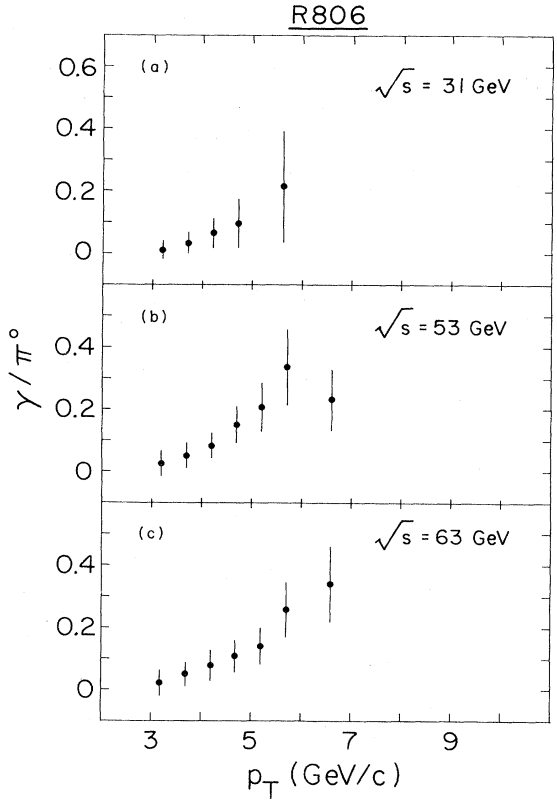

FIG. 14. The γ/π^0 ratio after background subtraction and correction for relative efficiencies for data from the first geometrical configuration for (a) $\sqrt{s}=31$ GeV, (b) $\sqrt{s}=53$ GeV, and (c) $\sqrt{s}=63$ GeV (Anassontzis *et al.*, 1982).

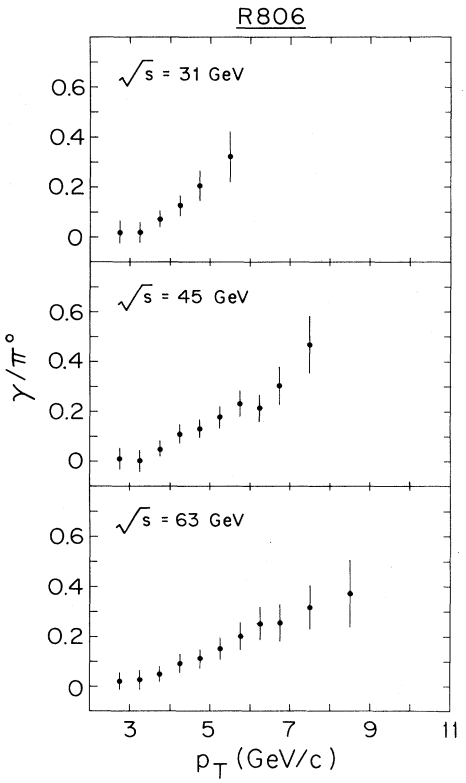

FIG. 15. The γ/π^0 corrected ratio obtained for the second geometrical configuration for (a) $\sqrt{s}=31$ GeV, (b) $\sqrt{s}=45$ GeV, and (c) $\sqrt{s}=63$ GeV (Anassontzis *et al.*, 1982).

geometrical configurations for $\sqrt{s}$ between 31 and 63 GeV. For the third geometrical configuration we compare the data with a sample calculation (Contogouris *et al.*, 1982) for the γ/π^0 ratio for different choices of gluon structure function, with and without higher-order soft-gluon corrections. Fits of similar quality, using somewhat different assumptions, have been obtained by others (Baier *et al.*, 1980; Cormell and Owens, 1980; Dechantsreiter *et al.*, 1981; Horgan and Sharbach, 1981).

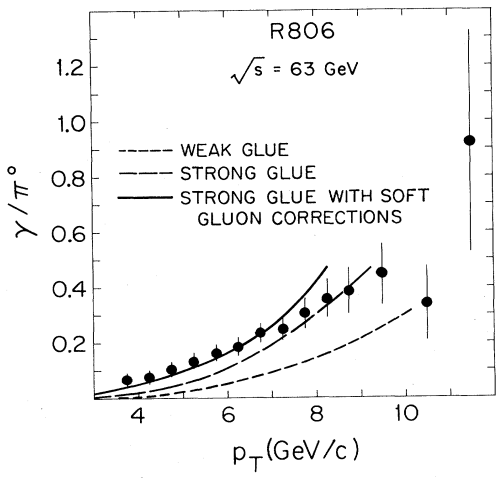

FIG. 16. The γ/π^0 corrected ratio obtained for the third geometrical configuration for $\sqrt{s}=63$ GeV (Anassontzis *et al.*, 1982). The curves are fits for different assumptions concerning the gluon structure functions and soft-gluon corrections (Contogouris *et al.*, 1982).

The group has pointed out that the ratio extracted in this manner is not a completely inclusive measurement because of the requirements on remnant energy and on the number of γ showers in the same calorimeter. Although similar criteria were applied to π^0 data, differences in production mechanisms could affect the extracted γ/π^0 ratio. In particular, because the diagrams expected to contribute to the γ signal predict fewer same-side associated particles than for π^0 events, the effect of the above restrictions would be to increase the observed γ/π^0 production ratio. As we discuss below, such correlations have, in fact, been observed in the data. However, because of the relatively small acceptance of the detectors, and the fact that minimum ionizing particles accompanying the electromagnetic showers did not always deposit sufficient energy to be detected in the calorimeters, this

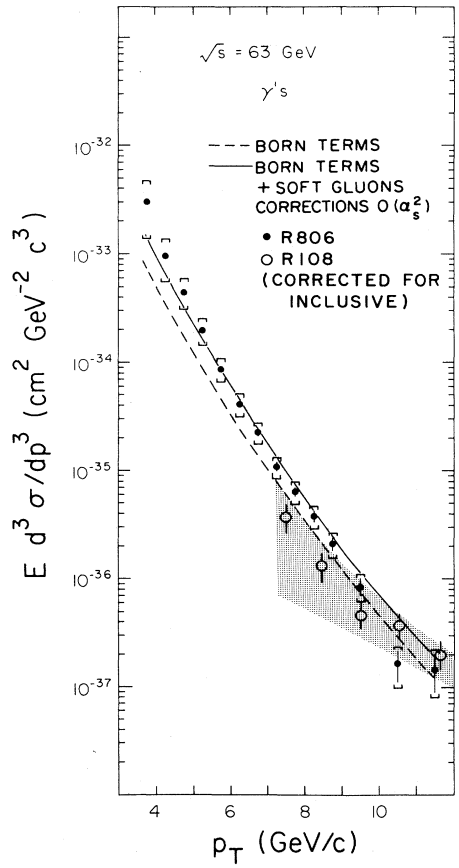

FIG. 17. The invariant inclusive cross section for direct-photon production in pp collisions at $\sqrt{s}=63$ GeV near 90° in the center of mass (Anassontzis *et al.*, 1982). The curves correspond to a hard-gluon structure function for the proton, calculated with and without soft-gluon corrections (Contogouris *et al.*, 1982). The additional data at larger p_T are from R108; the shaded region corresponds to the range of systematic uncertainty in the R108 data (Angelis *et al.*, 1980).

bias in the γ/π ratio was small; the group originally estimated a correction factor of 0.85 ± 0.15 to the observed γ/π^0 ratio to transform it to an inclusive measurement. Although the size of this correction appears reasonable, it was never fully explained in the published work of R806.

Utilizing information from experiment R807, the group refined the analysis and extracted the inclusive cross section for prompt γ production. From the observed density of charged particles near γ and π^0 triggers, and through an explicit measurement of the probability that a charged particle deposits sufficient energy in the detector to cause the event to be rejected, the loss of events due to the cuts on unassigned energy and on extra showers was determined to be about 25% (for both γ's and π^0s). The corrected invariant cross section for direct-photon production at $\sqrt{s}=63$ GeV is shown in Fig. 17. The curves represent phenomenological calculations which we will discuss in Sec. V. Also, for comparison, we show in Fig. 17 several data points from R108 (see next section).

2. The R108 experiment

Another experiment that provided convincing evidence for prompt γ's at high p_T was executed at the ISR using the conversion technique. The apparatus is shown in Fig. 18 (Angelis *et al.*, 1980). It consisted of two identical 12×14 arrays of lead glass blocks (each 15×15 cm^2 in transverse size) located at 1.1 m from the intersection region. Because of the center of mass motion of the colliding beams, each of the arrays covered different solid angles; one had $\Delta\Omega=0.87$ sr and the other 1.42 sr. The arrays were located outside a superconducting solenoid containing drift chambers and a scintillator hodoscope (the A counter). Two hodoscopes of 12 counters each (the B counters) were located outside the coil. The coil and cryostat corresponded to 1.0 radiation lengths of material, which served as the γ converter in the experiment.

Data were recorded whenever the total signal in either lead glass array was above some threshold and when at least one A counter had a signal. In the off-line analysis it was required that an interaction vertex had at least two reconstructed tracks, and that four A counters had signals. These criteria were effective in rejecting cosmic-ray events and beam-gas interactions. Clusters were defined as localized and isolated depositions of energy in 3×3 matrices of blocks; using this definition, π^0's with momenta above 3 GeV/c appeared as localized single clusters, as did (with varying efficiencies) other multiphoton decays of neutral mesons [η's, $\eta'(958)$'s, ω's, etc.]. A cluster was rejected from consideration as a neutral particle candidate if a reconstructed charged particle pointed to within 30 cm of that cluster. (The tracking efficiency was $\sim85\%$.) Various checks were made on the dependence of the efficiency of these selection criteria on p_T; little or no variation was observed. In addition, differences in response between the two arrays were compatible with expectations from just the difference in the solid angle they subtended in the center of mass.

Conversions in the coil were defined by the presence of signals in one of the two B counters nearest the candidate shower that had a pulse height corresponding to at least 1.5 times the value expected for a minimal ionizing particle. To reduce confusion from the presence of other particles, events with additional neutral clusters in the region that overlapped the two appropriate B counters, or with tracks in the drift chamber that pointed to these counters, were rejected. This eliminated 40% of the events. Data were collected at $\sqrt{s}=62.4$ GeV with an integrated luminosity of 7.6×10^{37} cm^{-2}.

Applying the above criteria, the observed nonconversion probability for the experiment as a function of p_T is plotted in Fig. 19. Also shown is the expected nonconversion fraction for a source consisting entirely of single γ's, and for sources without prompt γ's. The nonconversion probability per γ can be written as follows:

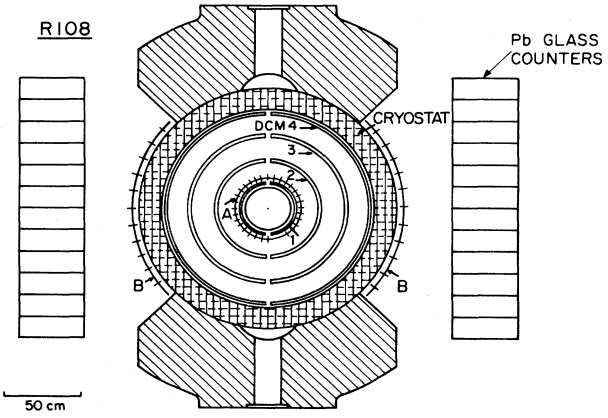

FIG. 18. A view of the R108 apparatus normal to the beams (Angelis *et al.*, 1980).

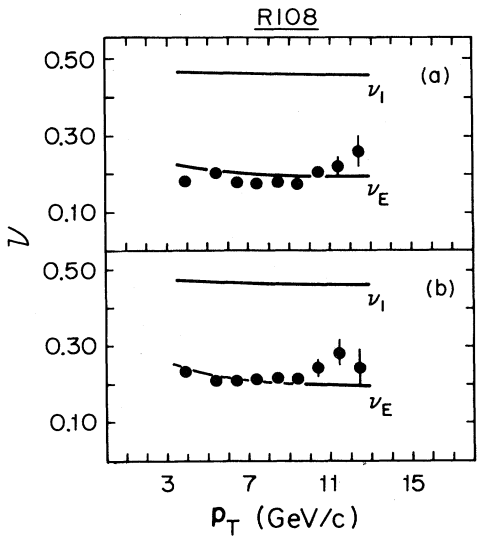

FIG. 19. Nonconversion fraction as a function of p_T for those events with no overlap in the B counters; (a) for the outside array, (b) for the inside array (Angelis *et al.*, 1980).

$$\nu=\exp[-\tfrac{7}{9}(t/x_0)(1-\xi)]\ , \tag{13}$$

where t is the converter thickness, x_0 is the radiation length of the material, and ξ is a small energy-dependent correction factor which was mentioned earlier in this section. The nonconversion probability for events without prompt γ's was calculated using a Monte Carlo program that averaged contributions from π^0's, η's, $\eta'(958)$'s, ω's, and K_s^0 decaying into all-neutral final states. Previously published particle-production ratios at the ISR were used as input to the Monte Carlo; these ratios were assumed to be independent of p_T.

The contribution to the nonconversion probability due to overlapping showers, such as two π^0's in the same cluster, was calculated using the measured probability of observing a charged particle near a high-p_T shower. The overlap probability was found to be small, typically, between 0.5% and 1.5%. It is not clear, however, whether the charged/neutral correlations are the same as correlations among only neutral particles. We shall return to this point later when we compare the various experiments.

As seen in Fig. 19, the measured nonconversion probability at low p_T lies below the level expected if there were no prompt γ's. As mentioned in the beginning of this section, this could be due to an error in the calculation of the absolute converter thickness, or due to a miscalculation of the energy loss in the converter. The discrepancy could also be due to additional sources with very high conversion probability that were not taken explicitly into account in the Monte Carlo. Because the measured nonconversion probability fell outside the allowed range, more input was required before any conclusions could be reached. The group used the measurements of the γ/π^0 ratio from Amaldi *et al.* (1979a) ($\gamma/\pi^0=0.021\pm0.012$ for $3.5<p_T<5.0$ GeV/c) to normalize their results at 4 GeV/c. After this adjustment of ν, f_γ [see Eq. (11)] was extracted for $p_T>5$ GeV/c. The results obtained for the two arrays of lead glass were consistent; the data were therefore combined and are given in Fig. 20. The results of R108 for $\sqrt{s}=44.8$ GeV (Angelis *et al.*, 1981) are also shown in Fig. 20. Only statistical errors are given in the figure; an additional total uncertainty of ±0.053 on f_γ was quoted because of systematic uncertainties in (1) corrections to the energy loss in the converter (0.028), (2) meson decays with more than two photons in the final state and possible overlap problems (0.037), and (3) the statistical uncertainty in the normalization at low p_T (0.026). The inclusive γ cross section at $\sqrt{s}=63$ GeV was obtained by multiplying the extracted value of f_γ by the inclusive neutral cross section (Angelis *et al.*, 1978). The result is shown in Fig. 21. A correction to the inclusive ratio f_γ had to be made to account for the requirement that no additional particles or clusters overlap with the B counters in the region of the detected shower. Assuming that direct photons are produced unaccompanied by same-side jet fragments, this correction was estimated (Angelis *et al.*, 1980) to be a factor of 0.8. Although this factor may overcorrect somewhat the value of f_γ, we have included it in the results shown in Fig. 21.

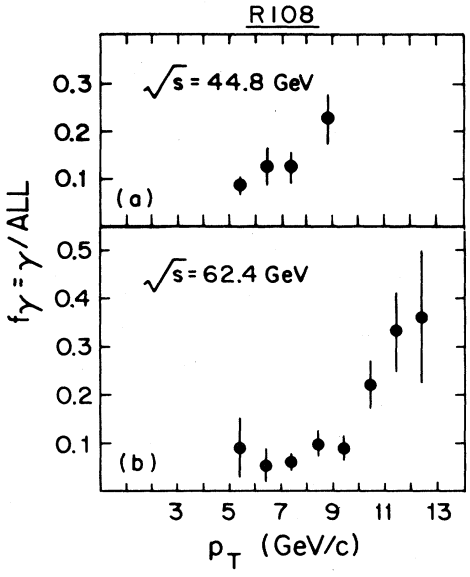

FIG. 20. The fraction of clusters attributed to direct single-photon production as a function of p_T. In addition to the errors shown, there is an overall additive systematic uncertainty of ±0.053, by which all the points may be adjusted together (Angelis *et al.*, 1981).

Also shown in Fig. 21 are two recent calculations for the direct photon yield (Duke and Owens, 1983). These will be discussed in Sec. V.

3. The E95 experiment

We next discuss the Fermilab—Johns Hopkins experiment (E95) that measured $p\text{Be}\rightarrow\gamma+x$ at $\sqrt{s}=19.4$ and

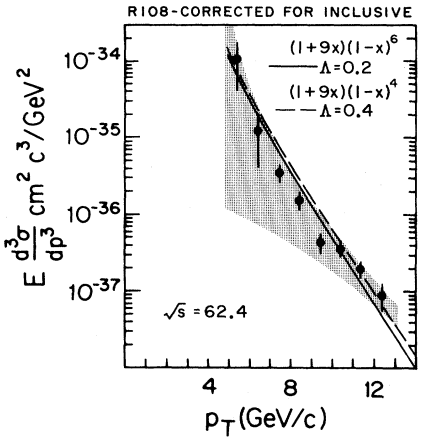

FIG. 21. Inclusive invariant cross section attributed to direct single-photon production at $\sqrt{s}=63$ GeV. The errors shown are statistical. The shaded region corresponds to smoothed limits showing the effect on the data of the ±0.05 systematic uncertainty in f_γ (Angelis *et al.*, 1980). The curves are recent calculations showing how a change in the input gluon structure function can be compensated by a change in the Λ parameter of QCD (Duke and Owens, 1983).

23.8 GeV in the p_T range $1.5 < p_T < 4.0$ GeV/c and for $-1.74 < y < 0.0$ (Baltrusaitis *et al.*, 1979).[10]

The apparatus consisted of a two-arm spectrometer with 5×5 arrays of lead glass blocks, each 6.3×6.3 cm^2 in area (Baltrusaitis *et al.*, 1980). Data were recorded whenever the signal in one of the lead glass arrays exceeded some threshold and there were no signals in lucite hodoscopes upstream of thin lead converters located in front of the arrays. The analysis of the data was similar to that described for the early ISR experiments in Sec. III.B. The expected single-γ background from π^0's and other mesons was normalized to the observed π^0 rate as determined from the reconstructed π^0 spectrum. Because of the small number of lead glass blocks in this experiment, the backgrounds were rather large. Backgrounds expected from η's and $\eta'(958)$'s were calculated using a Monte Carlo technique. Background from neutral hadrons was measured by inserting 11.3 radiation lengths of lead converter in front of the sweeping magnet; this removed any γ's that were in the beam and attenuated neutral hadrons by 31%. From events selected using this configuration, it was found that hadrons generated background events at a level of 10—30% of the observed direct-γ signal (worst at largest p_T).

Figure 22 shows the observed single-γ rate compared with various sources of background as calculated in the Monte Carlo. It is clear that an excess of γ's is observed over a p_T range of $2.6 < p_T < 3.7$ GeV/c. Figure 23 shows the ratio of cross sections for γ/π^0 as a function of p_T, corrected for backgrounds, reconstruction efficiencies, and acceptances.

Because of the small signal/background ratio in these data, particular care was required in sorting out possible systematic problems. The authors have considered a range of backgrounds and biases in their experiment, including errors stemming from losses due to photon conversions in the spectrometer, uncertainties in the calculated reconstruction efficiencies, and possible errors in the π^0 differential cross section and in the η/π^0 ratio used in the Monte Carlo. The total systematic error determined by adding the above uncertainties in quadrature is shown as the shaded band in Fig. 23.

A feature of this experiment was the ability to measure the γ and the π^0 yield over a relatively wide range of Feynman x values. Figure 24 shows the dependence of the γ/π^0 ratio on x_F. Although the systematic errors are large, there is some indication that the γ/π^0 ratio increases for large x_F in the backward hemisphere of the center of mass.

4. The E629 experiment

Another experiment to measure prompt photon production at Fermilab in pC collisions was performed at

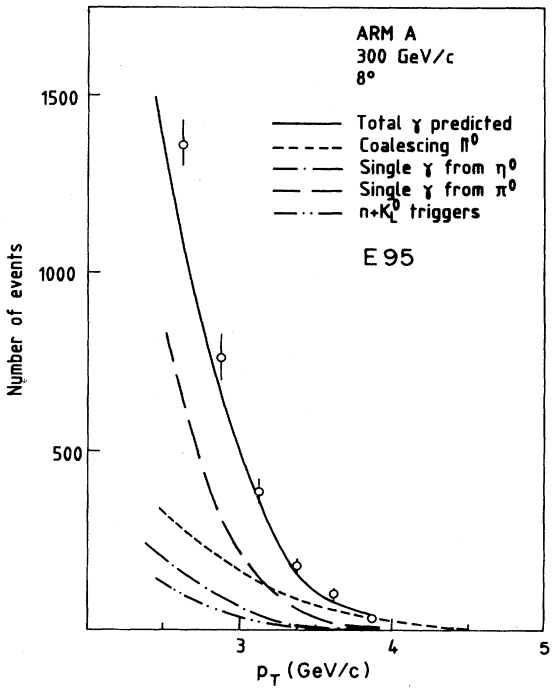

FIG. 22. Observed single-photonlike spectra for pBe collisions at 300 GeV, taken with a spectrometer at 8° in the laboratory. Also shown are the various components of the predicted background spectrum (Baltrusaitis *et al.*, 1979).

$\sqrt{s} = 19.4$ GeV by the Fermilab—Michigan State—Minnesota—Northeastern—Rochester group (E629). Although the experiment was only a test for a future experiment, a significant signal was seen for pC interactions, and an indication for a comparable signal in π^+C interactions was also found (McLaughlin *et al.*, 1983).

The experiment used a lead—liquid-argon calorimeter of fine transverse segmentation to detect the γ's and π^0's (Nelson *et al.*, 1983). It was situated at 100 mr relative

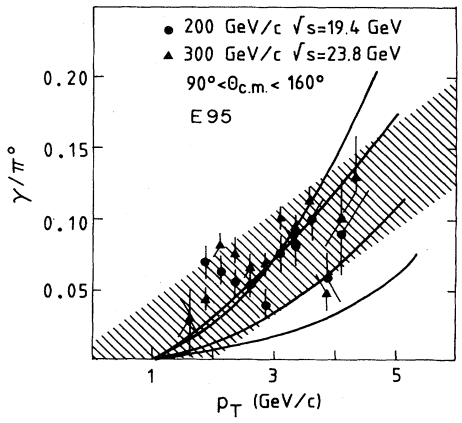

FIG. 23. The γ/π^0 ratio as a function of p_T for pBe collisions at 200 and 300 GeV/c. The shaded bands indicate the magnitude of the systematic error. The curves shown are various QCD predictions (Baltrusaitis *et al.*, 1979).

[10]Data on γ/π^0 at $\sqrt{s} = 27.4$ GeV were presented earlier by this group. [See the review of Cronin (1977).] Those results are consistent with the improved measurements to be discussed here.

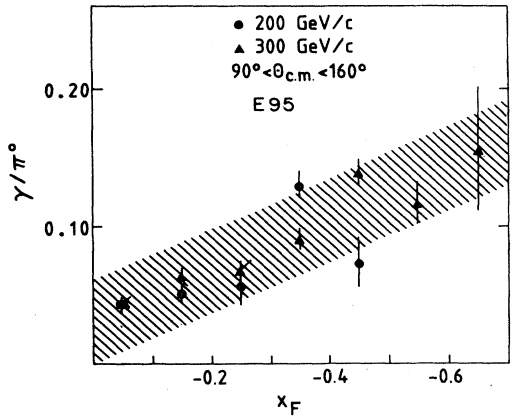

FIG. 24. The γ/π^0 ratio as a function of x_F for pBe collisions at 200 and 300 GeV/c. The shaded bands indicate the magnitude of the systematic uncertainty (Baltrusaitis *et al.*, 1979).

to the beam at a distance of 8 m from the target; it subtended ~ 0.8 sr in the center of mass, centered at a c.m. production angle of 90°. The transverse segmentation was in strips of x and y orientation with 1.27-cm pitch.

Data were collected whenever the total transverse momentum in the detector exceeded a threshold of 2.3—3.0 GeV/c (depending on position in the detector) and when any set of three adjacent strips had a signal corresponding to more than 0.6 GeV/c. The analysis in many respects was similar to that of experiment R806. Cuts were made on longitudinal energy deposition, on the timing of the calorimeter signal with respect to the interaction time, and on the direction of the shower as determined from signals in the front and back of the detector. The experiment was unique in that no requirements were imposed on energy accompanying reconstructed showers in the calorimeter, or on the number of showers per event. Consequently, the measurement was truly inclusive. Prompt γ candidates were defined as showers which, when paired with all other detected showers, were inconsistent with originating from either π^0 or η decays; corrections were made for the loss of events due to accidental matches falling within the π^0 or η mass region.

Background from meson decays was calculated using a Monte Carlo program which incorporated the rate for π^0 and η production measured in the same experiment. Various aspects of the observed π^0 signal were well reproduced by the Monte Carlo calculation; in particular, the distribution in the asymmetry parameter, important for verifying the contribution of π^0 background in the γ sample was well reproduced. The asymmetry distributions for π^0 and η events are shown in Fig. 25.

In Fig. 26 we show the γ/π^0 ratio, corrected for relative reconstruction efficiencies of γ's and π^0's; the background expected from all sources is given by the shaded band in the figure. A clear excess is observed in the pC data for $p_T > 2.5$ GeV/c; a similar excess is observed for π^+C collisions, although the statistical significance in any one bin is marginal.

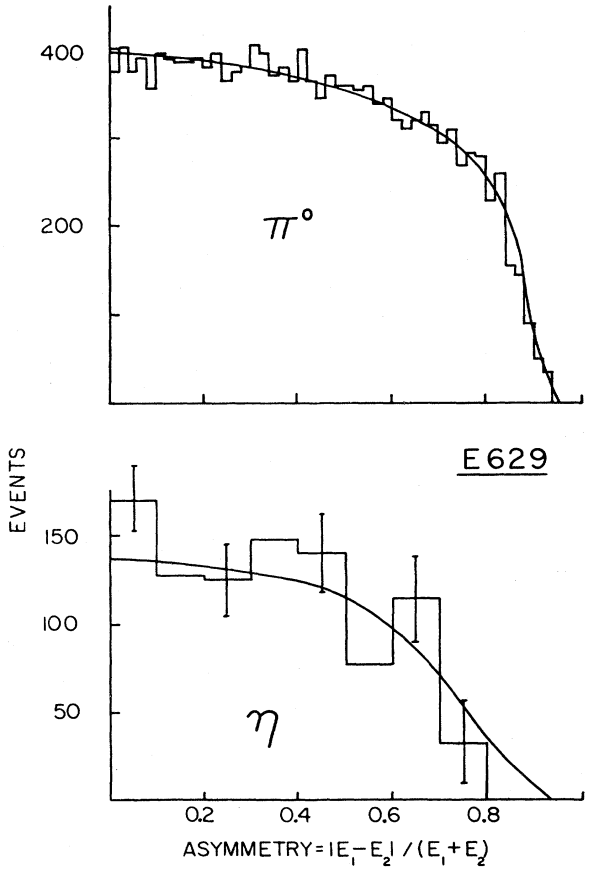

FIG. 25. Asymmetry decay distributions for π^0's and η's in E629 compared to predictions from the Monte Carlo (McLaughlin *et al.*, 1983).

5. The R807 experiment

Finally, we discuss a recent result on production of γ's and π^0's at small angles at the ISR (Åkesson *et al.*, 1983b). The experiment was intended to test the prediction of certain models that γ production at small scatter-

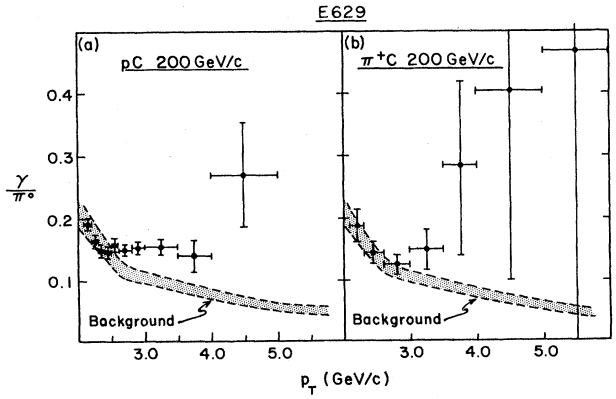

FIG. 26. Acceptance corrected γ/π^0 inclusive ratio in pC and π^+C collisions at 200 GeV/c. The expected background to the direct-photon signal is indicated by the shaded band (McLaughlin *et al.*, 1983).

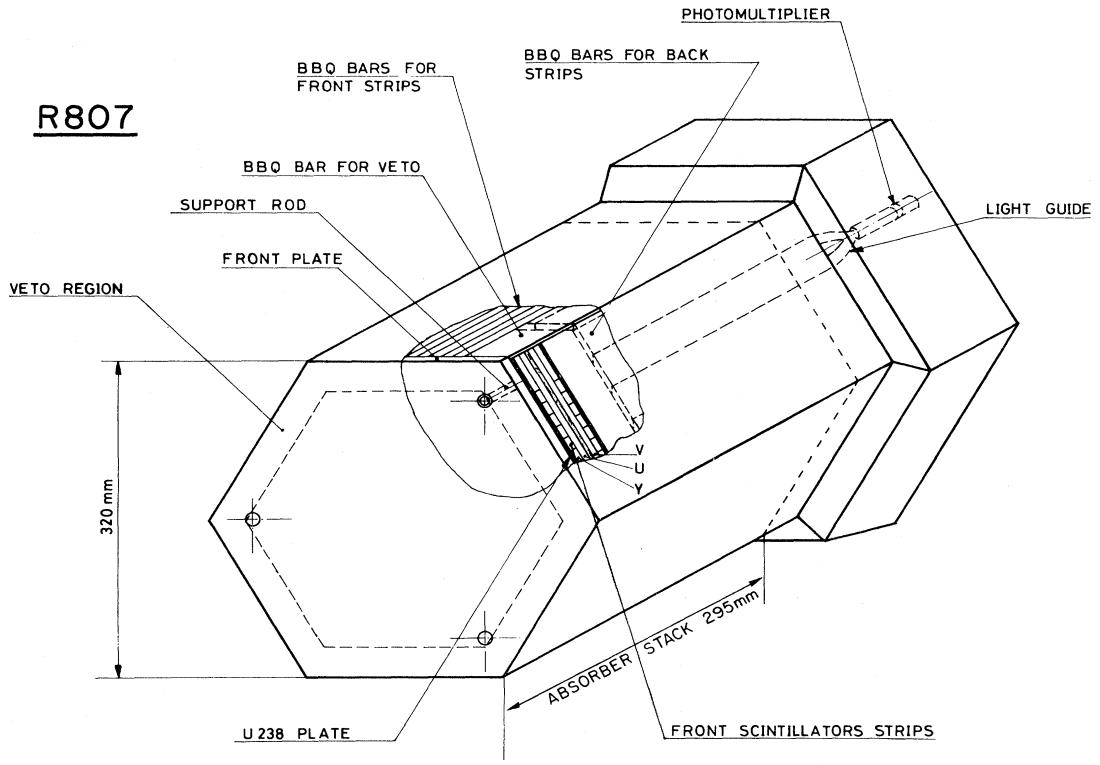

FIG. 27. Schematic of the hexagon detector used in R807 (Åkesson *et al.*, 1983b).

ing angles may be enhanced because of contributions from bremsstrahlung and higher twist effects.

The detector is shown in Fig. 27. It was centered at a production angle of 11° in the center of mass and subtended a solid angle of 25 msr. The rapidity range was $2.00 < y < 2.75$, and the useful p_T interval extended over the range $1.5 < p_T < 4.5$ GeV/c. The detector consisted of a uranium-scintillator sandwich separated longitudinally into two layers. The front section (6.5 radiation lengths) was divided into 24 strips, each 1 cm wide; the transverse segmentation of the back section (13 radiation lengths) was in 3-cm strips. In each section, three sets of strips were interleaved at 60° with respect to each other to provide stereoscopic reconstruction of the showers. In addition, a 3.5-cm-wide border at the perimeter of the front section was used as a veto region to minimize background from π^0 and η decays in which only one of the photons was contained within the fiducial region.

Data were recorded when the transverse energy in the calorimeter was above a given threshold and there was either a signal in a hodoscope of counters around the intersection region or in a hodoscope surrounding the outgoing beam pipe. The data sample was for an integrated luminosity of 7.1×10^{35} cm^{-2} at $\sqrt{s} = 63$ GeV.

Channel-to-channel response of the detector was measured in a test beam with electrons and monitored with a light flasher system. The absolute energy scale was set by monitoring the π^0 mass, and was known to $\pm 3\%$. Strips with energy above a threshold of 25 MeV were used in the analysis, which was very similar to that of experiment R806. Clusters were formed by correlating the detected signals in each of the three interleaved views, using both stereoscopic reconstruction and pulse-height matching. Analysis cuts were also similar to those of experiment R806; in particular, any excess energy not assigned to showers was restricted to be less than 400 MeV for the front section and less than 800 MeV for the back section of the detector; only single- or two-shower events were used; and all showers were required to be within a fiducial region excluding the perimeter of the detector.

The acceptance, reconstruction efficiency, and meson background to the direct-γ signal were calculated via a Monte Carlo program using the EGS code. The dependence of the γ and π^0 yields on both p_T and y were taken into account in the calculation. The η/π^0 ratio was measured in the same experiment; other mesons were assumed to be produced relative to π^0's at the same rate as observed at 90°.

Figure 28 shows the detected ratio of γ/π^0, along with the sources of background expected from meson decays. An excess is observed for $p_T > 2.0$ GeV/c. The calculated curves show, separately, background from different meson decays; the shaded region shows the sum of all contributions, and the width of the band indicates the systematic uncertainty of the prediction.

In addition to meson-induced backgrounds, possible backgrounds due to charged or neutral hadrons simulating γ's, cosmic-ray—induced events, and beam-

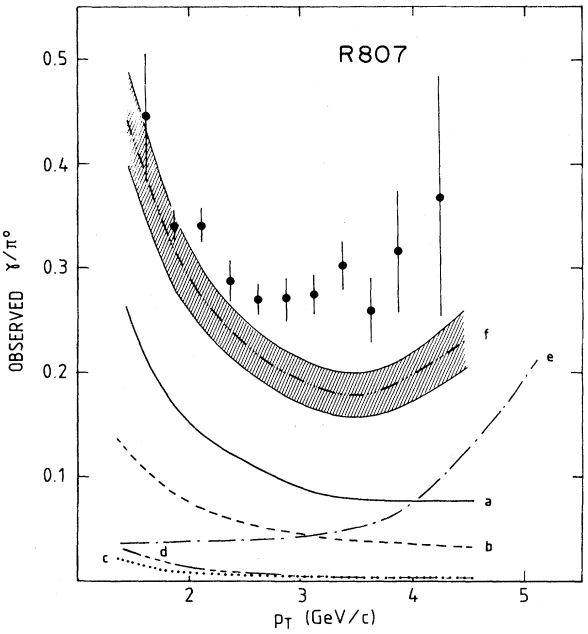

FIG. 28. The detected γ/π^0 ratio and the expected sources of background for production at 11° in the ISR at $\sqrt{s}=63$ GeV (Åkesson *et al.*, 1983b).

gas—induced events were considered. All were found to be negligible. Finally, the detector nonlinearity ($<1\%$ at 20 GeV) was measured and corrected using a light flasher system.

Figure 29 shows the γ/π^0 production ratio as a function of p_T, after subtraction of background and correction for reconstruction efficiencies and acceptances. As in most other experiments, the ratio presented is not truly inclusive because of the requirements on the unassigned energy and accompanying reconstructed showers. However, the criteria used in the analysis permitted several accompanying minimum ionizing particles to traverse the detector; the correction needed to make the ratio inclusive is therefore not expected to be large. In fact, the effect of the restriction on the number of showers and on the unassigned energy was shown to change the *absolute* π^0 production cross section by only 25%. The curve in Fig. 29 is a QCD prediction for the inclusive γ/π^0 ratio (Benary *et al.*, 1983).

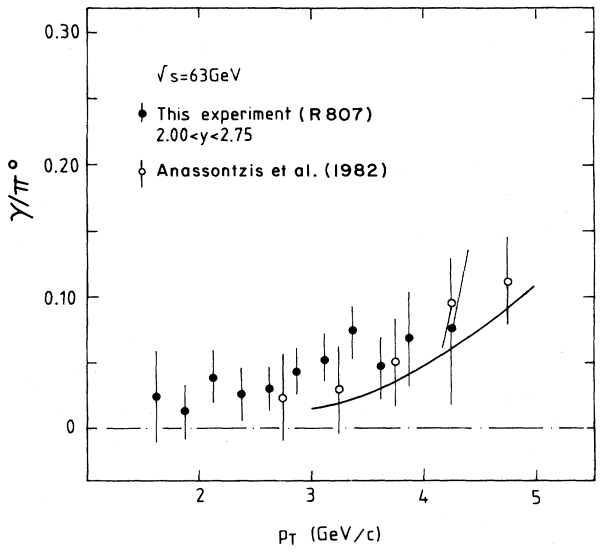

FIG. 29. The γ/π^0 production ratio as a function of p_T after all corrections. The data are for 11° at $\sqrt{s}=63$ GeV (Åkesson *et al.*, 1983b). The calculated curve is from Benary *et al.*, 1983.

D. Comparison of results

We next turn to a comparison of the experiments. As mentioned earlier, the first measurements were rather qualitative. Of the more recent experiments on prompt γ production, the R806 and R108 efforts cover a comparable energy and p_T range. Although the results can be considered in qualitative agreement, at least in the sense that a substantial prompt γ signal is observed, the numerical measurements are not completely compatible. It is useful therefore to examine possible causes of discrepancy.

We first note that R108 measured the ratio of γ's to all neutral clusters that satisfied their selection criteria, whereas R806 measured γ/π^0. To compare analogous results, the data of R108 can be corrected for contributions from meson decays and background from neutral hadrons. This correction factor depends on p_T, because the yields change with p_T, as do the probabilities that any given meson will produce a single isolated shower. In Fig. 30 we show the R806 and R108 data superimposed after multiplying the R108 data by the appropriate factor, which is approximately 1.6 for this p_T range.[11] The error bars shown have the statistical and systematic uncertainties added in quadrature. We see that for $p_T<10$ GeV/c, the two sets of data disagree by about a factor of 2; nevertheless, considering the size of the error bars, the discrepancy cannot be regarded as very significant.

Although the discrepancy is not very serious, it is useful to try to identify difficulties that could contribute to this disagreement. Three points are worth discussing. First, in order to account for their "unphysical" value of the measured nonconversion fraction, and to minimize sensitivity to the absolute conversion probability, R108 normalized their result to the γ/π^0 measurement of 0.02 ± 0.01 of Amaldi *et al.* (1979a), at $\sqrt{s}=53$ GeV. The most recent value of γ/π^0 from R806 at $p_T=4$ GeV/c is 0.07 ± 0.03. We infer from Eq. (12) that by renormalizing to a γ/π^0 ratio of 0.07, the additive change in γ/π^0 would be 0.05, and the upward change in γ/all would be 0.032. While this change is within the systematic errors quoted by R108, this choice of normalization im-

[11]We thank M. Tannenbaum for providing the p_T dependence of the correction.

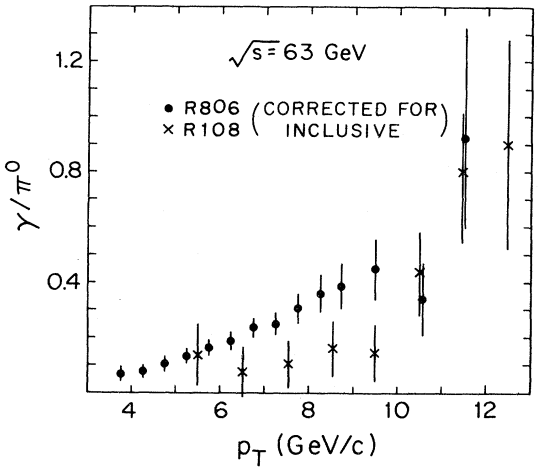

FIG. 30. A comparison of the γ/π^0 production ratios as a function of p_T for R108 and R806 data. Data have been corrected to provide inclusive yields. The error bars have systematic and statistical uncertainties added in quadrature.

proves the agreement between the two data sets.

The second possible source of discrepancy is due to the fact that neither measurement is inclusive. However, this correction was small and similar in both experiments. In fact, the trigger biases in the two experiments, and the solid angles over which the accompanying particles affected γ detection were comparable in R108 and R806; consequently, it is not likely that any differences in this small correction could account for the observed discrepancy.

Finally, the fact that the experiments normalized their direct γ results to different quantities could possibly cause some difference. The R806 measurement is inherently cleaner in the sense that the prompt γ signal is normalized to a well-defined and measured π^0 yield. In R108 normalization is to a mixture of meson decays and neutral hadron background contributions. Substantial systematic uncertainties were attributed to assumptions in R108 concerning cross sections for meson production used in the Monte Carlo simulation. However, it is difficult to estimate the effect of jet structure on the observed shower conversion probability. One point in particular deserves further mention. The effect of having overlapping particles coalesce to single showers was estimated from the data by observing the correlation between *charged* tracks and a *trigger* particle. However, because neutral particles contribute to the trigger energy, more neutral than charged overlaps could be expected. It is difficult to precisely determine the effect of this trigger bias on the overlap correction (it would, of course, be expected to be largest at high momentum); any such additional background from multipion events, if not taken into account, would decrease the γ/π^0 ratio in R108 because of the larger conversion probabilities involved. The correction factor is clearly sensitive to details of jet fragmentation. Again, it seems unlikely that this possible bias would alleviate the discrepancy between R108 and R806, because no discrepancy exists at highest p_T, and the $\sqrt{s}=45$ GeV data from R108 appear consistent with the R806 measurements.

In addition to the normalized photon yields, both groups have extracted a production cross section for direct γ's from their data. As discussed earlier, the R806 data shown in Fig. 17 have been corrected so that the distribution corresponds to an inclusive measurement. We have already adjusted the R108 measurements shown in Fig. 21, using the estimated correction that we mentioned at the end of Sec. III.C.2 (corresponds to a decrease of 20% in the γ cross section). Within the substantial systematic errors (see Fig. 21), the agreement between the experiments is surprisingly good. Renormalizing the R108 data to the measurement of γ/π^0 by R806 at low p_T would raise the cross section presented by R108 by about 50% at low p_T and by $\sim 10\%$ at largest p_T values. Uncertainties in just the absolute energy scale (5% for R108 and 2% for R806) correspond to shifts in relative cross sections of order 50% and 20% for the two experiments at $p_T=8$ GeV/c.

Because of the systematic uncertainties discussed above, we conclude that the results of R108 and R806 cannot be regarded as inconsistent with one another. There is no question that both groups have observed clear signals for the production of direct photons. The R806 data have more checks and appear to be less subject to uncertainties in normalization.

Of the other recent experiments, those of E95 and E629 at Fermilab also cover comparable kinematic regions, although the center-of-mass rapidity coverage of E95 is somewhat larger. For p_T greater than 2.5 GeV/c, the experiments are essentially in agreement. However, for smaller values of p_T, E629 finds an upper limit of $\gamma/\pi^0<0.02$, well below that of E95. The latter result is in better agreement with recent ISR measurements, at somewhat larger center-of-mass energy. Given the small value of the signal-to-noise ratio in the E95 experiment, we tend to consider the later work of E629 to be more reliable. Although it is difficult to identify any clear source for this minor discrepancy, a possibility is that, unlike the E629 data, the E95 results are not fully inclusive.

Information on the dependence of the direct-photon yield on Feynman-x is very sparse. The results of Fig. 29 compare data from R807 at large rapidities (x_F from ~ 0.2 to ~ 0.4) to data from R806 at $\theta_{\text{c.m.}}=90°$; these exhibit no dependence of the γ/π^0 ratio on x_F. This is somewhat contradictory to the data of E95 (Fig. 24). However, it should be recalled that the E95 measurements were on a beryllium target and, of course, the ISR and Fermilab experiments were performed at different energies.

Finally, there have been several recent attempts to determine the scaling behavior of inclusive photon production with energy (Anassontzis *et al.*, 1982b; Burkert, 1983; Huston, 1983). In Fig. 31 we show a fit to the results of E629 and R806 in terms of the functional form $E\,d\sigma/d^3p=C(1-x_T)^N p_T^{-M}$, where C is a normalization

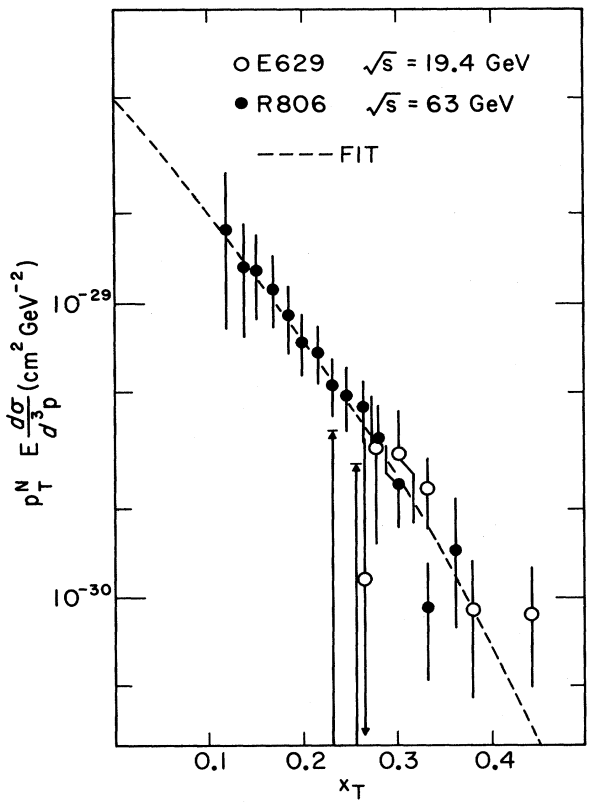

FIG. 31. A fit of the inclusive photon data of E629 and R806 to a function of p_T and x_T: $(49\pm18)(1-x_T)^{8.4\pm1.0}p_T^{-6.6\pm0.2}$ μb/GeV^2 (Huston, 1983; McLaughlin *et al.*, 1983).

factor. The fit has an excellent χ^2; the extracted parameters are $C=48\pm18$ μb/GeV^2, $N=8.4\pm1.0$, and $M=6.6\pm0.3$ (Huston, 1983; McLaughlin *et al.*, 1983). The p_T dependence is similar to that found for production of jets at the ISR (Åkesson *et al.*, 1983c). It should be pointed out that to obtain a direct-photon yield on a nucleon target, E629 assumed a linear dependence of the cross section on nucleon number. Approximately 10—20% discrepancies in relative normalization could result because of this assumption.[12] The effect on the value of M, however, is rather weak (30% change in relative normalization provides a change of ~0.2 in the value of M).

Although the γ/π^0 ratio does not appear to have a very significant energy dependence, there is some evidence that, for fixed p_T, it drops with increasing energy. This qualitative conclusion can be inferred from a comparison of the data sets shown in Figs. 15, where the effect is small, and Fig. 20, where the effect is very strong, and deduced from the x_T dependence for direct photons obtained in Fig. 31. (Note, however, that the R806 data from the second configuration in Fig. 14 do not display any energy dependence.) Comparing a fit to the photon yield, of the kind shown in Fig. 31, with a similar fit (for $\theta_{\text{c.m.}}\approx90°$) performed to π^0 data, both restricted to $p_T>3$ GeV/c, yields the following estimate for the γ/π^0 ratio in pp collisions:[13]

$$\frac{E\,d\sigma_\gamma/d^3p}{E\,d\sigma_{\pi^0}/d^3p}\approx(9\pm5)\times10^{-3}\frac{p_T^{1.3\pm0.3}}{(1-x_T)^{1.4\pm0.9}}\ . \qquad (14)$$

We see that there is substantial uncertainty in the energy dependence of the γ/π^0 ratio that will not be resolved before the next generation experiments are completed.

E. Results on correlations

We now turn to a discussion of experiments which have studied production of particles accompanying γ and π^0 triggers. Two questions concerning correlations have been addressed in recent pp experiments. First is whether the particle density near the prompt γ (same side) is consistent with expectations based on the Compton diagram. That is, are γ's produced predominantly unaccompanied by other particles, or is there evidence for an additional contribution from bremsstrahlung? Second is whether the character of the recoil (away-side) jet is different for γ and π^0 events, as would be expected if the recoil jets from direct γ's were dominantly remnants of u quarks (the Compton diagram). Three experiments have studied these questions. The R806 group searched for accompanying particles in their liquid-argon calorimeters (Kourkoumelis *et al.*, 1981). Also, R806, in conjunction with R807, measured the presence of accompanying charged particles in scintillation counters and in a large cylindrical drift chamber (Diakonou *et al.*, 1980c; Åkesson *et al.*, 1982a). Finally, the R108 experiment measured accompanying charged tracks in scintillators and in their central drift chambers (Angelis *et al.*, 1981).

Two early reports from R806 and R806/R807 provided qualitative information on the particle density that accompanied prompt γ and π^0 candidates. The first result (Diakonou *et al.*, 1980c) was based on the second geometrical arrangement discussed in Sec. III.C. Charged particles were identified through signals in a 44-element scintillator hodoscope that surrounded the intersection region and subtended ~2 units of pseudorapidity. Figure 32 shows the multiplicity of signals in the scintillators, separately for γ and π^0 candidates, as a function of p_T of the trigger particle. The γ triggers in this sample were not corrected for contamination from mesons. It is seen that, as p_T increases, the near-side multiplicity for γ can-

[12]The dependence of the structure functions on nuclear target could provide an additional A dependence (see Sec. II.C); also, the contribution from the specific graph shown in Fig. 1(c) depends somewhat on the quark content of the nucleus.

[13]A fit to the π^0 cross sections of E629 and R806 (at $\sqrt{s}=63$ GeV) for $p_T>3$ GeV/c provided the scaled form $(10\pm1)(1-x_T)^{9.2\pm0.2}p_T^{-8.3\pm0.1}$ mb/GeV^2, where the error bars are statistical (Povlis, 1983). We should point out that the parameters in Eq. (14) are somewhat sensitive to the p_T cutoff used in the fits. In addition, we wish to mention that, at such low p_T, k_T effects must be substantial. Consequently, this result must be used with some care, particularly for extrapolations to high (e.g., collider) energies.

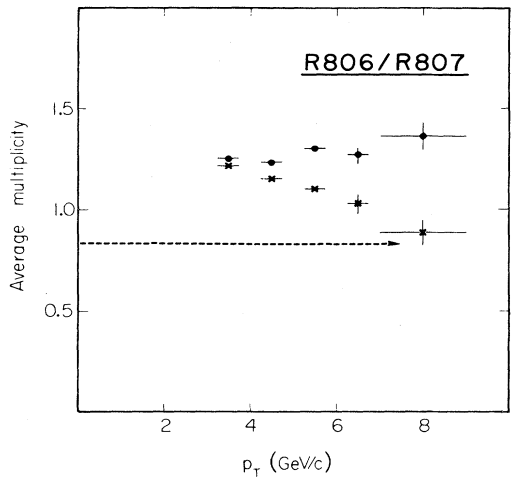

FIG. 32. The average multiplicity of scintillator-counter hits for π^0 (dots) and single-photon candidates (crosses) for the six scintillators within $\pm 24°$ of the trigger particle. The dashed line corresponds to the mean value of the multiplicity in untriggered (minimum bias) data (Diakonou *et al.*, 1980c).

didates decreases. This change with p_T can be attributed primarily to the changing signal to background ratio in the γ sample (see Fig. 13). At larger p_T (>7 GeV/c), where the background from mesons is relatively small, the accompanying particle density for γ's approaches that found for low-p_T (minimum bias) data, while the π^0 events show a higher accompanying particle density. The result demonstrates a qualitative difference between γ and π^0 events and speaks for the presence of a contribution to prompt γ production from processes such as the Compton or $q\bar{q}$ annihilation, that is, mechanisms that provide isolated direct photons.

A similar result was obtained by the R806 collaboration using four calorimeters of the kind used in the prompt γ analysis (Kourkoumelis *et al.*, 1981). The detectors were operated at 0.8 m from the interaction region and each subtended a solid angle of 1.0 sr. Although the prompt γ candidates in this configuration had substantially larger background contaminations from coalescing π^0's, it was possible to isolate a prompt γ signal for $p_T > 7.0$ GeV/c. The signal-to-background ratio was estimated to be about 1.4:1 in this sample. The probability of detecting an additional π^0 in another calorimeter was then measured for γ and π^0 triggers. Again, a tendency was observed for γ's to be produced unaccompanied by additional π^0's on the same side. For example, Fig. 33 shows, for two regions of accompanying momentum, the distribution in the difference in azimuth between the trigger particle and the accompanying π^0. The distributions for γ and π^0 candidates are clearly different. Similar differences were observed for rapidity correlation between the γ or π^0 triggers and their accompanying π^0's.

Additional confirmation for differences in the density of particles accompanying γ and π^0 triggers was obtained by the R108 experiment (Angelis *et al.*, 1981). They

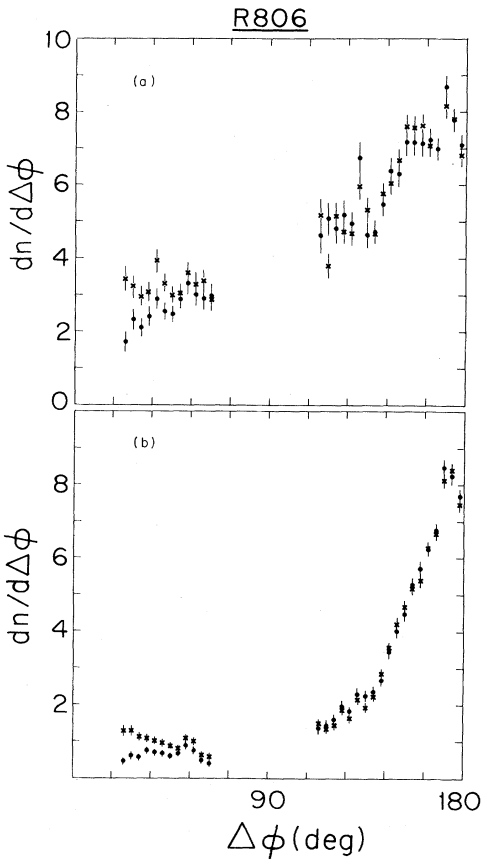

FIG. 33. The distribution in the difference in azimuth between π^0 (crosses) and single-photon (dots) triggers and reconstructed accompanying π^0's with transverse momentum (a) $p_T < 0.5$ GeV/c, and (b) $p_T > 0.5$ GeV/c (Kourkoumelis *et al.*, 1981).

studied charged particles detected in their central drift chamber system located within a 1.5-T solenoidal field (Camilleri *et al.*, 1978). The data were analyzed as discussed in Sec. III.C; the results at $\sqrt{s} = 63$ GeV and at $\sqrt{s} = 45$ GeV were combined for this analysis. To examine whether γ's tend to be produced unaccompanied, the data were divided into two samples, depending on whether there was at least one charged or neutral particle with $p_T > 0.3$ GeV/c produced within an azimuth of 90° of the direction of the trigger particle ($\Delta\phi < 90°$) in a range of pseudorapidity $|\eta| < 0.7$. As shown in Fig. 34, substantial differences were found in the γ/all ratio for the two data sets. The fraction of prompt γ events in the sample with no accompanying same-side particles is much larger than in the sample with accompanying particles. It should be pointed out that requiring that no charged or neutral particles appear within a 90° azimuthal range of the trigger is a very severe criterion. As R108 and other experiments have shown (e.g., Darriulat, 1980), a large fraction of the charged tracks with $p_T > 0.3$ GeV/c that are produced in that region are not associated with the trigger, that is, they are not part of the jet that caused the trigger. Nevertheless, the qualitative result is still clear; at moderate p_T, the direct-photon signal is greatly

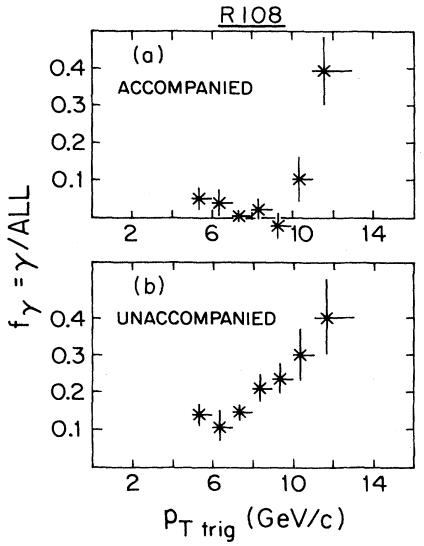

FIG. 34. (a) The fraction of events attributed to direct-photon production as a function of $p_{T\,\mathrm{trig}}$, for those events where the trigger was accompanied by a particle in the trigger hemisphere; (b) the same for those events where the trigger was not accompanied by a particle in the trigger hemisphere (Angelis *et al.*, 1981).

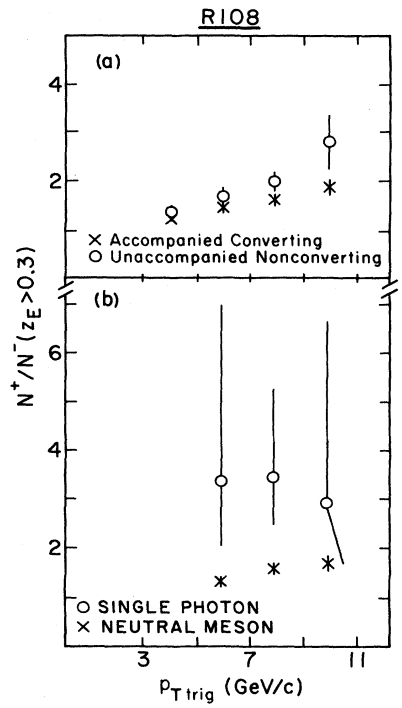

FIG. 35. The charge ratio (N^+/N^-) for $z_E > 0.3$ (away side) plotted as a function of $p_{T\,\mathrm{trig}}$ for (a) unaccompanied nonconverting events and accompanied converting events, and (b) direct photons and π^0 events (Angelis *et al.*, 1981).

enhanced for unaccompanied showers. There is also an indication in these data that, at very large p_T, γ's are produced along with other particles; although the effect is in only one bin, this can be interpreted as evidence for a bremsstrahlung contribution for $p_T > 10$ GeV/c.

Other attempts were made to study the event structure in R108 (Angelis *et al.*, 1981) by capitalizing on the observation that events with a nonconverting shower, and with no accompanying particles on the same side, were often γ's. In such a sample of data, the particle composition was determined to consist 39% of photons and 61% of neutral mesons and other hadrons. On the other hand, events that had a conversion, and were, in addition, accompanied by other particles, consisted almost entirely of neutral mesons and other hadrons (96%). The character of the away-side particles was investigated using these two types of data samples. As discussed previously, for Compton production, the expectation is for an enhancement in the number of positively charged particles in the away side, especially for large away-side momentum. A charge asymmetry N^+/N^- was defined as the ratio of the average number of positive to the average number of negative particles for any given range of z_E, where z_E (a z-like variable—see footnote 4) for any accompanying track is

$$z_E \equiv -\frac{\mathbf{p}\cdot\mathbf{p}_{\mathrm{trig}}}{|\mathbf{p}_{\mathrm{trig}}|^2}, \tag{15}$$

where $\mathbf{p}$ and $\mathbf{p}_{\mathrm{trig}}$ are the momenta of the accompanying track and the trigger particle, respectively. For both γ and π^0 candidates, N^+/N^- was found to be greater than one, as might be expected from an initial state with a net charge of 2. At low z_E, N^+/N^- was nearly the same for γ and π^0 candidates. Figure 35 shows the charge ratio for $z_E > 0.3$ as a function of p_T of the trigger particle. The data in part (a) are for unaccompanied nonconverting and accompanied converting triggers, while (b) displays the results after a statistical subtraction of the meson-induced background in the γ sample.[14] The ratio is clearly larger for γ's than for π^0's, both in the primary (trigger) data as well as in the background-subtracted distribution. [The increased error bars in (b) are due to the presence of systematic uncertainties inherent in the background subtraction.] The data therefore provide support for the expectation that the recoiling jet is often due to the fragmentation of a u quark.

Finally, we discuss the results of the R806/R807 collaboration, which measured correlations between charged tracks accompanying high-p_T γ's and π^0's (Åkesson *et al.*, 1982a). The γ's and π^0's were detected using the same lead—liquid-argon calorimeters used in the prompt-γ measurement of R806. The γ/π^0 ratio measured in this experiment agreed well with earlier results (Diakanou *et al.*, 1980b); the signal-to-background ratio varied from $\sim$0.3 at 3.0 GeV/c to more than 3.0 at 7 GeV/c. The direct-photon data presented by R806/R807 were corrected for meson-induced background using the observed

[14]The result shown in Fig. 35(b) is different from that given in Angelis *et al.*, 1981, because a recalculation of the effect of the background in the prompt-γ sample changed the ratio (Camilleri, 1981).

signal-to-background ratios in the single γ sample.

Charged particles were measured in a large cylindrical drift chamber situated in a 0.5-T axially symmetric magnetic field (Botner *et al.*, 1982). The chamber had 42 sampling layers and was segmented into 4° regions in azimuth. It provided space points (three dimensions) with a transverse resolution of ~ 250 μm from drift time, and ~ 2 cm resolution along the beam direction from charge division. The acceptance was $\sim 90\%$ of 2π in azimuth, and about two units of pseudorapidity, centered on $\eta = 0$.

The experiment had two aims, (1) to measure properties of the recoil jet and (2) to examine the particles produced at small angles with respect to the trigger; the goal was to test predictions based on the Compton production diagram and other mechanisms.

Figure 36 shows the azimuthal distribution ($\Delta\phi$) of particles (with $p_T > 1.0$ GeV/c) relative to the direction of the trigger γ or π^0. A clear difference in the density near the trigger is seen for the two data samples. (Similar differences are observed for accompanying particles of lower p_T, but the effect is not as striking.)

To examine further the character of the events for γ triggers, the distribution in accompanying transverse momentum as a function of azimuth (again with respect to the trigger particle) is shown in Fig. 37 for different values of trigger p_T. Here also, a clear difference is observed between γ and π^0 data. A principal aim of these studies was to ascertain the fractions of bremsstrahlung and Compton contributions to prompt-γ production. The fact that the transverse momentum associated with the charged particles accompanying photons did not show an enhancement at small $\Delta\phi$ indicated that the bremsstrahlung contribution was small. To extract the amount of bremsstrahlung production from the kind of distributions shown in Fig. 37, it was necessary to quantify the amount of accompanying energy expected for bremsstrahlung production and to determine the amount of accompanying "background" energy expected, at random, for small $\Delta\phi$ from the fragmentation of other constituents in an event. A ratio of bremsstrahlung to Compton production was extracted using plausible assumptions[15] for these two energy quantities (Åkesson *et al.*, 1982a); the results are shown in Fig. 38. (The calculation shown in the figure is from Dechanstreiter *et al.*, 1981.) Substantial systematic uncertainties in this ratio arise from the π^0 and η background subtraction, as well as from uncertainties in the accompanying energies from bremsstrahlung and background fragmentations. The bremsstrahlung/prompt production ratio is consistent with zero for all p_T; however, only a large upper limit can be placed on $\sigma_{\text{brems}}/\sigma_{\text{prompt}}$ of < 0.3, at a 95% confidence level, for $p_T > 5.5$ GeV/c. The limit is within the range of recent expectation for this ratio (Dechantsreiter *et al.*, 1981; Contogouris, Papadoupolos, and Papavassiliou, 1981; Nowak and Praszalowicz, 1983).

Experiment R806/R807 also provided additional information on the properties of recoil jets. As can be inferred from Fig. 36, the multiplicity of the away-side jet is essen-

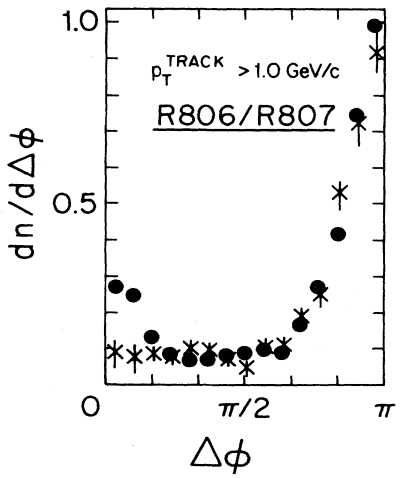

FIG. 36. The distribution in the difference in azimuthal angle ($\Delta\phi$) between the neutral trigger and a charged track, for p_T of the trigger greater than 4.5 GeV/c and for charged-particle transverse momenta > 1.0 GeV/c. The γ-triggered data have been corrected for effects of meson-induced background (Åkesson *et al.*, 1982a).

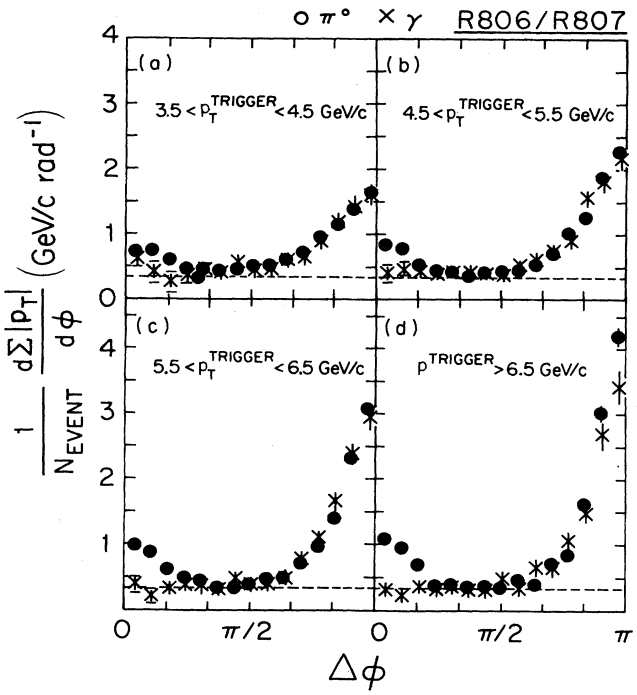

FIG. 37. For different bins in the neutral trigger momentum, the distribution in the average of the sum of the p_T values per interval in $\Delta\phi$. The γ-triggered data have been corrected for effects of meson-induced background (Åkesson *et al.*, 1982a).

[15]Basically, it was assumed that for the γ and π^0 triggers the average fraction of the energy of the initial quark that accompanies a bremsstrahlung photon to the fraction of the energy that accompanies the emitted π^0 is 0.83 ± 0.34. For justification see Åkesson *et al.*, 1982a.

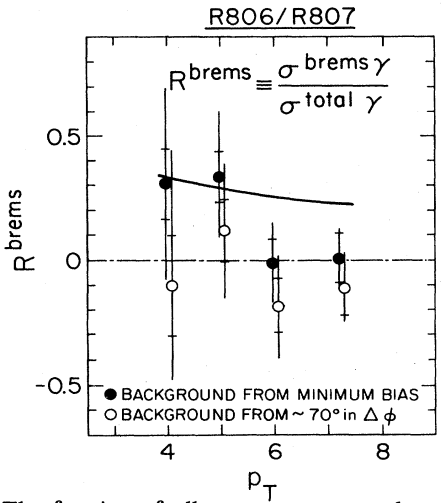

FIG. 38. The fraction of all prompt-γ events due to bremsstrahlung production, for two different assumptions about the energy of charged particles near the neutral trigger from the fragmentation of other partons. Inner error bars are statistical; outer error bars include systematic uncertainties added in quadrature (Åkesson *et al.*, 1982a). The curve is the result of a QCD-motivated calculation (Dechantsreiter *et al.*, 1981).

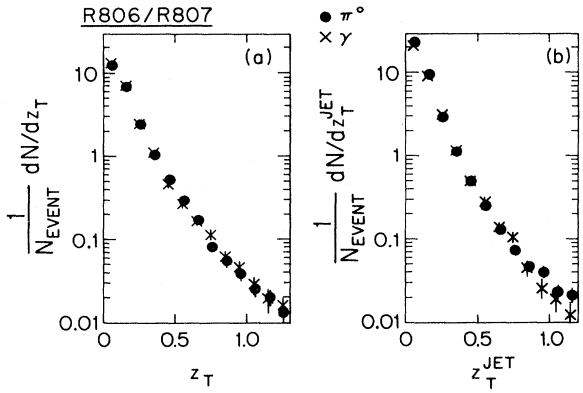

FIG. 39. The density of recoil particles ($\Delta\phi > 90°$) vs (a) z_T, or (b) z_T^{jet}, for p_T of the trigger greater than 4.5 GeV/c. The γ-triggered data have not been corrected for the effects of meson-induced background (Åkesson *et al.*, 1982a).

tially identical for γ and π^0 triggers. Differences between quark- and gluon-initiated jets might be expected to be observed in the z distribution of the recoil particles (z is the fraction of the jet momentum carried away by an individual hadron). In particular, gluon fragments are expected to exhibit a softer z distribution than quarks. Because the entire recoil jet was not detected in this experiment, another z-like variable z_T was defined for these investigations:

$$z_T \equiv |\mathbf{p}_T^{h^\pm} \cdot \mathbf{p}_T^{trig} / |p_T^{trig}|^2| \ , \tag{16}$$

where $\mathbf{p}_T^{trig}$ and $\mathbf{p}_T^h$ are the *transverse* momenta of the trigger γ's or π^0's, and away-side charged hadrons, respectively. Because a triggering π^0 carries a large fraction of its jet momentum, and because, in principle (except for k_T), the recoil jet has the same p_T as the trigger photon (or as the jet that provided the trigger π^0), z_T should approximately equal z. The data are displayed in Fig. 39(a); the distribution in z_T extends past a value of 1.0, and no appreciable difference is observed between γ and π^0 events.

Because γ's carry away the full momentum of the collision, whereas π^0's carry away only a large fraction of the constituent's momentum, using z_T as an approximation for z produces a different bias for γ and π^0 events. Consequently, the data were examined using a corrected value of z by defining the variable

$$z_T^{JET} = |\mathbf{p}_T^{h^\pm} \cdot \mathbf{p}_T^{JET} / |p_T^{JET}|^2| \ , \tag{17}$$

where $\mathbf{p}_T^{JET}$ was calculated by adding to the γ or π^0 momentum the momenta of all charged particles within a cone of 45° around the trigger. Corrections were applied for tracking inefficiencies, acceptance, and for the fact that neutral accompanying hadrons were not detected in the experiment. The distributions in z_T^{JET} for γ and π^0 events are shown in Fig. 39(b). Although no strong conclusion can be drawn from these data, a possible difference in the distribution can be seen at large values of z_T^{JET}. It should be pointed out that no correction was made in the sample to account for meson-induced background; nevertheless, this would not change the qualitative conclusions garnered from Fig. 39.

We might remark that the fact that the two z_T distributions in Fig. 39(a) are the same implies that there is, in fact, a difference between the γ and π^0 events. This is because γ's carry the full constituent momentum, while π^0's do not.[16] Estimates for p_T^{trig}/p_T^{JET} for data selected with a high-p_T hadron trigger vary from about 0.8 to 0.9 (Albrow *et al.*, 1978; Buchanan, 1982; Angelis *et al.*, 1982). Consequently, rescaling the values of z_T for π^0 events by this factor would provide a significantly softer z_T distribution for π^0-triggered data. Although this result is consistent with the expectation that π^0 triggers have a combination of gluon and quark recoils, whereas γ triggers are associated primarily with quark recoils, the argument is only qualitative.

The final topic addressed by R806/R807 was the charge distribution of recoiling particles. As discussed earlier, because of the enhanced fraction of u-quark—initiated jet recoils expected from γ's, a charge asymmetry is expected, especially at high z. Because of the admixture of u, d, and gluon jets that are expected to recoil from π^0 triggers, a smaller asymmetry is expected for π^0's. The results are shown in Fig. 40, for two bins of trigger momentum; the relative density of positive to negative particles is plotted as a function of z_T, separately for γ and π^0 events. (A statistical subtraction, to account largely for the π^0 background, has been made in the γ sample.) For both sets of data, the positive/negative ratio increases with increasing z_T. A marginally significant

[16]This has been emphasized by G. Bellettini (1981).

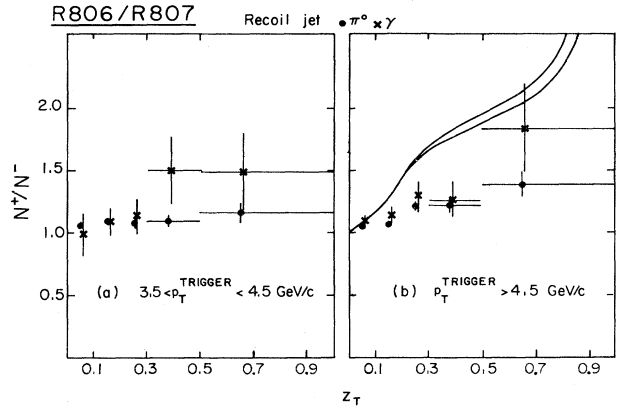

FIG. 40. For two bins in trigger momentum, the ratio of the density of positive to negative particles for $\Delta\phi > 90°$ as a function of z_T. The γ-triggered events have been corrected for effects of meson-induced background. The curves shown in (b) are from the calculation of Halzen *et al.*, 1980, for $p_T=6.0$ GeV/c. The data have $\langle p_T\rangle=5.8$ GeV/c. The curves are for extreme variations in gluon fragmentation for the small contribution from quark-antiquark annihilation to prompt-γ production. Including scale breaking effects in the fragmentation increases the predicted charge ratio somewhat (Åkesson *et al.*, 1982a).

difference can be seen between γ and π^0 events. Also shown for comparison are predictions of a calculation based on QCD (Halzen *et al.*, 1980). The data are consistently below the prediction of the model and lower than the results of R108 (Fig. 35). Unfortunately, at high z_T, where the predictive power of the QCD models are most reliable, the data are statistically limited.

It is clear that the measurements of associated charged-particle correlations in γ and π^0 events are rather limited by either statistical or systematical uncertainties. Results on the density of same-side particles indicate a convincing difference between γ and π^0 triggers. Nevertheless, the quantitative conclusion from R806/R807 on the fraction of events due to bremsstrahlung production is weak because of poor statistics, because of uncertainties from the meson-induced background, and because of the uncertainties in assumptions concerning charged-particle distributions, which are required in the extraction of $\sigma_{\text{brems}}/\sigma_{\text{prompt}}$.

Other results from correlation studies are even more ambiguous. Very little difference is observed in the away-side jet properties between γ and π^0 triggers. The z_T distributions are nearly identical. Here, however, there is not much theoretical guidance for the difference to be expected between gluon and quark jets; in addition, there is no reliable information on the admixture of quark and gluon jets that are expected to recoil against π^0 triggers. The charge asymmetry, especially at large z, is expected to show substantial differences between γ's and π^0's, but, here again, the experimental results are weak. The R108 data show a one to two standard deviation difference between γ's and π^0's in each of three p_T bins. However, because of the small signal-to-background ratio for γ's, the charge asymmetry has large uncertainties. Although the charge asymmetry measured in R807 is lower, it also has substantial errors, and it is difficult to draw any conclusions about the discrepancy with R108, particularly since the two sets of data do not cover the same regions of p_T. At best, both measurements can be taken as indicative of a difference in the charge asymmetry of away-side jets that accompany γ's and π^0's. More data at higher z_T would be required to provide stringent tests of the theoretical predictions.

IV. NEXT-GENERATION EXPERIMENTS

A. Upcoming experiments on direct photons

It is perhaps not surprising that the most informative experiments on direct photons to date have been those performed at the ISR. The high energies that were available there, and the consequent large cross sections at high p_T, coupled with the excellent luminosities, made the ISR an almost ideal accelerator for studying direct photons. With the closing of the ISR in late 1983, the two remaining efforts in this field will also be terminated. In this section we first discuss these last two contributions to the physics of direct photons from the ISR. We subsequently turn to a new investigation of direct photons at the SPS, where the circulating $\bar{p}$ beam for the collider will be used for studying interactions on a gas-jet target. Finally, we discuss experiments that will use fixed targets. The main advantages of the fixed-target program, namely, the ability to examine the projectile and target dependence of prompt photon production, is expected to be exploited maximally in the next few years both at CERN and at Fermilab.

B. Final studies at the ISR

To take greater advantage of the $\bar{p}p$ option at the ISR that was initiated in 1981, the R-110 collaboration (Camilleri *et al.*, 1981) installed arrays of active lead glass converters and *MWPC* planes in front of their two existent lead glass electromagnetic shower detectors. A sketch of the modification to their apparatus is shown in Fig. 41. The *MWPC*'s are present to measure the positions of converted photons and thereby provide discrimination between π^0 and γ conversions, something that was not available in this group's initial experiments (Fig. 18). Through a comparison of $\bar{p}p$ and pp data in the same apparatus, the experimenters hope to extract information on the relative importance of the annihilation and Compton diagrams in $\bar{p}p$ collisions, and on any differences that might manifest themselves in the character of the away-side quark and gluon jets. Although this experiment covers a reasonably large solid angle (arrays of 0.82 and 1.4 sr), the ability to resolve π^0's from γ's will be limited to $p_T \lesssim 6$ GeV/c. This is somewhat unfortunate, because the annihilation graph starts dominating the Compton graph only at $x_T \gtrsim 0.2$ (Benary *et al.*, 1981; Contogouris,

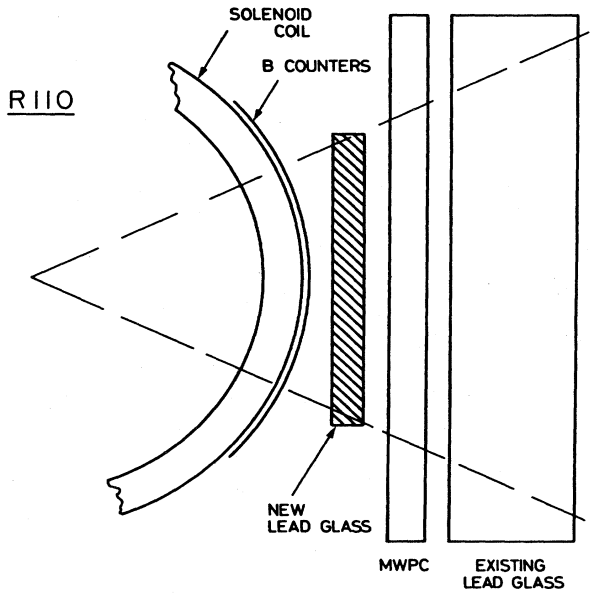

FIG. 41. Schematic drawing of the upgraded version of the R110 apparatus (Camilleri *et al.*, 1981).

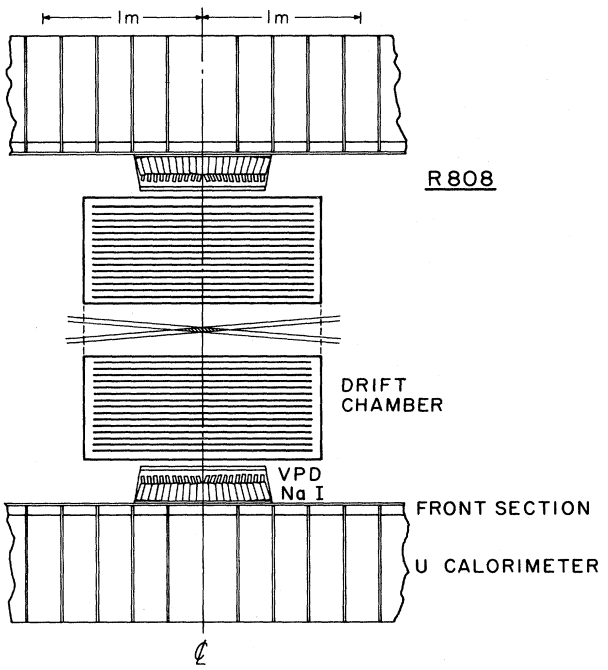

FIG. 42. The added NaI arrays and uranium calorimeters in R808 (Anassontzis *et al.*, 1981).

Papadoupolos, and Papavassiliou, 1981). However, the major problem with the experiment will undoubtedly be that the $\bar{p}$ luminosity (and the running time at the ISR) may be too limited to even reach p_T values of ~ 6 GeV/c.

The R808 collaboration at the ISR (Anassontzis *et al.*, 1981) has improved their capability for measuring direct photons below p_T values of 8 GeV/c. This was done by installing two arrays of NaI blocks in front of their walls of uranium calorimeters. (The liquid-argon detectors used by this group in previous experiments were incompatible with the uranium towers that were introduced for studying unbiased production of hadron jets.) Each of the two NaI arrays consists of 600 crystals ($3.5 \times 3.5 \times 13.8$ cm^3) mounted so as to point towards the ISR intersection region. The arrays are located on opposite sides of the intersection point in order to be also sensitive to diphotons produced back-to-back at $\sim 90°$ in the c.m. Figure 42 illustrates the geometry. Vacuum photodiodes (VPD) are mounted on the front of the NaI blocks. These arrays can be used to reconstruct π^0's for $p_T < 8$ GeV/c, at which point the two showers from π^0 decays cannot be separated. Nevertheless, π^0's can be distinguished from single γ showers beyond 8 GeV/c on the basis of transverse shower shape. Because the NaI crystals are only ~ 5 radiation lengths thick (2.6 cm corresponds to one radiation length), a substantial amount of the electromagnetic energy from any shower will be deposited in the electromagnetic front sections of the uranium towers. Although the NaI arrays cover only a total of 1.2 sr of solid angle, the ability to discriminate π^0's and η's from prompt γ's should be quite good because of the additional coverage provided by the uranium calorimeters; these calorimeters can be used to establish the presence of any other electromagnetic showers outside of the acceptance of the NaI arrays, as well as to obtain measurements on any jets that accompany the γ's or π^0's.

Experiment R808 should provide valuable information on direct photon production in pp collisions in the regime of low p_T values that could not be well studied in previous investigations. The granularity of the NaI arrays and the excellent resolution, particularly for low-energy showers, will be important for improving the signal to noise for direct photons in the 4—8 GeV/c p_T region. A comparison with $\bar{p}p$ interactions will, again, be limited by low-$\bar{p}$ luminosity and the minimal amount of running time that will be available prior to the closing of the ISR.

C. Internal gas-jet target at the SPS

A new two-arm forward spectrometer is being completed for operation in late 1984 in the SPS tunnel (Antille *et al.*, 1980). The overall purpose of this UA-6 effort is to study rare processes in $\bar{p}p$ collisions at $\sqrt{s} \simeq 23$ GeV. Using a specially designed internal gas-jet target to interact with the stored $\bar{p}$ beam, the experiment can attain a luminosity of $\sim 10^{31}$ cm^{-2} sec^{-1}, with minimal loss of luminosity for the $\bar{p}p$ collider program. The equipment is designed so that it can be turned around by 180° in order to study similar pp processes and thereby provide a comparison of $\bar{p}p$ and pp interactions in the same apparatus. A perspective view of the set-up is shown in Fig. 43.

Each arm will have an acceptance of 1.5 sr in the c.m. ($30° < \theta_{\text{c.m.}} < 100°$). Photons will be detected using an electromagnetic shower detector located ~ 10 m downstream of the target; the detector will consist of interleaved lead plates and 0.5-cm proportional tubes (alternate

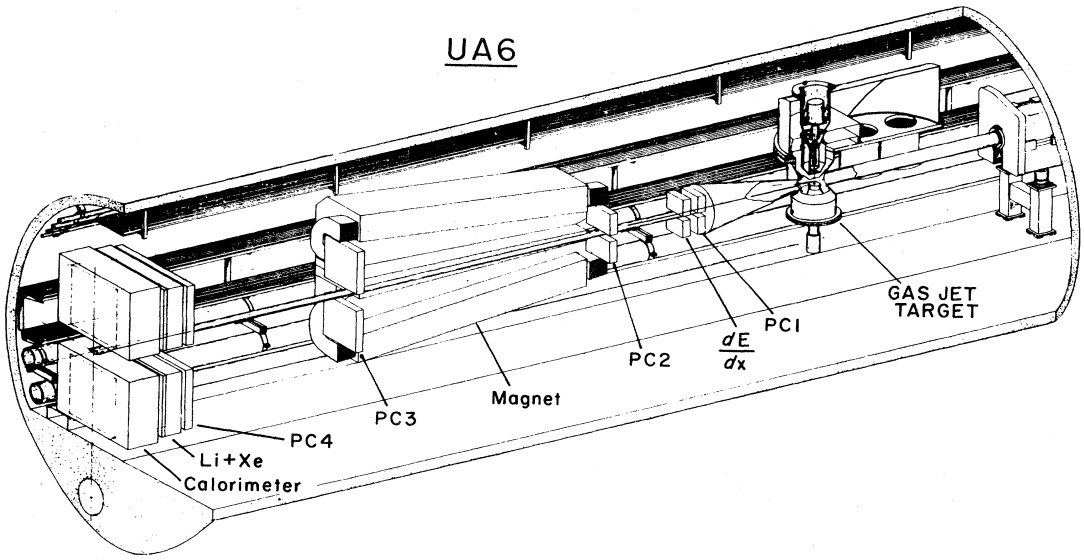

FIG. 43. A perspective view of the setup of experiment UA-6 in the SPS tunnel (Antille *et al.*, 1980).

x-y readout). The system will be segmented longitudinally into three sections to provide good hadron rejection. Momenta of the charged particles that accompany the prompt photons will be measured using the PWC system in conjunction with the analyzing magnets. The resolution of the electromagnetic calorimeter should be more than adequate for investigating the p_T range of 4—8 GeV/c of direct photon production; however, the proportional tube technique as used in UA-6 has still to be proven effective for measuring photon positions and energies under experimental conditions. Also, if UA-6 produces substantial background to the $\bar{p}p$ collider experiments, then its total amount of running time may be restricted.

D. Fixed-target program at the SPS

There are two fixed-target experiments at the SPS that have had some running during 1982—1983 (Giannini *et al.*, 1983; Bamberger *et al.*, 1983) and one that is about to be installed into the Ω' spectrometer (Bachman *et al.*, 1980).

Farthest along is the NA3 group, whose spectrometer is shown in Fig. 44. The segmentation of their electromagnetic shower detector (9 cm$\times$2.5 m lead/scintillator strips) has been improved for this experiment by installing in the old set-up a "shower localizer" at about 5 radiation lengths into the calorimeter (Costantini, 1983b). This device is a PWC system with strip and pad readout on the cathode planes. A position precision of about ± 3 mm for electrons has been achieved to date.[17] The main focus of this experiment is a comparison of γ production in 200 GeV/c π^+C and π^-C channels, in an attempt to extract information on the annihilation graph (pC data will also be taken). There are basically three triggers in the experiment, which are described below.

(1) A direct photon (or a photon from a π^0) converts in a thin (0.15 radiation lengths) lead converter that is located in front of the analyzing magnet. The electron pair opens horizontally in crossing the magnet and is detected in trigger chambers ($M1/M2$) and in the electromagnetic calorimeter. A minimum energy requirement in the calorimeter is used in conjunction with the trigger PWC's to select events of some minimum p_T. This method has the advantage in that it provides a way of separating the two γ's from π^0 decays by simply converting one of them (and detecting the other one in the calorimeter). The problem is that only $\sim 10\%$ of the direct photons convert in the thin radiator; consequently this technique requires a lot of running time. The threshold for this trigger is set typically at ~ 2 GeV/c for the vertically projected part of p_T.

(2) NA3 also has an electromagnetic calorimeter trigger of large acceptance. However, because of the poor granularity, to avoid saturation from multi-π^0 events, the threshold has to be set high to keep the trigger rate at a reasonable level. The threshold in this mode is kept typically at 4 GeV/c p_T (projected along vertical direction).

(3) The third trigger is a two-shower requirement (one in the upper and one in the lower spectrometer arm), each typically $\gtrsim 1.5$ GeV/c in projected transverse momentum. This should enable NA3 to study $\gamma\gamma$ events of lower threshold than could be obtained with the single-shower trigger modes. The results from NA3 are still too preliminary to tell whether the experiment will be able to measure, with precision, the contribution of the annihilation graph to direct-photon production.

The NA-24 collaboration (Bamberger *et al.*, 1983) has thus far had only calibration and test time but no data

[17] This is about a factor of 3 or 4 worse than has been obtained using other calorimetry techniques (Nelson *et al.*, 1983; Bachman *et al.*, 1983).

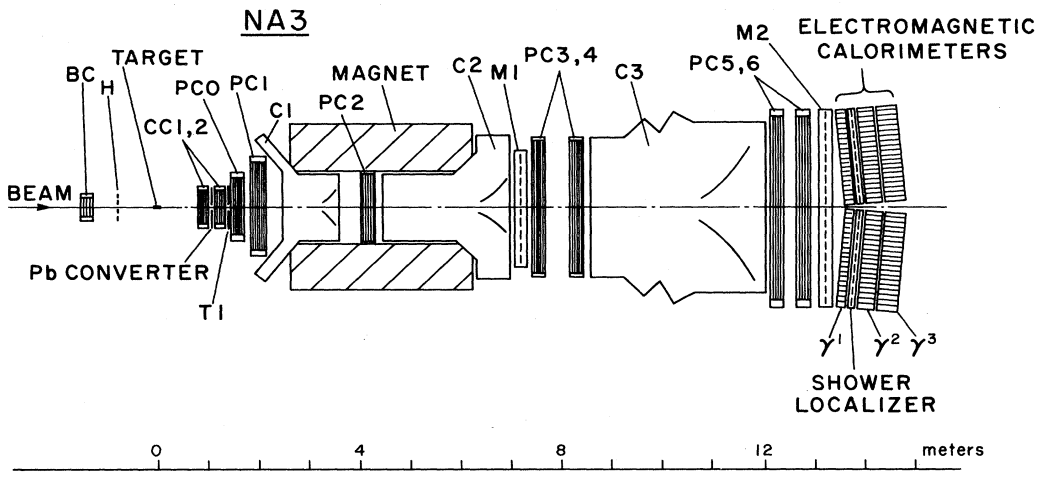

FIG. 44. Schematic of the NA-3 spectrometer showing additional instrumentation for improving detection of photons (Giannini *et al.*, 1983).

taking. Approval has been obtained for 40 days of beam time in 1983. A layout of the experiment is shown in Fig. 45, where an enlargement showing the nature of the new photon detector is also given. The photons convert in eight lead sheets, each of 1 radiation length; every one of these is followed, alternately, by x and y proportional tubes, of triangular cell shape, with wire spacing of 7.7 mm. An additional plane of proportional tubes, rotated by 45°, is placed behind every x-y doublet. Four modules of this type surround the beam hole and are located just up-stream of the electromagnetic section of the NA-5 2π calorimeter. Although the results of the test runs on the performance of the photon detector are not yet available, the trigger rates achieved thus far appear to be encouraging. NA-24 utilizes a 1-m hydrogen target in a 300-GeV beam. The hope is to investigate with good statistics single-photon production in π^+p, π^-p, and and pp collisions up to p_T of ~ 7 GeV/c, and diphotons in π^-p collisions up to masses of ~ 8 GeV. As in the case of UA-6, the technique to be used for measuring direct photons has still to be proven effective. The advantage that this experiment has over NA-3 is the factor of 1.5 in beam energy, which provides, typically, a factor of ~ 5 in yield for $p_T > 5$ GeV/c. The dramatic increase in yield expected at large p_T with increasing beam energy is displayed in Fig. 46 (Baker *et al.*, 1981). (The anticipated increase in π^0 production from Fig. 46 is conistent with that expected for direct photons based on Fig. 31.)

The WA 70 collaboration has designed and tested a novel electromagnetic calorimeter for their direct photon experiment at the CERN SPS (Bachman *et al.*, 1983). The device will consist of twelve identical modules, arranged in four quadrants around the beam axis, with each quadrant being three modules deep. These modules will be 2×2 m^2 in area and ~ 10 cm thick. The showers will be sampled ten times, alternately in x and y directions, through 2-m-long and 5-mm-diam Teflon tubes containing liquid scintillator. These tubes will be stacked vertically in planes, embedded in epoxy, banded with thin steel and fiberglass layers for structural rigidity, and glued to 0.5-cm-thick lead plates. The details of the construction are indicated in Fig. 47. The detector will be placed about 10 m downstream of a hydrogen target, which will be located within the upgraded Omega spectrometer (Ω'). Differential pulse-height and timing information for each set of x and y strips provides shower localization to an accuracy of about 2 cm, without reliance on stereoscopic reconstruction. The results of the test of the prototype calorimeter are very promising, and the detector should enable WA 70 to obtain precise information on prompt photons. The goals of this experiment are similar to those of NA-24.

E. Fixed-target experiments at Fermilab

Fermilab has two major experiments that will investigate direct photon production. The E705 group has upgraded its electromagnetic shower detection capabilities through the installation of modules of scintillating barium glass (composed primarily of BaO and SiO_2). The response of this glass to positrons has been studied recently (Cox *et al.*, 1982) and appears to be excellent. The energy resolution of the glass will certainly be adequate for studying direct photons. With the anticipated installation of 0.5-cm gas tubes (operated in a saturated avalanche mode) in the scintillation glass array, the position resolution and the ability to distinguish π^0's from direct photons should also be adequate. The main purpose of the experiment is the investigation of heavy-quark resonances; however, the availability of scintillation glass should provide extensive data on direct photons as well. A sketch of the E705 spectrometer is given in Fig. 48. The experiment should be running in late 1984 using a one-meter

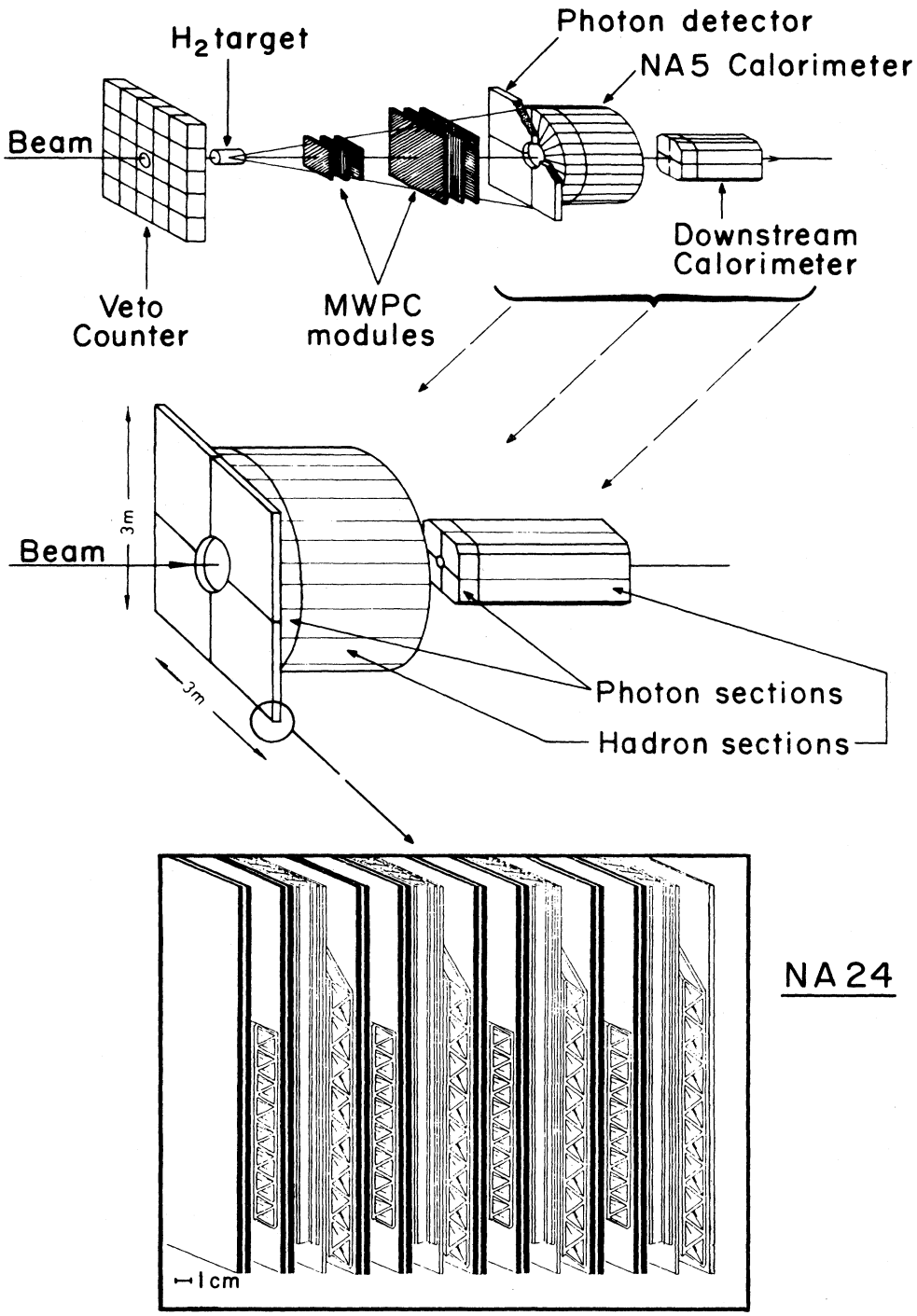

FIG. 45. Layout of the NA-5 apparatus supplemented with additional photon detection capability for NA-24 (Bamberger *et al.*, 1983).

hydrogen/deuterium target and 300-GeV positive and 300-GeV negative (highly $\bar{p}$ enriched) beams. Additional beam time is anticipated at $\sim$750 GeV once the Proton-West Area at Fermilab gets upgraded.

Experiment E706 was designated to be a second-generation experiment for investigating direct-photon physics (Baker *et al.*, 1981). A new beam and a new experimental hall are being constructed in the Meson Area of Fermilab for occupancy in 1985. A sketch of the elements of the spectrometer is given in Fig. 49. Photon detection will be based on liquid-argon calorimetry. Two electromagnetic sections will be followed by two hadronic

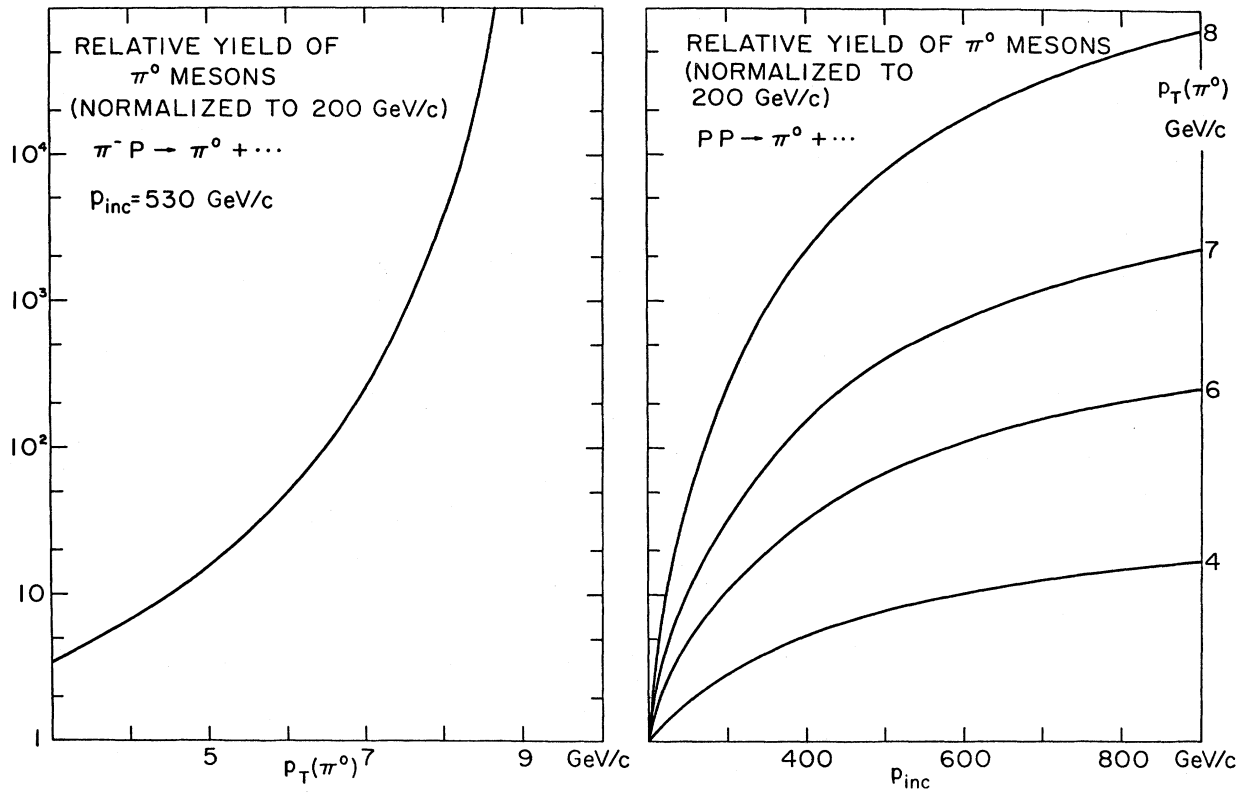

FIG. 46. Comparison of the anticipated production ratio for π^0's at 530 and at 200 GeV/c in $\pi^- p$ reactions as a function of p_T. Also shown is the ratio of π^0 production in pp collisions, for fixed p_T values, as a function of incident momentum, normalized to the yield at 200 GeV/c (Baker *et al.*, 1981).

sectors; both will be contained within one dewar. The electromagnetic detector will have r and ϕ readout geometry (total of $\sim$6500 channels), while the hadronic sections will have equilateral triangle tesselations. The electromagnetic segmentation will be typically about 0.5 cm in the transverse dimension and the triangles will have areas of $\sim$70 cm^2. The calorimeter will be focused—i.e., the consecutive readout elements along any ray from the

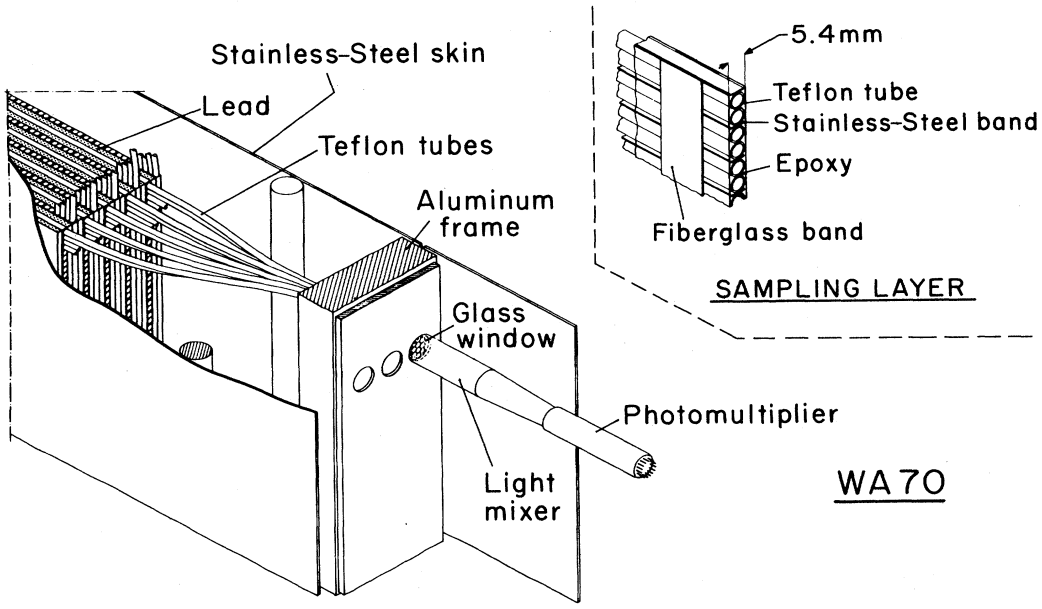

FIG. 47. The details of the construction of the photon detector for experiment WA 70 (Bachman *et al.*, 1983).

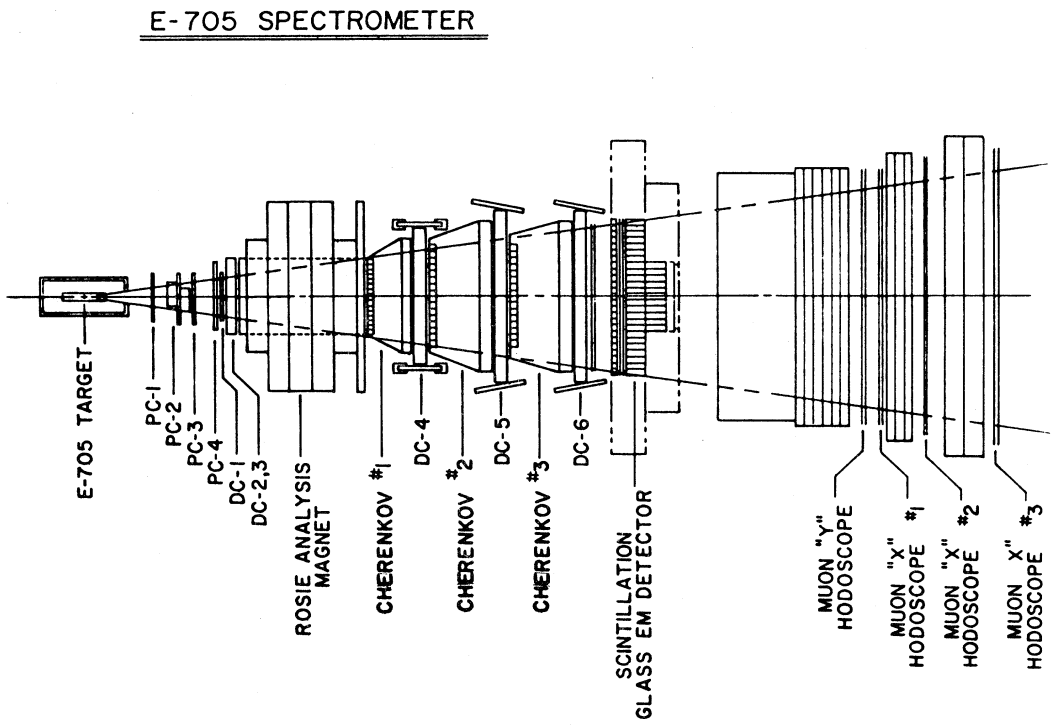

FIG. 48. Sketch of the spectrometer for experiment E705 (Binkley *et al.*, 1981).

target will subtend the same solid angle. The charged particles accompanying photons, π^0 or η's, will be measured using a silicon microstrip system in front of the analyzing magnet and PWC's downstream of the magnet. A novel scintillation calorimeter, to be read out with cylindrical wave-shifter bars interspersed through the

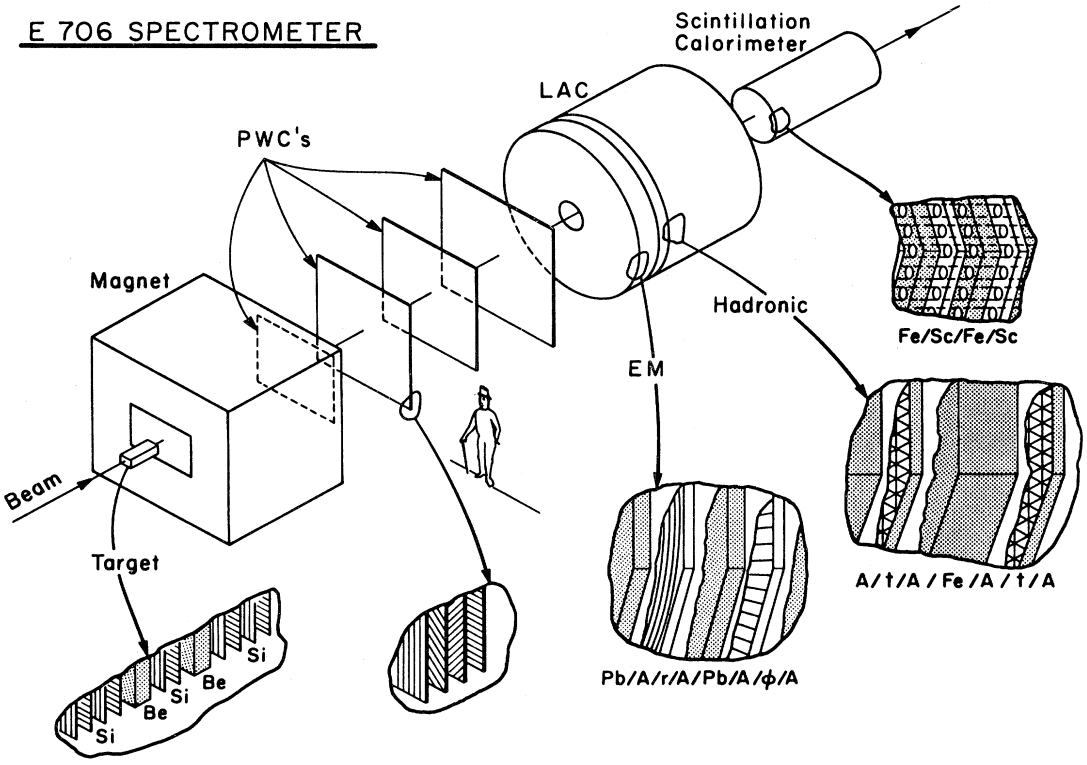

FIG. 49. Elements of the spectrometer for experiment E706 (Baker *et al.*, 1981).

iron/scintillator stack, will measure forward-produced particles. The acceptance of the system will be $\sim 80\%$ of 4π for photons and $\sim 90\%$ of 4π for charged particles. The hope is to study direct-photon production using 400—800 GeV beams (mesons and baryons of both sign) on various nuclear targets, for p_T values of 5—10 GeV/c. In addition, E706 expects to provide useful data on $\gamma\gamma$ and e^+e^- production for masses up to ~ 15 GeV.

F. Summary of expectations

In Table II we present an update of a previous summary by Costantini (Costantini, 1983a; Pretzl, 1983) of results anticipated from direct-photon experiments over the next few years. It is clear that the experiments presently set up at CERN, as well as E705 at Fermilab, will shortly make significant contributions to the available data on direct-photon production. Nevertheless, because the direct-photon yield at $p_T \gtrsim 7$ GeV/c should be several magnitudes greater for Tevatron running than at the SPS, E706, being an experiment dedicated to direct photons, should eventually have major impact on the field.

V. DISCUSSION AND SUMMARY

The data presented in this review leave no doubt that prompt photons have been observed in hadronic collisions. Although there is some disagreement among experiments, the essential result, namely, that the yield of direct photons at large transverse momenta is comparable to that of pions, is indisputable. In the range of Fermilab-ISR energies, the γ/π^0 production ratio in pp collisions increases with p_T, from a value of ~ 0.05 at ~ 3 GeV/c to ~ 0.5 at ~ 10 GeV/c.

The general level of the direct-photon signal is certainly consistent with that predicted from QCD calculations. This is in itself a great triumph for QCD. Comparisons of theory with data in Figs. 17, 21, and 30, for example, demonstrate the kind of good agreement that has been obtained. What has emerged from data on correlations is also encouraging. Results for same-side associated particles show unambigously that a substantial fraction of the γ's are produced unaccompanied, as would be expected from dominance of the Compton diagram (and a relatively small contribution from bremsstrahlung). From away-side investigations it appears that the charge asymmetry is at least roughly consistent with expectation. Qualitatively, therefore, the direct-photon data are in excellent agreement with QCD.

Although it is beyond the scope of this review to provide a full critical evaluation of the present status of the phenomenology, it is appropriate to discuss several features of the QCD fits presented with the data in Sec. III. This is particularly important for providing guidance to the next-generation experiments and for setting goals for new calculations that could be used to extract from the data parameters of physical interest.

Because of the phenomenological ambiguities discussed in Sec. II, and because of a lack of a complete calculation of higher-order contributions to direct-photon production, a comparison with data necessarily involves certain steps in the modeling. First, calculations can be taken to a specific order in α_s (usually the leading-log QCD approximation) to establish the kinematic domain over which there is agreement with the data. Subsequently, the leading terms can be supplemented either with phenomenological (model-dependent) corrections (e.g., k_T smearing) or with direct calculations of specific higher-order contributions (e.g., soft-gluon corrections, or higher-order bremsstrahlung contributions). As an example, the calculations of Contogouris *et al.* (1982), in Figs. 16 and 17 [for the strong gluon structure function $xG(g,p;x) \sim 0.9(1+9x)(1-x)^4$ at $Q^2=4$ GeV^2], can be compared with the calculations of Duke and Owens (dashed curve) in Fig. 21. Both calculations have essentially the same input quark and gluon structure functions. Duke and Owens use the leading-log approximation (including bremsstrahlung) while Contogouris *et al.* introduce, in addition, k_T smearing and soft-gluon corrections. For $p_T \gtrsim 7$ GeV/c the calculation of Duke and Owens lies about half way between the two curves of Contogouris *et al.* in Fig. 17. (The discrepancy between the Born terms of Contogouris *et al.* and the calculation of Duke and Owens can be attributed to differences in the Q^2 evolution of the structure functions provided by Duke and Owens.) Below p_T values of 7 GeV/c, as expected, Contogouris *et al.* have an increasing contribution relative to Duke and Owens, primarily because of the presence of k_T smearing in the former calculation ($\langle k_T \rangle = 0.5$ GeV/c). Both calculations have some difficulty in accounting for the direct-γ excess at low p_T observed in the data of R806. From these comparisons, and particularly from Fig. 16, we would conclude that a reasonably hard-gluon distribution is required to account for the direct-photon signal, and that some k_T smearing is needed to account for the data at lower p_T. However, because of uncertainties in the structure functions and in the absolute normalization of R108 and R806 data, nothing convincing can be said about the need for the soft-gluon corrections.

Unfortunately, the interesting result concerning the hardness of the input gluon structure function may be in doubt because of the second calculation of Duke and Owens shown in Fig. 21. In the calculation already mentioned (the dashed curve), Duke and Owens used the strong-gluon distribution and $\Lambda = 0.4$ GeV/c, while in the calculation for the unbroken curve a far weaker gluon structure function [$xG(g,p;x) \sim 1.6(1+9x)(1-x)^6$ at $Q^2=4$ GeV^2] and $\Lambda = 0.2$ GeV/c was used. The conclusion that can be drawn is that present direct-γ data cannot distinguish between these two rather different possibilities for the gluon structure of protons at low Q^2. That is, although the gluon structure function may be reasonably well determined by the data at $Q^2 \approx 90$ GeV^2, the correlation between the value of the QCD parameter Λ and the Q^2 evolution of the structure functions makes it difficult to reach a unique conclusion concerning the nature of the gluon distribution at small Q^2. If Λ is, in fact, close to 0.2 GeV/c, then the softer-gluon distribution is preferred.

Considering the rather imprecise nature of current ex-

TABLE II. List of approved prompt-photon experiments at CERN and at Fermilab.

Group	Start of data taking	Beam/target	Laboratory energy (GeV)	Photon detection	Photon energy resolution $\sigma(E)/E$; value at 50 GeV	Two-shower separation (mm)	Hadron measurement	Sensitivity events/nb day
ISR								
R110	82	$\bar{p},p/p$	2100	lead glass and PWC's	$\frac{0.05}{\sqrt{E}}$	~ 50	magnet spectrometer	$\sim 2\times 10^3$ (pp)
R808	82	$\bar{p},p/p$	2100	NaI and U calorimeters	$\frac{0.11}{\sqrt{E}}$	>35	magnet spectrometer, calorimeters	$\sim 10^3$ (pp)
SPS								
NA-3	82	$\pi^{\pm},p/C$	200	scintillator/lead and shower chamber	$<\frac{0.21}{\sqrt{E}};0.04$	<50	magnet spectrometer, Cherenkov	600
NA-24	83	$\pi^{\pm},p/p$	200 300	proportional tube/lead and scintillator/lead	$<\frac{0.24}{\sqrt{E}}$	15	segmented hadron calorimeter	800
WA-70	83	$\pi^{\pm},p/p$	200 300	liquid scintillator/lead	$<\frac{0.16}{\sqrt{E}};0.04$	15	Ω' spectrometer RICH counter	800
UA-6	84	$\bar{p},p/p$, other nuclei, polarized p	270	proportional tube/lead	$<\frac{0.23}{\sqrt{E}}$	$\gtrsim 15$	magnet spectrometer, dE/dx, transition radiation	40 $\bar{p}p$ (main user) 300 pp
FERMILAB								
E-705	84	$p,\bar{p},\pi^{\pm}/d$	300	scintillating barium glass	$<\frac{0.015}{\sqrt{E}};0.02$	10	magnet spectrometer, Cherenkov	$\sim 10^3$
E-706	86	$\pi^{\pm},p,\bar{p}$ some $K^{\pm}$ tagging/Be,C,Al	400 530 800	liquid argon/lead	$\sim\frac{0.14}{\sqrt{E}};0.03$	10	magnet spectrometer, calorimeter, silicon microstrips	$\sim 10^3$

periments, it is remarkable how far the phenomenology of direct photons has progressed. Based on calculations in the literature, the following conclusions appear to be noncontroversial: (1) Higher-twist contributions are expected to be small, except, as indicated previously, at large x_T (Owens, 1981; Berger, 1982; Farrar and Fox, 1980). (2) Bremsstrahlung corrections to the yield of direct photons should be incorporated, although these are expected to be small (Nowak and Praszalowicz, 1983; Benary *et al.*, 1983; Duke and Owens, 1983). (3) Scaling violations, particularly in the gluon structure functions, are important and cannot be ignored (Contogouris *et al.*, 1979; Baier *et al.*, 1980).

Other phenomenological questions are not so clearly resolved. There is, of course, the matter of defining Q^2, that we alluded to in Sec. II.B, and will not expand on here. There is also the problem of transverse motion of partons. Here there is agreement that at small p_T some kind of k_T smearing is needed to account for this internal motion. There is still controversy, however, in just how these corrections should be applied. For example, should on-shell or off-shell kinematics be used? Also, some of the k_T smearing must have origin in higher-order gluon corrections, and, in fact, some calculations use a large $\langle k_T \rangle$ to take partial account of such QCD radiation effects (Benary *et al.*, 1983).

A still open phenomenological question involves the nature of the higher-order QCD contributions to direct photon production. It is not presently known to what extent these terms can be ignored (Furmanski, 1981). The soft-gluon corrections of Contogouris, Papadoupoulos, and Papavassiliou (1981) and Contogouris, Papadopoulos, and Ralston (1981) are quite large; however, the complete calculation for corrections to order α_s^2 has not been done, and it is uncertain whether the neglected terms or even higher-order terms are, in fact, negligible. This is unquestionably an important area for future phenomenological investigation.

As we have indicated above, there is at present reasonable agreement among the various experiments on the magnitude of the direct-photon cross section and on the correlations between photons and their accompanying hadrons. The data are still very sparse. When more precise measurements on prompt photons become available some of the phenomenological uncertainties could be eliminated. Measuring correlations between the photons and their accompanying jets at different x_T would be particularly valuable and would provide detailed information on quark and gluon structure functions (Cormell and Owens, 1980). Precise data on the annihilation graph would provide unique information on the Q^2 dependence of gluon fragmentation. Also, ignoring correlations, if k_T smearing and α_s are deduced from other sources, e.g., Drell-Yan or diphoton production for $\langle k_T \rangle$ and e^+e^- annihilations for α_s,[18] then direct-photon data could be used to establish the character of the gluon structure functions and the overall self-consistency of QCD formalism. All these possibilities are, in fact, the goals of the next-generation experiments.

[18] For a critical analysis of procedures for determining α_s, see Duke and Roberts (1984).

ACKNOWLEDGMENTS

We thank our colleagues who have provided us with comments and with information that is contained in this review. We wish to acknowledge helpful correspondence with V. Burkert, L. Camilleri, F. Costantini, R. Cool, B. Cox, M. Martin, and K. Pretzl, and valuable discussions with S. Frankel, J. Huston, K. McDonald, C. Quigg, and C. Woody. We have greatly appreciated the detailed and illuminating remarks of J. Owens on the phenomenological sections, and the incisive and exhaustive comments of M. Tannenbaum on the entire manuscript.

REFERENCES

Adeva, B., *et al.*, 1983, Phys. Rev. Lett. **50**, 2051.
Aitchson, I. J. R., and A. J. G. Hey, 1982, *Gauge Theories in Particle Physics* (Adam Hilger Ltd., Bristol).
Åkesson, T., *et al.*, 1982a, Phys. Lett. **118B**, 178.
Åkesson, T., *et al.*, 1982b, Phys. Lett. **118B**, 185.
Åkesson, T., *et al.*, 1983a, Phys. Lett. **123B**, 133.
Åkesson, T., *et al.*, 1983b, Phys. Lett. **123B**, 367.
Åkesson, T., 1983c, Z. Phys. C **18**, 5.
Albrow, M. G., *et al.*, 1978, Nucl. Phys. B **145**, 305.
Altarelli, G., R. K. Ellis, and G. Martinelli, 1979, Nucl. Phys. B **158**, 461.
Altarelli, G., and G. Parisi, 1977, Nucl. Phys. B **126**, 298.
Amaldi, E., M. Beneventano, B. Borgia, A. Capone, F. de Notaristefani, U. Dore, F. Ferroni, E. Longo, L. Luminari, P. Pistilli, I. Sestili, G. F. Dell, L. C. L. Yuan, and G. Kantardjian, 1978, Phys. Lett. **77B**, 240.
Amaldi, E., M. Beneventano, B. Borgia, A. Capone, F. de Notaristefani, U. Dore, F. Ferroni, E. Longo, L. Luminari, P. Pistelli, I. Sestili, G. F. Dell, L. C. L. Yuan, G. Kantardjian, and J. Dooker, 1979a, Nucl. Phys. B **150**, 326.
Amaldi, E., M. Beneventano, B. Borgia, A. Capone, F. de Notaristefani, U. Dore, F. Ferroni, E. Longo, L. Luminari, P. Pistilli, I. Sestili, G. F. Dell, L. C. L. Yuan, and G. Kantardjian, 1979b, Phys. Lett. **84B**, 360.
Anassontzis, E., *et al.*, 1981, "A study of direct photon production," CERN/ISRC/81-16 (R808 collaboration at ISR).
Anassontzis, E., *et al.*, 1982a, Z. Phys. C **13**, 277.
Anassontzis, E., *et al.*, 1982b, in *Proceedings of the XIII International Symposium on Multiparticle Dynamics,* edited by W. Kittel, (Nijmegen University).
Andersson, B., G. Gustafson, and T. Sjöstrand, 1980, Phys. Lett. **94B**, 211.
Angelis, A. L. S., *et al.*, 1978, Phys. Lett. **79B**, 505.
Angelis, A. L. S., *et al.*, 1980, Phys. Lett. **94B**, 106.
Angelis, A. L. S., *et al.*, 1981, Phys. Lett. **98B**, 115.
Angelis, A. L. S., *et al.*, 1982, Nucl. Phys. B **209**, 284.
Antille, J., *et al.*, 1980, "Proposal for the study of e^+e^-, γ, π^0 and hyperon production in pp reactions at $\sqrt{s}=22.5$ GeV using an internal jet target at the SPS," CERN/SPSC/80-63 (UA-6 collaboration at SPS).
Arnison, G., *et al.*, 1983, Phys. Lett. **123B**, 115.
Aubert, J. J., *et al.*, 1983, Phys. Lett. **123B**, 275.
Aurenche, P., and J. Lindfors, 1980, Nucl. Phys. B **168**, 296.

Bachman, L., L. Fluri, M. N. Kienzle-Focacci, M. Martin, R. Mermod, D. Perrin, and J. Rutschmann, 1980, "Proposal to the SPSC study of direct photon events in hadronic collisions," CERN/SPSC/80-61 (WA 70 collaboration at SPS).
Bachman, L., *et al.*, 1983, Nucl. Instrum. Methods **206**, 85.
Badier, J., *et al.*, 1979, in *Proceedings of an International Symposium on Lepton and Photon Interactions—Fermilab*, edited by T. Kirk and H. Abarbanel (Fermilab, Batavia).
Baier, R., J. Engels, and B. Petterson, 1979, Z. Phys. C **2**, 265.
Baier, R., J. Engels, and B. Petterson, 1980, Z. Phys. C **6**, 309.
Baker, W., *et al.*, 1981, "A proposal to measure direct photon production at tevatron energies" (E706 collaboration at Fermilab).
Baltrusaitis, R. M., M. Binkley, B. Cox, T. Kondo, C. T. Murphy, W. Yang, L. Ettlinger, M. S. Goodman, J. A. J. Matthews, and J. Nagy, 1979, Phys. Lett. **88B**, 372.
Baltrusaitis, R. M., M. Binkley, B. Cox, T. Kondo, C. T. Murphy, W. Yang, L. Ettlinger, M. S. Goodman, J. A. J. Matthews, and J. Nagy, 1980, Phys. Rev. Lett. **44**, 122.
Bamberger, A., *et al.*, 1980, "A proposal to investigate deep inelastic scattering processes involving photons in either the initial or the final state," CERN/SPSC/80-83 (NA-24 collaboration at SPS).
Bamberger, A., *et al.*, 1983, CERN/SPSC/83-3, SPSC/M 344 (NA-24 collaboration at SPS).
Banner, M., *et al.*, 1982, Phys. Lett. **118B**, 203.
Bellettini, G., 1981, private communication.
Benary, O., E. Gotsman, and D. Lissauer, 1981, Z. Phys. C **9**, 81.
Benary, O., E. Gotsman, and D. Lissauer, 1983, Z. Phys. C **16**, 211.
Berger, E. L., 1982a Phys. Rev. D **26**, 105.
Berger, E. L., 1982b, in *Proceedings, Drell Yan Workshop* (Fermilab, October 1982).
Berger, E. L., 1981, private communication.
Berman, S. M., J. D. Bjorken, and J. Kogut, 1971, Phys. Rev. D **4**, 3388.
Binkley, M., *et al.*, 1981, "A comparison of the production of direct photons and resonances decaying to lepton pairs by antiproton/π^- and proton/π^+ beams" (E-537 phase II: revised objective, Fermilab proposal 669).
Bodek, A., N. Giokaris, W. B. Atwood, D. H. Coward, D. J. Sherden, D. L. Dubin, J. E. Elias, J. I. Friedman, H. W. Kendall, J. S. Poucher, and E. M. Riordan, 1983, Phys. Rev. Lett. **50**, 1431.
Bøggild, H., and T. Ferbel, 1974, Ann. Rev. Nucl. Sci. **24**, 451.
Botner, O., *et al.*, Nucl. Instrum. Methods **196**, 315.
Brodsky, S. J., and G. R. Farrar, 1975, Phys. Rev. D **11**, 1309.
Buchanan, C. D., 1982, "Comparison of single particle trigger, high p results in proton-proton collisions at $\sqrt{s}=45$ and 63 GeV," in *Elementary Hadronic Processes and Heavy Ion Interactions* (Proceedings Recontre de Moriond XVII), edited by J. Tran Thanh Van (Editions, Frontières, France), Vol. II, 139.
Buras, A. J., and K. J. F. Gaemers, 1978, Nucl. Phys. B **132**, 249.
Burkert, V., 1983, in Proceedings, XIV International Symposium on Multiple Dynamics (Lake Tahoe), edited by J. Gunion (to be published).
Camilleri, L., 1981, private communication.
Camilleri, L., *et al.*, 1978, Nucl. Instrum. Methods **156**, 275.
Camilleri, L., *et al.*, 1981, CERN/ISRC/81-9 (R110 collaboration at ISR).
Carimalo, S., M. Crozon, P. Kessler, and J. Parisi, 1981, Phys. Lett. **98B**, 105.
Caswell, W. E., R. R. Horgan, and S. J. Brodsky, 1978, Phys. Rev. D **18**, 2415.
Cobb J., *et al.*, 1978, Phys. Lett. **78B**, 519.
Cobb, J. H., S. Iwata, D. C. Rahm, P. Rehak, I. Stumer, C. W. Fabjan, M. Harris, J. Lindsay, I. Mannelli, K. Nakamura, A. Nappi, W. Struczinski, W. J. Willis, C. Kourkoumelis, and A. J. Lankford, 1979, Nucl. Instrum. Methods **158**, 93.
Combridge, B. L., 1980, CIT report CALT-68-766.
Contogouris, A. P., S. Papadopoulos, and M. Hongoh, 1979, Phys. Rev. D **19**, 2607.
Contogouris, A. P., S. Papadopoulos, and C. Papavassiliou, 1981, Nucl. Phys. B **179**, 461.
Contogouris, A. P., S. Papadopoulos, and J. Ralston, 1981, Phys. Lett. **104B**, 70.
Contogouris, A. P., S. Papadopoulos, and J. Ralston, 1982, Phys. Rev. D **25**, 1280.
Cormell, L., and J. F. Owens, 1980, Phys. Rev. D. **22**, 1609.
Constantini, F., 1983a, *SPS Workshop on Fixed Target Physics in 1984—1989*, Vol. II, CERN 83/02.
Constantini, F., 1983b, in Proceedings of the Second International Pisa Meeting on Advanced Detectors (to be published).
Cronin, J., 1977, in *Proceedings of an International Symposium on Lepton and Photon Interactions, Hamburg*, edited by F. Gutbrod (DESY, Hamburg).
Cox, B., G. Hale, P. O. Mazur, R. L. Wagner, D. E. Wagoner, H. Areti, S. Conetti, P. Lebrun, T. Ryan, J. E. Brau, and R. A. Gearhart, 1982, "A measurement of the response of an SCG1-C scintillation glass shower detector to 2—17.5 GeV positrons," Fermilab-Conf-82/75-EXP.
Darriulat, P., 1980, Ann. Rev. Nucl. Sci. **30**, 159.
Darriulat, P., P. Dittman, K. Eggert, M. Holder, K. T. McDonald, T. Modis, F. L. Navarria, A. Seiden, J. Strauss, G. Vesztergombi, and E. G. H. Williams, Nucl. Phys. B **110**, 365.
Dechantsreiter, M., F. Halzen, and D. M. Scott, 1981, Phys. Rev. D **24**, 2856.
De Marzo, C., *et al.*, 1982, Phys. Lett. **112B**, 173.
De Rujula, A., H. Georgi, and H. D. Politzer, 1977, Ann. Phys. **103**, 315.
Diakonou, M., *et al.*, 1979, Phys. Lett. **87B**, 292.
Diakonou, M., *et al.*, 1980a, Phys. Lett. **89B**, 432.
Diakonou, M., *et al.*, 1980b, Phys. Lett. **91B**, 296.
Diakonou, M., *et al.*, 1980c, Phys. Lett. **91B**, 301.
Donaldson, G., H. Gordon, K.-W. Lai, I. Stumer, A. Barnes, J. Mellema, A. Tollestrup, R. Walker, O. Dahl, R. Johnson, A. Ogawa, M. Pripstein, and S. Shannon, 1976, Bull. Am. Phys. Soc. **21**, 568.
Duke, D. W., and J. F. Owens, 1983, Florida State Preprint, FSU-HEP-831115.
Duke, D. W., and R. G. Roberts, 1984, Phys. Rep. (in press).
Escobar, C. O., 1975, Nucl. Phys. B **98**, 173.
Farrar, G. R., 1974, Nucl. Phys. B **77**, 429.
Farrar, G. R., 1977, Phys. Lett. **67B**, 337.
Farrar, G. R., and G. C. Fox, 1980, Nucl. Phys. B **167**, 205.
Farrar, G. R., and S. C. Frautschi, 1976, Phys. Rev. Lett. **36**, 1017.
Feinberg, E. L., 1976, Nuovo Cimento A **34**, 391.
Feynman, R. P., R. D. Field, and G. C. Fox, 1978, Phys. Rev. D **18**, 3320.
Field, R. D., 1978, "Dynamics of high-energy reactions," in *Proceedings of the XIXth International Conference on High-Energy Physics, Tokyo*, edited by S. Homma, M. Kawaguchi, and H. Miyazawa (Physical Society of Japan, Tokyo) p. 743.
Ford, R. L., and W. R. Nelson, 1978, SLAC 210.
Frazer, W. R., and J. F. Gunion, 1979, Phys. Rev. D **20**, 147.

Fritzsch, M., and P. Minkowski, 1977, Phys. Lett. **69B**, 316.
Furmanski, W., 1981, Jagellonion University report TPJU-12/81.
Georgi, H., and H. D. Politzer, 1974, Phys. Rev. D **9**, 416.
Giannini, G., *et al.,* 1983, NA3 status report to SPSC.
Goshaw, A. T., P. W. Lucas, W. D. Walker, J. R. Elliot, L. E. Evans, L. R Fortney, and W. J. Robertson, 1979, Phys. Rev. Lett. **43**, 1065.
Gross, D. J., and F. Wilczek, 1973, Phys. Rev. Lett. **30**, 1343.
Gross, D. J., and F. Wilczek, 1974, Phys. Rev. D **9**, 980.
Gunion, J. F., 1974, Phys. Rev. D **10**, 242.
Hagelberg, R., *et al.,* 1980, "Direct photon production in hadron-hadron collisions at the SPS," CERN/SPSC/80-106 (NA-3 collaboration at SPS).
Halzen, F., M. Dechantsreiter, and D. M. Scott, 1980, Phys. Rev. D **22**, 1617.
Halzen, F., and D. M. Scott, 1978a, Phys. Rev. Lett. **40**, 1117.
Halzen, F., and D. M. Scott, 1978b, Phys. Rev. D **18**, 3378.
Halzen, F., and D. M. Scott, 1981, University of Wisconsin Report MAD/PH/21.
Horgan, R. R., and P. N. Scharbach, 1979, Phys. Lett. **81B**, 215.
Horgan, R. R., and P. N. Scharbach, Nucl. Phys. B **181**, 421.
Hoyer, P., P. Osland, H. G. Sander, T. F. Walsh, and P. M. Zerwas, 1979, Nucl. Phys. B **161**, 349.
Huston, J., 1983, in Proceedings, XIV International Symposium on Multiparticle Dynamics (Lake Tahoe), edited by J. Gunion (to be published).
Jaffe, R. L., 1983, Phys. Rev. Lett. **50**, 228.
Kotański, A., and J. Kubar, 1980, Acta Phys. Pol. B **11**, 669.
Kourkoumelis, C., *et al.,* 1979, Phys. Lett. **84B**, 277.
Kourkoumelis, C., *et al.,* 1980, Z. Phys. C **5**, 95.
Kourkoumelis, C., *et al.,* 1981, Nucl. Phys. B **179**, 1.
Kourkoumelis, C., *et al.,* 1982, Z. Phys. C **16**, 101.
Krawczyk, M., and W. Ochs, 1978, Phys. Lett. **79B**, 119.
Krzywicki, A., 1976, Phys. Rev. D **14**, 152.
Krzywicki, A., J. Engels, B. Petersen, and U. Sukhatme, Phys. Lett. **85B**, 407.
Kubar-Andre, J., and F. Paige, 1979, Phys. Rev. D **19**, 221.
Lederman, L. M., 1975, in *Proceedings, International Symposium on Lepton and Photon Interactions at High Energies,* edited by W. T. Kirk (Stanford University).
Llewellyn Smith, C. H., 1983, Oxford preprint 18/83.
McLaughlin, M., *et al.,* 1983, Phys. Rev. Lett. **51**, 971.
Nelson, C. A., *et al.,* 1983, Nucl. Instrum. Methods **216**, 381.
Newman, C. B., K. J. Anderson, R. N. Coleman, G. E. Hogan, K. P. Karhi, K. T. McDonald, J. E. Pilcher, E. I. Rosenberg, G. H. Sanders, A. J. S. Smith, and J. J. Thaler, 1979, Phys. Rev. Lett. **42**, 951.
Nowak, M., and M. Praszalowicz, 1983, Z. Phys. C **17**, 249.
Owens, J. F., 1981, Florida State University report FSU-HEP-820315.
Owens, J. F., and E. Reya, 1978, Phys. Rev. D **17**, 3003.
Perkins, D. H., 1981, "Deep inelastic lepton-nucleon scattering," in *Techniques and Concepts of High-Energy Physics,* edited by T. Ferbel (Plenum, New York), p. 279.
Perl, M. L., 1974, *High Energy Hadron Physics* (Wiley, New York).
Petrarca, S., and F. Rapuano, 1979, Phys. Lett. **88B**, 167.
Politzer, H. D., 1973, Phys. Rev. Lett. **30**, 1346.
Povlis, J., 1983, private communication.
Povlis, J., *et al.,* 1983, Phys. Rev. Lett. **51**, 968.
Pretzl, K., *et al.,* 1983, "Investigation of deep inelastic scattering processes involving large $p+$ direct photons in the final state," in *Workshop on SPS Fixed-Target Physics in the Years 1984—1989,* p. 105, Vol. II, CERN 83/02.
Quigg, C., 1983, *Gauge Theories of the Strong, Weak and Electromagnetic Interactions* (Benjamin-Cummings, Reading).
Rosner, J., 1981, "Quark models," in *Techniques and Concepts of High-Energy Physics,* edited by T. Ferbel (Plenum, New York), p. 1.
Rückl, R., S. J. Brodsky, and J. F. Gunion, 1978, Phys. Rev. D **18**, 2469.
Sehgal, L. M., 1977, "Hadron production by leptons," in *Proceedings, International Symposium on Lepton and Photon Interactions,* edited by F. Gutbrod (Deutsches Elektronen-Synchrotron, Hamburg), p. 837.
Willis, W. J., 1981, CERN-EP/81-45, presented at *Colloquium on Photon-Photon Interactions,* Paris.
Wolf, G., 1982, "Jet production and fragmentation," in *Proceedings of the XXIth International Conference on High-Energy Physics,* edited by P. Petiau and M. Porneuf, J. Phys. (Paris), Colloq. **43**, 525.
Yan, T-M., 1976, Ann. Rev. Nucl. Sci. **26**, 199.